

*The base map on the front cover shows geophysical survey locations overlaying a geologic map of U.S. Geological Survey, Windham, New Hampshire, 1:24,000-scale quadrangle. Geology is by G.S. Walsh and S.F. Clark, Jr. (1999) and lineaments are from Ferguson and others (1997) and R.B. Moore and Garrick Marcoux, 1998.*

*The photographs and graphics overlying the base map are showing, counterclockwise from the left, a USGS scientist using a resistivity meter and surveying equipment (background) to survey the bedrock beneath the surface using a geophysical method called azimuthal square-array direct-current resistivity. In the lower left, this cross section is showing the results of a survey along line 3 in Windham, N.H., using another method called two-dimensional direct-current resistivity. In the lower right, the photograph is showing a bedrock outcrop located between red lines 3 and 4 (on base map) at Windham, in which the fractures and parting parallel to foliation have the same strike as the azimuthal square-array direct-current resistivity survey results, and remotely sensed lineaments (purple and green lines on base map). The upper right graphic shows a polar plot of the results of an azimuthal square-array direct-current resistivity survey at Windham for array 1 (red circle on base map).*

**U.S. Department of the Interior  
U.S. Geological Survey**

**In cooperation with the  
NEW HAMPSHIRE DEPARTMENT OF ENVIRONMENTAL SERVICES**

# **Geophysical Investigations of Well Fields to Characterize Fractured-Bedrock Aquifers in Southern New Hampshire**

By James R. Degnan, Richard Bridge Moore, and Thomas J. Mack

**Water-Resources Investigations Report 01-4183**

**Pembroke, New Hampshire  
2001**

## **U.S. Department of the Interior**

Gale A. Norton, Secretary

## **U.S. Geological Survey**

Charles G. Groat, Director

The use of firm, trade, and brand names in this report is for identification purposes only and does not constitute endorsement by the U.S. Government.

For additional information write to:

District Chief  
U.S. Geological Survey  
New Hampshire/Vermont District  
361 Commerce Way  
Pembroke, NH 03275-3718

or through our Web site at  
**<http://nh.water.usgs.gov>**

Copies of this report can be purchased from:

U.S. Geological Survey  
Branch of Information Services  
Box 25286  
Federal Center  
Denver, CO 80225

# CONTENTS

- Abstract..... 1
- Introduction ..... 2
  - Purpose and Scope..... 2
  - Previous Investigations ..... 2
  - Site Selection ..... 3
  - Geohydrologic Settings ..... 3
  - Acknowledgments ..... 4
- Approach and Methods..... 4
  - P-Wave Seismic Refraction ..... 5
  - Ground-Penetrating Radar ..... 6
  - Magnetics..... 6
  - Very-Low-Frequency Electromagnetics ..... 6
  - Inductive Electromagnetic Terrain Conductivity ..... 7
  - Two-Dimensional Direct-Current Resistivity ..... 7
  - Azimuthal-Square Array Direct-Current Resistivity ..... 8
  - Borehole Geophysical Surveys..... 8
- Analysis and Results of Geophysical Investigations of Well Fields..... 9
  - Site 1, Bedford, New Hampshire ..... 10
    - Geophysical Surveys and Interpretation..... 10
    - Integration of Results..... 14
  - Site 2, Windham, New Hampshire ..... 16
    - Geophysical Surveys and Interpretation..... 18
    - Integration of Results..... 19
  - Site 3, Pelham, New Hampshire ..... 25
    - Geophysical Surveys and Interpretation..... 27
    - Integration of Results..... 29
  - Site 4, Goffstown, New Hampshire ..... 30
    - Geophysical Surveys and Interpretation..... 32
    - Integration of Results..... 35
  - Site 5, Goffstown, New Hampshire ..... 35
    - Geophysical Surveys and Interpretation..... 37
    - Integration of Results..... 39
  - Site 6, Salem, New Hampshire ..... 39
    - Geophysical Surveys and Interpretation..... 41
    - Integration of Results..... 44
- Summary and Conclusions ..... 47
- Selected References ..... 48
- Appendix 1. Graphs Showing Borehole Geophysical Logs of Three Sites in New Hampshire..... 51

## FIGURES

1-2. Maps showing:	
1. Location of the geophysical study area in the Pinardville, Windham, and Salem Depot 7.5-minute quadrangles in southern New Hampshire.....	2
2. Geophysical survey locations, bedrock geology, and lineaments at site 1, Bedford, N.H. ....	11
3-4. Graphs showing:	
3. Processed ground-penetrating radar profile at site 1 from line 1, Bedford, N.H.....	12
4. Magnetic and electromagnetic surveys at site 1 from line 1.....	13
5. Magnetic and electromagnetic surveys at site 1 from line 2.....	13
6-7. Cross sections showing inverted resistivity sections of two-dimensional, direct-current resistivity data at:	
6. Site 1 from line 1, Bedford, N.H. ....	14
7. Site 1 from line 2 .....	15
8. Polar plots showing azimuthal square-array direct-current resistivity at site 1 for arrays 1 and 2, Bedford, N.H.....	16
9. Map showing geophysical survey locations, bedrock geology, and lineaments at site 2, Windham, N.H.....	17
10-14. Graphs showing:	
10. Processed ground-penetrating radar profile at site 2 from line 1, Windham, N.H. ....	19
11. Magnetic and electromagnetic surveys at site 2 from line 1.....	20
12. Magnetic and electromagnetic surveys at site 2 from line 2.....	20
13. Magnetic and electromagnetic surveys at site 2 from line 3.....	21
14. Magnetic and electromagnetic surveys at site 2 from line 4.....	21
15-18. Cross sections showing inverted resistivity sections of two-dimensional, direct-current resistivity data at:	
15. Site 2 from line 1, Windham, N.H. ....	22
16. Site 2 from line 2 .....	23
17. Site 2 from line 3 .....	23
18. Site 2 from line 4 .....	24
19. Polar plot showing azimuthal square-array direct-current resistivity at site 2 for array 1, Windham, N.H. ....	24
20. Map showing geophysical survey locations, bedrock geology, and lineaments at site 3, Pelham, N.H. ....	26
21-22. Graphs showing magnetic and electromagnetic surveys at:	
21. Site 3 from line 1, Pelham, N.H.....	27
22. Site 3 from line 2 .....	28
23-24. Cross sections showing inverted resistivity sections of two-dimensional, direct-current resistivity data at:	
23. Site 3 from line 1, Pelham, N.H.....	28
24. Site 3 from line 2 .....	29
25. Polar plots showing azimuthal square-array direct-current resistivity at site 3 for arrays 1 and 2, Pelham, N.H.....	30
26. Map showing geophysical survey locations, bedrock geology, and lineaments at site 4, Goffstown, N.H. ....	31
27-28. Graphs showing magnetic and electromagnetic surveys at:	
27. Site 4 from line 1, Goffstown, N.H.....	32
28. Site 4 from line 2 .....	33
29-30. Cross sections showing inverted resistivity sections of two-dimensional, direct-current resistivity data at:	
29. Site 4 from line 1, Goffstown, N.H.....	33
30. Site 4 from line 2 .....	34
31. Polar plot showing azimuthal square-array direct-current resistivity at site 4 for array 1, Goffstown, N.H.....	34
32. Diagram showing lower hemisphere equal-area nets from bedrock well GNW 406 at site 4, Goffstown, N.H.....	35
33. Map showing geophysical survey locations, bedrock geology, and lineaments at site 5, Goffstown, N.H. ....	36
34-35. Graphs showing magnetic and electromagnetic surveys at:	
34. Site 5 from line 1, Goffstown, N.H.....	38
35. Site 5 from line 2 .....	38
36-37. Cross sections showing inverted resistivity sections of two-dimensional, direct-current resistivity data at:	
36. Site 5 from line 1, Goffstown, N.H.....	40
37. Site 5 from line 2 .....	40
38. Polar plot showing azimuthal square-array direct-current resistivity at site 5 for array 1, Goffstown, N.H.....	41
39. Diagram showing lower hemisphere equal-area nets from bedrock well GNW 408 at site 5, Goffstown, N.H.....	41
40. Map showing geophysical survey locations, bedrock geology, and lineaments at site 6, Salem, N.H. ....	42

41-43. Graphs showing electromagnetic surveys at:

41. Site 6 from line 1, Salem, N.H..... 43

42. Site 6 from line 2 ..... 43

43. Site 6 from line 3 ..... 43

44-46. Cross sections showing inverted resistivity sections of two-dimensional, direct-current resistivity data at:

44. Site 6 from line 1, Salem, N.H..... 45

45. Site 6 from line 2 ..... 46

46. Site 6 from line 3 ..... 46

47. Polar plot showing azimuthal square-array direct-current resistivity at site 6 for array 1, Salem, N.H..... 47

48. Diagram showing lower hemisphere equal-area nets from bedrock well SAW 272 at site 6, Salem, N.H..... 47

1A-C. Appendix graphs showing borehole geophysical logs of:

A. Well GNW 406 at site 4, Goffstown, N.H. .... 52

B. Well GNW 408 at site 5..... 53

C. Well SAW 272 at site 6, Salem, N.H. .... 54

**CONVERSION FACTORS, ABBREVIATIONS, AND VERTICAL DATUM**

<b>Multiply</b>	<b>By</b>	<b>To obtain</b>
<b>Length</b>		
inch (in.)	25.4	millimeter
foot (ft)	0.3048	meter
<b>Flow</b>		
gallon per minute (gal/min)	0.06308	liter per second
<b>Hydraulic Conductivity</b>		
foot per day (ft/d)	0.3048	meter per day
Temperature in degrees Celsius (°C) can be converted to degrees Fahrenheit (°F) as follows: $^{\circ}\text{F} = (^{\circ}\text{C} \div 5/9) + 32.$		

**Sea Level:** In this report “sea level” refers to the National Geodetic Vertical Datum of 1929 (NGVD of 1929)—a geodetic datum derived from a general adjustment of the first-order level nets of both the United States and Canada, formerly called Sea Level Datum of 1929.

**ABBREVIATIONS USED IN THIS REPORT**

Ω m	ohmmeter
mmho/m	millimohos per meter
MHz	megahertz
kHz	kilohertz
ft/s	foot per second
mS/m	millisiemens per meter
°	degree
m	meter
nT	nanotesla

# Geophysical Investigations of Well Fields to Characterize Fractured-Bedrock Aquifers in Southern New Hampshire

By James R. Degnan, Richard Bridge Moore, and Thomas J. Mack

## Abstract

Bedrock-fracture zones near high-yield bedrock wells in southern New Hampshire well fields were located and characterized using seven surface and six borehole geophysical survey methods. Detailed surveys of six sites with various methods provide an opportunity to integrate and compare survey results. Borehole geophysical surveys were conducted at three of the sites to confirm subsurface features. Hydrogeologic settings, including a variety of bedrock and surface geologic materials, were sought to gain an insight into the usefulness of the methods in varied terrains. Results from 15 survey lines, 8 arrays, and 3 boreholes were processed and interpreted from the 6 sites.

The surface geophysical methods used provided physical properties of fractured bedrock. Seismic refraction and ground-penetrating radar (GPR) primarily were used to characterize the overburden materials, but in a few cases indicated bedrock-fracture zones. Magnetometer surveys were used to obtain background information about the bedrock to compare with other results, and to search for magnetic lows, which may result from weathered fractured rock. Electromagnetic terrain conductivity surveys (EM) and very-low-frequency electromagnetic surveys (VLF) were used as rapid reconnaissance techniques with the primary purpose of identifying electrical anomalies, indicating potential fracture zones in bedrock.

Direct-current (dc) resistivity methods were used to gather detailed subsurface information about fracture depth and orientation. Two-dimensional (2-D) dc-resistivity surveys using dipole-dipole and Schlumberger arrays located and characterized the overburden, bedrock, and bedrock-fracture zones through analysis of data inversions. Azimuthal square array dc-resistivity survey results indicated orientations of conductive steep-dipping bedrock-fracture zones that were located and characterized by previously applied geophysical methods.

Various available data sets were used for site selection, characterizations, and interpretations. Lineament data, developed as a part of a statewide and regional scale investigation of the bedrock aquifer, were available to identify potential near-vertical fracture zones. Geophysical surveys indicated fracture zones coincident with lineaments at 4 of the sites. Geologic data collected as a part of the regional scale investigation provided outcrop fracture measurements, ductile fabric, and contact information. Dominant fracture trends correspond to the trends of geophysical anomalies at 4 of the sites. Water-well drillers' logs from water supply and environmental data sets also were used where available to characterize sites. Regional overburden information was compiled from stratified-drift aquifer maps and surficial-geological maps.

## INTRODUCTION

Many towns and communities in New Hampshire have limited amounts, or an absence of, sand and gravel aquifers, which are favorable for constructing high-yield wells. These towns must look for additional water resources in crystalline bedrock. The average bedrock well yield in New Hampshire is about 6 gal/min. An adequate municipal or commercial well typically requires tens to hundreds of gallons per minute. The U.S. Geological Survey (USGS), in cooperation with the New Hampshire Department of Environmental Services (NHDES), has done a statewide assessment of ground-water resources in the bedrock aquifers of New Hampshire (R.B. Moore and others, U.S. Geological Survey, written commun., 2001), which provides regional and statewide information regarding bedrock aquifer areas that are likely to be favorable for resource investigation. In identified potential high-yield bedrock aquifers, individual boreholes must be targeted to intercept a fracture or fracture zone that could be from 5-10 ft to less than 1 ft wide. The water-resources professional needs additional, site-specific information, to precisely locate boreholes to intercept specific bedrock-fracture zones. If such fractures are steeply dipping, the "target" surface area overlying the high-yield bedrock aquifer can be small. As part of the statewide bedrock-aquifer assessment, the USGS, in cooperation with the NHDES, assessed the use of geophysical methods to identify high-yield bedrock-fracture zones at six sites in New Hampshire (fig. 1).

## Purpose and Scope

This report describes the results of surface and borehole geophysical investigations of bedrock aquifers at selected well-field sites in New Hampshire. Included in this report are analyses of the data from various types of geophysical surveys to provide bedrock-fracture zone locations and characteristics and specifically to characterize fracture zones at high-yield well sites. The area of study includes six well field sites that were surveyed with surface methods from February to December 1999. Three sites were surveyed with borehole geophysical methods in December 2000. Geologic and lineament data were used to ensure that a variety of sites were selected, and were considered during the interpretation and discussion of the results of surface and borehole geophysical surveys.

## Previous Investigations

The use of geophysical techniques are well documented for water-supply (Haeni, 1995) and contaminant investigations in unconsolidated environments. Whereas fracture zones were correlated with photolinear features in some settings by geophysical methods, for example in karst environments in Florida (Spratt, 1996) and in sandstones in West Africa (Taylor and others, 1999), few publications document the use of geophysical techniques for investigation of water supply in fractured crystalline rock, particularly in the northeastern United States. Previous investigations using various geophysical methods to study high-yield crystalline bedrock aquifers include those of Chapman and Lane, 1996; Mack and others, 1998; and Johnson and others, 1999. Direct-current resistivity and borehole radar techniques were used by Chapman and Lane (1996) to determine the orientations of fracture zones in a crystalline bedrock aquifer in Lawrenceville, Ga. Advanced borehole techniques were used in Rye, N.H., to identify fractures in wells and in the surrounding area. Strikes of fracture sets in the wells in Rye, identified by Johnson and others (1999), were coincident with remotely sensed lineaments identified by Ferguson and others (1997). Complex fracture patterns emerged between two wells using radar tomography results in Seabrook, N.H.,

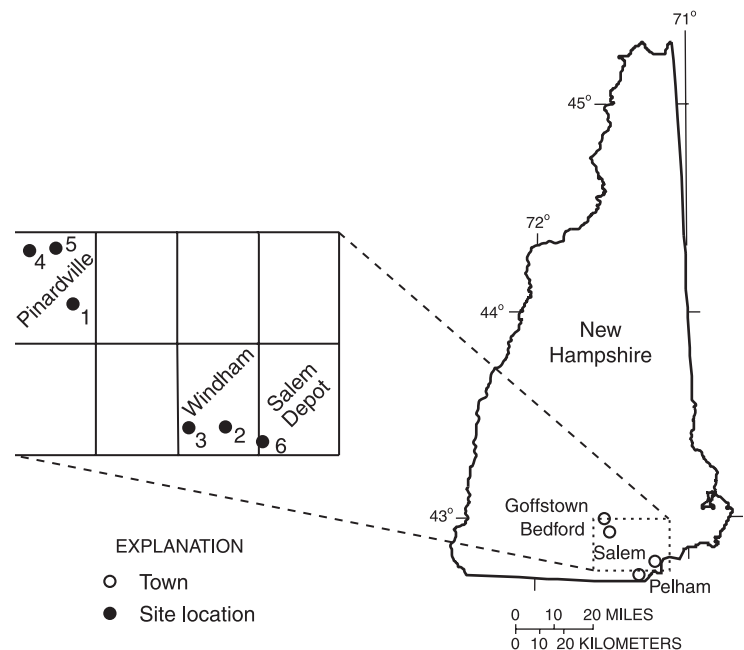


**Figure 1.** Location of the geophysical study area in the Pinardville, Windham, and Salem Depot 7.5-minute quadrangles in southern New Hampshire. Numbers on the quadrangles refer to sites.

one of which is one of the highest yielding bedrock wells in the State (greater than 560 gal/min). The trend of a lineament at this site (Ferguson and others, 1997) correlated with results of borehole geophysical log interpretations and results of aquifer tests (Mack and others, 1998).

## Site Selection

Geophysical investigation sites for this study were selected in or near two 7.5-minute quadrangles (Pinardville and Windham, N.H.) where detailed geology (including bedrock-outcrop fracture data) was mapped as a part of this project by Walsh and Clark (1998), and T.R. Armstrong and W.C. Burton (U.S. Geological Survey, written commun., 1999). These quadrangles are the first two quadrangles in New Hampshire mapped in detail by the USGS at the 1:24000 scale. Sites were selected within these quadrangles to provide a more complete geohydrologic setting for the geophysical investigations. Additional lineament data were identified and correlated with fractures in bedrock outcrops within the two quadrangles (R.B. Moore and others, U.S. Geological Survey, written commun., 2001). Lineaments are straight line features observed on the Earth's surface that may represent bedrock fracture zones (Clark and others, 1996). Wells within 500 ft of a lineament were chosen so these data could be included in site characterizations and interpretations. Sites with bedrock-well yields greater than 75 gal/min were selected to ensure the presence of high-yield fractured rock.

Sites were assessed for potential cultural noise and were avoided if the noise potential was high. A total of 17 sites initially were selected for reconnaissance investigations. Techniques that allowed for rapid data collection (ground-penetrating radar (GPR), electromagnetic terrain conductivity surveys (EM) and very-low-frequency electromagnetic surveys (VLF)) were used at the initial sites. Six of the 17 sites were selected for detailed investigation, representing a variety of geologic and physiographic settings, and are the subject of this report.

## Geohydrologic Settings

Physiographic settings for the study sites ranged from wetland valleys to mountainsides. Over the two-

quadrangle region, elevations of the sites ranged from 150 to 930 ft. The maximum relief between survey lines at a site is 80 ft (at site 4 on the side of a mountain). Two sites had little to no relief between survey lines; a flat field on the side of a hill at site 5 and a wet lowland setting at site 6 (fig. 1).

At all of the sites the crystalline bedrock was covered with unconsolidated materials, which are glacial and glacial fluvial in origin. Four of the sites were covered in till that ranged in thickness from inches to tens of feet. Till generally is an unsorted mixture of clay, silt, sand, pebbles, cobbles, and boulders. Stratified drift overlays bedrock at site 3 and site 6 (fig. 1). It is not known if till is present beneath stratified drift at these sites. Stratified drift at these sites ranged from inches to tens of feet thick. Generally, stratified drift is deposited in streams or quiet water bodies fed by meltwater flowing from glaciers and consists of sorted and layered unconsolidated material.

The bedrock geology of the Pinardville quadrangle includes a suite of metamorphosed intrusives, metamorphosed layered extrusives, and interlayered metasediments (T.R. Armstrong and W.C. Burton, U.S. Geological Survey, written commun., 1999). The rocks range in age from Permian to Late Proterozoic. Sites 1, 4, and 5 were in the Massabesic Gneiss and Rangely Formations. Rocks in the Massabesic Gneiss Complex are coarse grained and include well-foliated felsic and mafic gneiss and weakly foliated to well-layered migmatitic gneiss. Rocks of the Rangely Formation have a strong parallel bedding ductile fabric composed of well-layered pelitic metasediments.

Bedrock in the Windham quadrangle consists of Ordovician and Silurian metasedimentary rocks of the Merrimack Trough, with intrusive rocks as young as Mesozoic (Walsh and Clark, 1998). Sites 2, 3, and 6, in the Windham and neighboring Salem quadrangles are in the Berwick Formation, with site 2 on a contact between the Berwick Formation and the Ayer Granodiorite. The Berwick Formation is a biotite-plagioclase-quartz granofels schist with interbedded calc-silicate rocks and feldspathic quartzite. The Ayer Granodiorite is a Silurian-age intrusive rock. The Ayer Granodiorite is mapped as two phases at site 2, one phase being porphyritic granite to granodiorite, and a second phase of granodiorite (Walsh and Clark, 1999).

Brittle (fracture) geologic data from Walsh and Clark (1999) and T.R. Armstrong and W.C. Burton (U.S. Geological Survey, written commun., 1999) were analyzed on a site-by-site basis to define fracture families. All measurements within a 4,000-ft radius of each study site with a dip greater than 45° were compiled from a geographic information system (GIS) database. Fracture families were defined for each site by plotting azimuth-frequency (rose) diagrams in the Structural Data Integrated System Analyzer (DAISY 2.19) by Salvini (2000). The DAISY software uses a Gaussian curve-fitting routine for determining peaks in directional data (Salvini and others, 1999). Peak orientations, error ranges, and normalized fracture peak heights were compiled for site characterization and comparison with geophysical data. The error range indicates the range of trends associated with the peak. The normalized fracture-peak height indicates how large the peak is, in percent, in relation to the largest (100 percent) peak at a site.

Hundreds of remotely sensed lineaments are present in the study area (Clark and others, 1997; Ferguson and others, 1997). The lineament data used in the analysis for this study were observed based on the methods of Clark and others (1996). Lineaments associated with the sites were observed from the following observation platforms: side looking airborne radar (SLAR), satellite photography (Landsat), low-altitude black and white aerial photography (LOWALT), high-altitude black and white aerial photography (HIGHALT), color infrared aerial photography (CIR), and 1:24,000-scale topographic map (TOPO). Several of the remotely sensed lineaments at the sites have been correlated with physiographic features seen in the field at ground level. Many lineaments were correlated with fractures measured in outcrop; these lineaments are noted in this report when observed at the study sites. Domain-analysis and 1,000-ft buffer analysis fracture-correlation techniques and the full data set are described by (R.B. Moore and others, U.S. Geological Survey, written commun., 2001), a companion report for this project.

High-yield wells at the study sites are used for irrigation, and domestic and public water supply. The reported water yield from the wells ranged from 75 to 630 gal/min. The depth of the wells ranged from 150 to 500 ft. The maximum depth to bedrock was estimated at 22 ft from drilling logs (casing length

minus 12 ft). Water-table depth in the bedrock ranged from at the surface (0 ft) to 64 ft deep.

Well-yield probabilities, throughout the Pinardville and Windham quadrangles, were estimated by (R.B. Moore and others, U.S. Geological Survey, written commun., 2001) for a grid of cells, 98.4 x 98.4 ft per cell. Probabilities of obtaining at least 40 gal/min were estimated for theoretical wells drilled 400 ft deep. These estimates were based on a large database of actual bedrock well yields of wells with varying depths and site characteristics. Well-site characteristics were derived from Statewide databases and quadrangle-scale topographic, geologic, and lineament maps. Probabilities at the geophysical sites ranged from 5 to 38 percent. Locations of the high-yield wells at the geophysical sites had probabilities ranging from 12 to 38 percent based on the well-site characteristics.

## Acknowledgments

The authors thank the State, Federal, and municipal officials, residents, and well contractors that provided data for this study. Appreciation is expressed to the members of the Geophysical Advisory Committee for providing insight and guidance for the study plans. Members of the Geophysical Advisory Committee include Richard Chormann, James Vernon, Joseph Ingari, Garrick Marcoux, John Jemzeck, and John Brooks. Dr. James H. Vernon provided data examples from surveys at a site just north of the Windham quadrangle. Surface geophysical surveys and analysis by George Willard contributed significantly to this study. Special thanks are extended to the private and corporate landowners and managers who volunteered access to their land and wells making this study possible.

## APPROACH AND METHODS

Surface geophysical survey methods are useful in water-resource investigations of surficial aquifers (Haeni, 1995). Some of these methods can be applied to fractured-bedrock settings. For this study, surface geophysical techniques were selected that can yield interpretable anomalies if fracture zones are present, and can be detected on the basis of background geologic and cultural conditions. Borehole-

geophysical techniques were selected to provide the location and orientation of bedrock fractures at depth for comparison with the results of surface-geophysical surveys. Processed and interpreted geophysical data were compared to geologic outcrop and remotely sensed data.

Many geophysical-survey methods take advantage of the electrical anomaly associated with the large electrical contrast between fractures and the host rock. In general, the electrical conductivity of crystalline bedrock (such as granites, gneiss, and shists) in the State is low relative to other subsurface materials, and a fluid-filled fracture zone is more electrically conductive than the host rock. This electrical contrast creates a dielectric permittivity contrast (Beres and Haeni, 1991), for example, that makes it possible to image fluid-filled fractures with ground-penetrating radar. Sufficiently large fracture zones may have a slower average seismic velocity than competent rock; therefore, average bedrock seismic velocity can be high parallel to the dominant fracture strike. Low magnetic anomalies can indicate weathered fracture zones, which lowers the presence of magnetic minerals in the host rock.

Many other factors can cause geophysical anomalies and must be considered when interpreting fracture zones. Bedrock foliation, geologic contacts, or intrusions may produce electric or magnetic contrasts or anomalies depending on mineral constituents of the rocks. Bedrock and overburden type, ground-water saturation, ground-water chemistry, bedrock and surface topography, cultural, and atmospheric conditions all may have an effect on geophysical data. Variations in electrical properties result from different rock and overburden materials, pore-water chemistry, porosity, and degree of saturation of bedrock or overburden.

Up to seven surface-geophysical survey methods were used to characterize the subsurface at the sites—Primary wave (P-wave) seismic refraction, ground-penetrating radar, magnetics, very-low-frequency electromagnetics, inductive electromagnetic terrain conductivity, two-dimensional direct-current electrical resistivity, and azimuthal square-array electrical resistivity. Technique application was limited on the basis of the natural and cultural conditions at each site. Borehole-geophysical logs also were collected at three sites and included caliper, fluid temperature and resistivity, electromagnetic induction, natural-gamma radiation, and optical televiewer. The following sections describe the surface and borehole surveys.

## **P-Wave Seismic Refraction**

Seismic refraction uses refracted seismic waves to characterize the acoustic or seismic-velocity distribution of layered earth materials. A compression or primary (P) wave is generated at the Earth's surface, travels into the earth and is refracted and reflected back to the surface. The resulting waves are recorded by geophones. Only layers increasing in seismic velocity with depth can be accurately detected with seismic refraction. Thin, intermediate velocity layers are not detectable. A thorough description of theory and interpretation of seismic refraction data is given by Haeni (1988).

Variations in average bedrock seismic velocity were examined between survey lines with different orientations at the sites. Variations in bedrock seismic velocity can be attributed to vertical and sub-vertical fracture zones in which maximum velocity, the average of a line, is along the strike of these fracture zones (Hansen and Lane, 1995). Seismic surveys also were used to search for depressions in the bedrock surface, which might be indicative of a weathered fracture zone.

Seismic-refraction surveys were done at three of the sites primarily to identify seismic-velocity variations, but also to survey the depth to the water table and the depth to bedrock. Nine survey lines were collected at five locations using a geophone spacing of 10 ft. Four of the locations contained two orthogonal lines sharing a common center point. One line was oriented normal and one parallel to the suspected strike of a fracture zone on the basis of previously collected geophysical data. First arrivals of P-waves from 5 shot points on each survey line were recorded using a 24-channel signal enhancement seismograph. A sledgehammer and a metal plate were used to produce the seismic waves. The relative locations and elevation of each geophone and shot point were surveyed for data analysis.

Seismic data were processed using a computer program developed by Scott (1971) that uses time delay and ray-tracing methods. Where possible, identification of the water-table surface and underlying bedrock topography was made during processing to help interpret information gained from other techniques. Variations in seismic velocities and bedrock surface topography were compared with other geophysical data.

## Ground-Penetrating Radar

Ground-penetrating-radar (GPR) surveys done with a transmitting and receiving antenna were used to image the depth to bedrock and fracture zones. The antenna generates and detects electromagnetic (EM) waves at a 300 MHz frequency. The radar-wave propagation is affected by differences in electromagnetic properties of the medium. These properties include dielectric permittivity, electrical conductivity, and magnetic susceptibility (Beres and Haeni, 1991), which are affected by water content, overburden type, and lithology. Features identified in this study are bedrock-overburden interfaces and sub-horizontal bedrock fractures. Hansen and Lane (1995) used GPR to identify bedrock-fracture zones and overburden interfaces. The utility of GPR is limited at sites with electrically conductive clay-rich overburden (such as till) because the EM wave can be attenuated before it reaches bedrock (Ayotte and Dorgan, 1995; Ayotte and others, 1999). Where conditions are conducive to successful data collection, GPR provides a rapid means of providing detailed insight into subsurface conditions.

GPR survey design and resulting data presentation for this study differed at each site. Where the land surface was flat and open, the surveys were done in a continuous data-collection mode. Continuous data collection requires that the antenna be pulled at a constant speed while radar pulses are transmitted into the earth. A point-survey mode was used at sites that were heavily wooded or had rugged terrain. During a point survey, the antenna is placed at regular intervals along a line. A 5-ft data-collection interval was used for all point surveys. Repeated measurements at each point are stacked to filter out noise. Continuous and point profiles were adjusted for topographic relief. The results of the GPR surveys for two lines where anomalies indicate features in bedrock are presented in this report. Other GPR surveys are not included.

## Magnetics

Magnetometer surveys measure slight variations in the Earth's total magnetic field. Changes in the magnetic field can result from varying types and amounts of magnetic minerals present in the bedrock. Magnetic anomalies also can differ as a result of the sensor and bedrock separation caused by variations in overburden thickness. Magnetic anomalies related to

fracture zones could be low if the magnetic minerals of the host rock have been weathered. Magnetic lows were associated with fracture zones in an investigation by Frohlich (1989) of crystalline rocks across New England.

Total field surveys for each line were measured with a proton magnetometer at a measurement interval of 10 ft. Surveys done for this study were completed in less than an hour; therefore, diurnal corrections were not made. Results are reported in nanoteslas (nT) subtracting the regional base of roughly 54,000 nT.

## Very-Low-Frequency Electromagnetics

Very-low-frequency electromagnetic surveys (VLF) use very-low-frequency radio (3-30kHz) waves generated by distant transmitters. Measurements of a tilt-angle of the long axis of the primary magnetic field ellipse are made, which are affected by secondary magnetic fields. The secondary fields are a product of electrical galvanic currents induced in conductive media in the Earth from the primary magnetic field. This study used the VLF transmitter in Cutler, Me., that broadcasts at a frequency of 24 kHz at 1,000 kilowatts power. This transmitter provided a consistent and strong signal. Alternate transmitters in Jim Creek, Wa., and Aguada, P.R., were assessed but the signal strength was too weak for use here.

The tilt-angle mode of operation was used to detect conductive features in the bedrock. Measurements were taken every 10 ft along a line. Fracture zones that are fluid filled can produce high electrical conductivity anomalies. VLF surveys are best for detecting conductive anomalies when the feature is linear or elongated and oriented less than a 45° angle from the measurement point to the transmitter. The response of the tilt-angle percent when passing over a conductive feature is a high reading followed by a low reading. The inflection point between the high and low anomalies indicates the location of the feature (Iris Instruments, 1993). The width of the anomaly from peak to trough is proportional to one half of the depth to the top of the feature (Wright, 1994). Surface topography can cause subtle changes in the tilt-angle and must be considered. Ionospheric activity can affect VLF signal strength. VLF was used previously, in conjunction with other techniques, to identify fracture zones at a site in the Mirror Lake area, Grafton County, New Hampshire (Powers, Singha, and Haeni, 1999).

## Inductive Electromagnetic Terrain Conductivity

Inductive electromagnetic terrain conductivity (EM) surveys responded to induced electromagnetic signals to measure the electrical conductivity of subsurface media. A portable transmitter and receiver kept at a fixed distance (coil spacing) were used for EM surveys from point to point along a survey line. The transmitter emits an electromagnetic field by energizing a coil of wire with alternating current (AC). The resulting magnetic field (primary) induces an electrical current in the ground. A secondary magnetic field, caused by the induced current, is measured as a voltage difference from the primary field signal in the receiving coil. This induced voltage is proportional to the apparent conductivity of the Earth. The apparent conductivity measured is that of a hemisphere of all Earth materials between the coils where the effective measurement point is the mid-point between the coils.

The vertical dipole survey mode (VD) was used primarily in this study because it is better at detecting vertical conductive features and has a deeper range of sensitivity than the horizontal dipole survey mode. In the VD mode, the plane of the coils is held horizontally, with the axis of the coils oriented vertically. The VD survey is optimized to be most sensitive at depths of 0.4 times the coil spacing, and measures within a depth range of 0.1 to 1.5 times the coil spacing (McNeil, 1980). The modeled response of a vertically conductive feature detected with a VD survey, consists of a below background (sometimes negative) apparent conductivity measurement centered over a feature positioned between two above-average apparent conductivity measurement peaks. The distance between the inner limbs of the conductivity peaks must be equal to the coil spacing to be able to identify a vertical conductor (McNeil, 1980). The relative height of the above-average measurement peaks to each other can indicate the dip direction of the feature. The dip of a planar conductive feature is towards the higher conductivity peak.

The horizontal dipole (HD) mode is used to obtain a measurement of the near-surface conductivity. In the HD mode, the plane of the coils is held vertically, with the axis of the coils oriented horizontally in the plane of the survey line. The HD is more sensitive to electrical properties close to the surface; a measurement depth range extending to 0.75 times the coil spacing. HD measurements were used to provide

a qualitative indication of relative changes in overburden thickness, assuming the overburden is more electrically conductive than the underlying bedrock. Since bedrock generally is much more electrically resistive, a HD high can represent a thickening of the overburden, or a filled bedrock trough. This technique was used by Taylor and others (1999) to indicate depressions in a bedrock surface.

EM measurements were made using a 20-m coil spacing at most of the sites for this study. At sites where electromagnetic noise was a problem, a 10-m coil spacing was used. VD measurements were made every 10 ft and HD measurements were made every 20 ft along a survey line.

## Two-Dimensional Direct-Current Resistivity

Two-dimensional direct current (dc) resistivity surveys, termed 2-D resistivity, measure the electrical resistivity of the subsurface. Direct current is induced in the ground by two current electrodes and the voltage is measured at two potential electrodes. A resistance value is obtained by dividing the measured voltage by the induced current. The apparent resistivity is calculated from the resistance value and geometric factors that are different for each array type (arrangement of current and potential electrodes in relation to each other) and takes into account the electrode spacing. Dipole-dipole and Schlumberger array (Zohdy and others, 1974) survey configurations were used. A combination of 28 electrodes and addressable switches were used at a time to collect resistivity measurements. When needed, electrodes were moved from one end of the line to the other end to collect additional measurements. The relative elevation of the land surface at each electrode was surveyed and accounted for in processing of the data.

The apparent resistivity values collected in the field were inverted. Results are adjusted, during the processing, for topographic relief along a survey line. Field and model data sets were processed using RES2DINV version 3.42 (Loke, 1997) to produce inverted resistivity sections from the apparent resistivity data. Inversion gives a more realistic resistivity value projected to a relative elevation.

Model cross sections of the subsurface resistivity distribution were created and data collection was simulated using RES2DMOD version 2.2

(Loke, 1999). The input model cross sections were created on the basis of the known geology and the results and interpretations of the inverted field data. Synthetic apparent-resistivity data were calculated from the model cross-sections and inverted for comparison to the inverted field data. A model solution is reached after numerous iterations, each with a modified model, when the inverted resistivity section from the field data and inverted synthetic resistivity section from the model data approximately match. The model solutions are not unique but, with inclusion of known information to the model, such as depth to water table or depth to bedrock, the solutions represent a likely interpretation.

### **Azimuthal-Square Array Direct-Current Resistivity**

Azimuthal square-array dc-resistivity surveys, termed square-array resistivity, measure the subsurface resistivity in various orientations and allow for the determination of the strike of a conductive anomaly with depth (Habberjam and Watkins, 1967). To determine the strike of near-vertical conductive anomalies in the bedrock, a horizontal-layered overburden must be assumed. This technique cannot correct for bedrock or surface topography; therefore, surveys (arrays) were collected at areas without these conditions

Electrodes are set in square arrays, direct current is produced in the ground by two current electrodes on one side of the square and a potential difference is measured at two electrodes on the other side. The length of the side of the square is termed the A-spacing. From these four electrodes, apparent resistivity is calculated from electrode spacing and a geometric factor. For each square, the current and potential electrode connections are switched 90° to measure resistivity in another orientation using the same electrode locations. Making a measurement by placing the current and potential electrode connections diagonally on the square facilitates an error check.

Resistivity represents an average resistance of subsurface materials between the electrodes. The mid-point of resistivity can be projected to a specified depth and compass direction on the basis of the side length of the square, defined by A-spacing and the array orientation. The effective survey depth is approximately equal to the A-spacing. For each

survey, data were collected with array “squares” oriented 15° apart and with a number of different A-spacings. The size of the survey and effective depth of penetration depended on the amount of unobstructed terrain available. After preliminary evaluations of 2-D resistivity data, square array locations were chosen.

Graphical interpretations of the data were made by plotting the resistivity with radial orientation. Resistivity data were collected and interpreted according to the techniques described by Lane and others (1995). Primary conductive strikes are orthogonal to the resistivity maximum. Secondary conductive strikes are orthogonal to the second largest resistivity measurements. If a range of high resistivity measurements is observed, then a conductive range is orthogonal to the range of measurement orientations.

### **Borehole Geophysical Surveys**

Six borehole geophysical logs were collected including caliper (hole diameter), fluid temperature, fluid resistivity, electromagnetic induction, natural-gamma radiation, and optical televiewer. The first five logs can help identify water-bearing fractured zones, whereas the optical televiewer provides the fracture orientation. Borehole geophysical logs were interpreted together to characterize borehole fractures.

The caliper log was used to generate a continuous profile of the borehole diameter. This log shows the mechanically measured diameter of the borehole as a spring-loaded, three-arm caliper tool is pulled up the well. The arms open as they pass borehole enlargements. Increases in the borehole diameter generally are related to fractures, but also can be caused by changes in lithology or well construction. The profile indicates the roughness of the borehole wall. Some enlargements were larger than the caliper diameter (18 in.).

The electromagnetic induction (EM) log provides a profile of the electrical conductivity of the rocks and fluid in the materials surrounding the borehole. The conductivity changes measured by the EM log are caused by variations in the electrical conductance of the fluids in the formation, alteration of minerals, and increases in porosity and borehole enlargements. The log can be used to delineate changes in lithology and electrical properties of water in the formation. In crystalline rock in

New Hampshire, increases in conductivity were associated with fractured zones (Mack and others, 1998), primarily the result of increased water content in the fractures.

The fluid-temperature log displays a continuous measurement of fluid temperature in the borehole. In the absence of ground-water flow, the temperature gradually increases with the geothermal gradient, which is  $0.6^{\circ}\text{C}$  per 100 ft of depth (Keyes, 1988). A continuous plot of the fluid temperature with depth is used to identify zones that deviate from the expected geothermal gradient. Deviations from the gradient indicate locations where ground water enters or exits the borehole.

The fluid-resistivity log records the electrical resistance of the fluid in the borehole. Changes in the electrical resistance of the water in the borehole indicate differences in the total dissolved solid concentrations in borehole water. These differences typically indicate sources of water that have contrasting chemistry and have come from alternate water-bearing zones. Similar to the fluid-temperature profile, fluid-resistivity deviations from a straight-line gradient indicate locations where ground water enters or exits the borehole.

The natural gamma log measures the natural-gamma radioactivity of the formation surrounding the borehole. Gamma radiation is a natural product of the radioactive decay of potassium-40, and a daughter product of uranium and thorium decay. The gamma log used in this investigation does not differentiate between the sources of the gamma radiation. The gamma log is a count of total gamma-radiation emissions, which may be correlated with the rock type or with fracture infillings. Potassium-40 is abundant in potassium feldspar (microcline and orthoclase), which alters to sericite and clay. In the alteration process, potassium-40 is concentrated in the clay by processes of adsorption and ion exchange. Deviations in the gamma log trace indicate changes in the rock type or the presence of mineralized fractures. Clay minerals, which sometimes form in the fractures, generally have an elevated concentration of potassium-40 minerals from areas away from the fractures and cause an increase in the gamma values.

An optical televiewer (OTV) log was used to map the location and orientation of fractures that intersect a well. The OTV log collects oriented digital pictures of the borehole wall in  $360^{\circ}$  concurrently with borehole deviation. The product is a high-resolution,

digital picture of the borehole wall that can be used to determine the location and orientation (strike and dip) of fractures, lithologic contacts, or other borehole features. Boreholes drilled into crystalline rock frequently deviate from vertical because of variations in rock properties, the fabric of the bedrock, fracturing, or as a result of the drilling process or technique. Deviation is measured by a magnetometer and inclinometer, and is recorded as an azimuthal direction ( $0\text{-}360^{\circ}$  from magnetic north) and the inclination of the borehole ( $0\text{-}90^{\circ}$  from vertical) with depth. Measurements of borehole deviation are used to correct the apparent strike and dip of a feature in a deviated borehole to its true orientation.

Results of the OTV log for a borehole can be summarized in a fracture stereogram for comparison with surface or remote analyses. The stereogram, a lower-hemisphere, equal-area projection of poles to planes, was used to plot the orientation of fractures and contacts and foliation. Fractures include transmissive fractures, open fractures, contact fractures and cracks. A stereogram reduces each features plane to a point that represents the intersection of a pole, perpendicular to a features plane, with a lower hemisphere. For example, a horizontal fracture would be indicated by a point in the center of the stereogram, whereas a fracture striking  $215^{\circ}$  with a dip of  $89^{\circ}$  W would be indicated by a point towards the right (eastern) edge of the outer circle. The orientation of the fracture plane is reported as  $215^{\circ}, 89^{\circ}$ , which in the right-hand-rule format implies that a fracture that dips west ( $89^{\circ}$  dip, to the right of the  $215^{\circ}$  bearing).

## **ANALYSIS AND RESULTS OF GEOPHYSICAL INVESTIGATIONS OF WELL FIELDS**

Six sites in southern New Hampshire were selected for geophysical surveying. Detailed site maps and graphics of the data are used to describe survey results. Surface-geophysical surveys were done along survey lines, and around array centers at each of the six sites. The results are in terms of distance along each line or a trend for an array. Trends are reported in terms of azimuth degrees from true north. Borehole geophysical logs were collected at selected sites where wells were accessible (no pumps were installed), and (or) permission was obtained to remove water-supply pumps. Borehole-geophysical logs provide actual

fracture measurements for confirmation or comparison with analyses of surface and remotely sensed surveys.

Numerous anomalies were detected in the survey lines and arrays by various methods. Locations on the survey lines displaying anomalies from multiple methods, or strong anomalies, likely are related to actual features in the bedrock. Multiple geophysical methods, and geologic and remotely sensed data, were used to locate and characterize subsurface features to provide indication of bedrock-fracture zones. Square-array resistivity results, geologic data, and lineament locations and orientations provided information to determine the strike of likely fracture zones.

### Site 1, Bedford, New Hampshire

Site 1 on State Route 101 in Bedford, N.H., is a wooded hillside at an elevation of about 360 to 400 ft in the area of the surveys. T.R. Armstrong and W.C. Burton (U.S. Geological Survey, written commun., 1999), mapped the bedrock geology of this area as two variations of the Massabesic Gneiss Complex, specifically a migmatite gneiss and a layered paragneiss and orthogneiss (fig. 2). The bedrock is exposed at the surface on the west end of line 1 and in the central part of the site. The overburden is mapped as a till, which is unsorted to poorly sorted clay silt, sand, pebbles, cobbles and boulders with some gravel (Koteff, 1970). Mapped lineaments at the site were observed from SLAR, Landsat (Clark and others, 1997), and TOPO platforms trending 18°, 33°, and 22° (fig. 2). The SLAR and Landsat lineaments were fracture correlated using the 1,000-ft buffer analysis technique (R.B. Moore and others, U.S. Geological Survey, written commun., 2001). Fracture data within a 4,000-ft radius of the site have three peak orientations: 27°±7° (100 percent, normalized height), 295°±10° (25 percent, normalized height), and 301°±11° (23 percent, normalized height). Fractures in an outcrop between line 1 and line 2 have a strike and dip of 20° and 82°. Lineaments are visible at the site as swales at line 1 trending 5° and 20°.

Drilled to a depth of 485 ft, through approximately 24 ft of overburden, well BIW 889 (fig. 2) has a reported yield of 150 gal/min and a static water level depth of 30 ft. The drillers' log indicates that the high-yielding water-bearing zone is between 420 and 485 ft deep. Probabilities of exceeding a yield of 40 gal/min from a 400-ft deep well at this site ranged from 5 to

29 percent. A 14-percent probability is calculated for the 98.4-ft (30-m) square cell that well BIW 889 is located in (R.B. Moore and others, U.S. Geological Survey, written commun., 2001). Variations in probability at the site appear to reflect lithologic contacts, topography, and lineaments.

Three geophysical survey lines were selected to bisect lineament locations on either side of the well. Line 1 is in the woods to the south of the well, just east of State Route 101 and extending for 480 ft to the east. Line 2 is 900 ft long and begins in an open field east of State Route 101, crosses through a wooded area and into another open field to the north of the well. Two array center locations were placed on line 2 at locations where geophysical anomalies were detected along the survey line. Array 1 was centered at 660 ft along line 2. Array 2 was centered at 450 ft along line 2 (fig. 2).

### Geophysical Surveys and Interpretation

Seven geophysical methods were used to characterize site 1. Overburden thickness or physical properties were derived from the (P)-Wave Seismic-Refraction, GPR, EM, and 2-D resistivity survey results (figs. 3-7). Bedrock characteristics and anomalies that could be caused by bedrock fractures are observed in the seismic-refraction, GPR, magnetometer, VLF, EM, 2-D resistivity, and square-array resistivity-survey results.

Seismic-refraction (P)-wave data were collected along line 2 between 335 and 565 ft. The line was interpreted based on a three-layer model: unsaturated till, saturated till, and bedrock. The bedrock surface ranges from 15-40 ft below the ground surface, depending on the velocity chosen for the saturated till. The water table is about 8 ft below the ground surface. Three troughs are indicated in the bedrock surface. The deepest troughs are centered at 375 and 425 ft, with 10-20 ft of relief in the bedrock surface. A minor trough is centered at 525 ft with 5-10 ft of relief. Bedrock seismic velocity normal to the lineament was calculated to be approximately 8,000 ft/s. This velocity is significantly lower than bedrock velocities (10,000 to 20,000 ft/s) typically seen in New Hampshire (Medalie and Moore, 1995).

Ground-penetrating radar (GPR) data were collected along the entire lengths of line 1 and line 2 (fig. 2). The GPR profile of line 1 indicates subhorizontal reflectors at about 10-20 ft below the interpreted bedrock surface. These reflectors likely

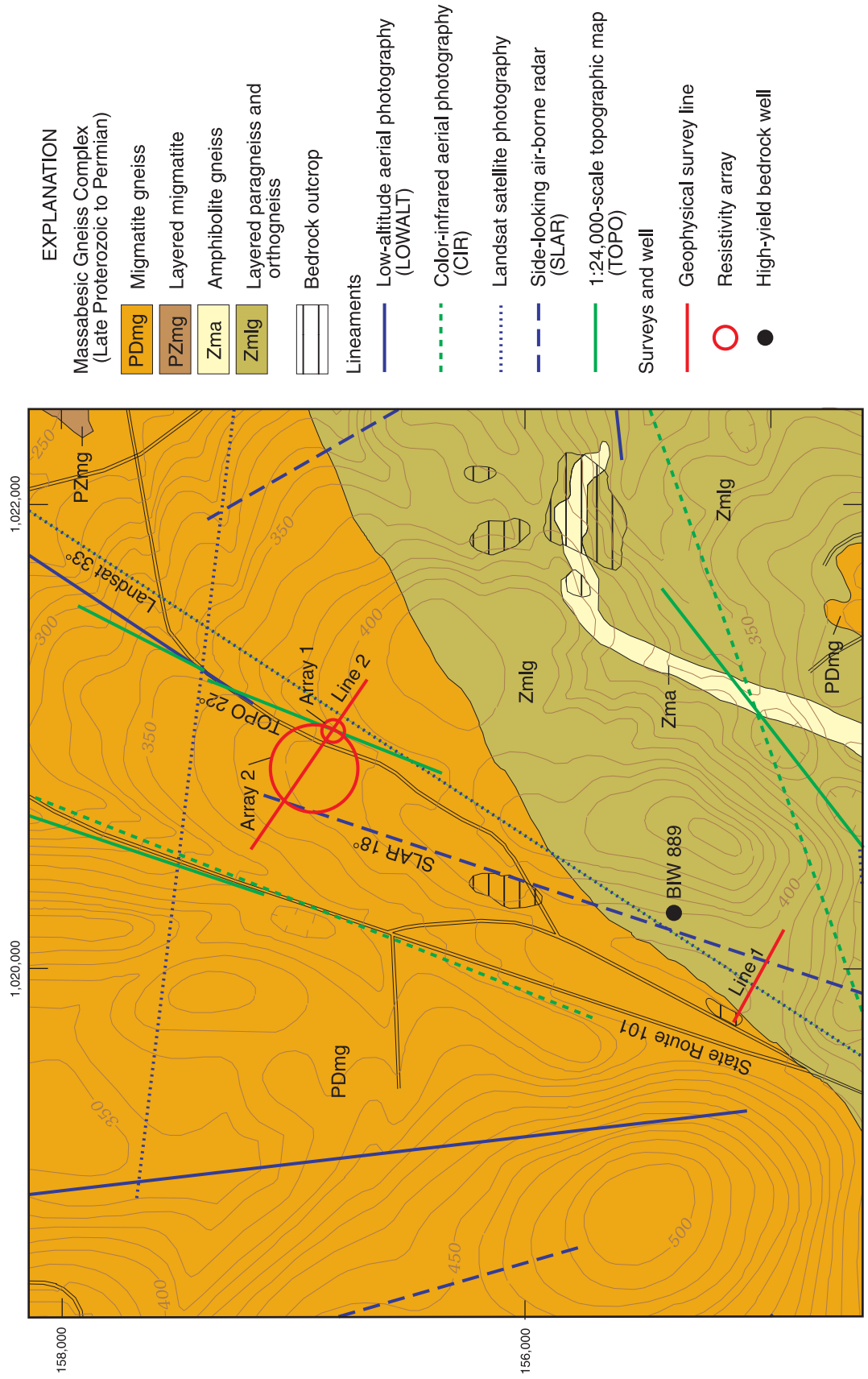


**Figure 2.** Geophysical survey locations, bedrock geology, and lineaments at site 1, Bedford, N.H. Site location is shown on figure 1.

## SITE 1, LINE 1

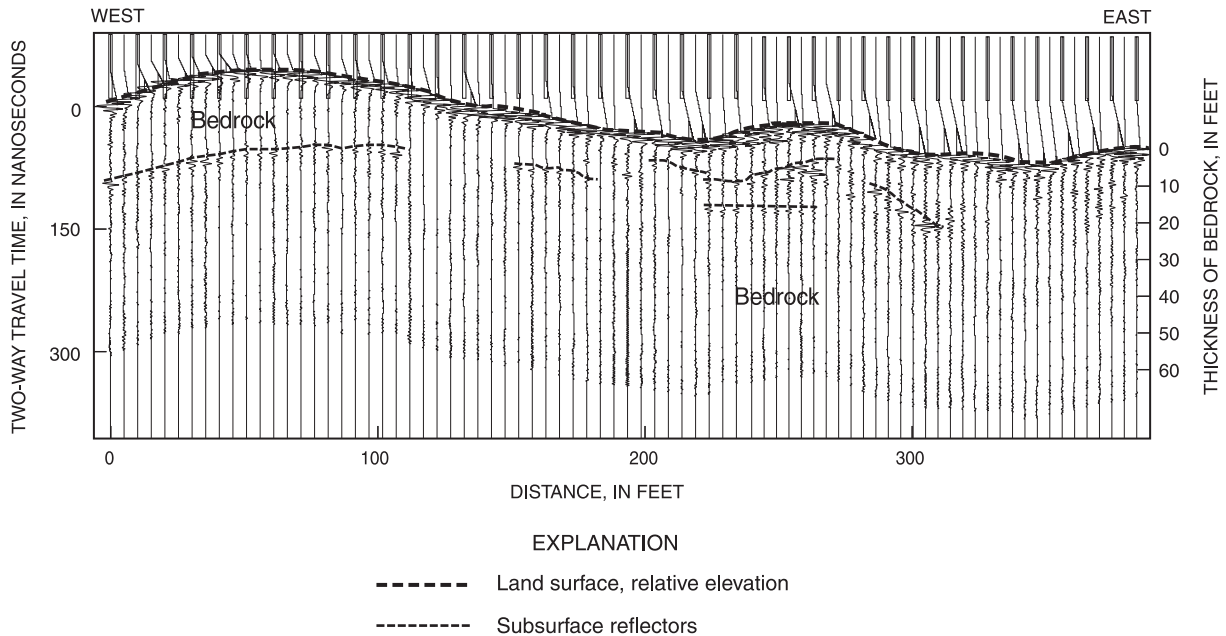


**Figure 3.** Processed ground-penetrating radar profile at site 1 from line 1, Bedford, N.H. Site and line locations are shown on figures 1 and 2, respectively.

are sheeting fractures (fig. 3). The GPR profile along line 2 indicates a reflector at approximately 10 ft deep from 600 to 900 ft, which is likely the water table in the overburden above bedrock.

Magnetometer measurements were made along line 1 and line 2 (figs. 4 and 5). The average magnetic field measurement (after subtracting the regional trend of 54,000 nT) at this site during the surveys is about 500 nT. Results at line 1 indicate an anomalous magnetic low of 445 nT between 270 and 310 ft; a magnetic low of 470 nT occurs at about 410 ft (fig. 4a). The survey results at line 2 (fig. 5a) indicate a low of 480 nT between 0 and 200 ft. The total field increases to a high of 575 nT at 455 ft. Results at line 2 indicate a low of 525 nT between 640 and 690 ft, and a low of 515 nT at 845 ft (fig. 5a).

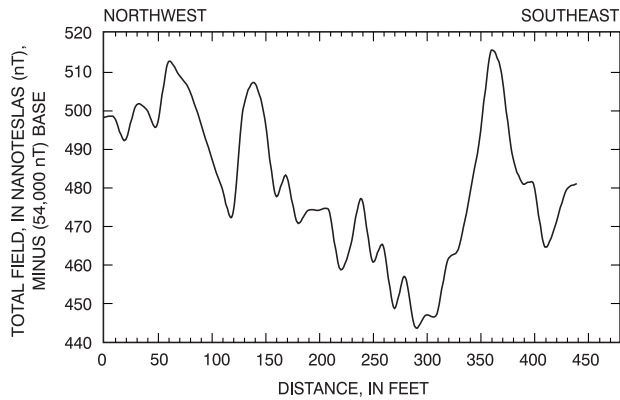
VLF tilt-angle surveys at line 1 and line 2 indicate anomalies. Overhead power lines nearby affected results along approximately the first 100 ft of line 1. Line 1 had inflection points at 110, 195, 240, and 310 ft (fig. 4b). Inflections were detected at line 2 at 130, 300, 375, 530, 640, 800, and 880 ft; overlapping anomalies are observed between 300 and 375 ft (fig. 5b).

EM surveys were collected on line 1 and line 2 at site 1. Nearby power lines caused signal noise. To avoid this noise, the survey coil spacing was shortened from 20 (65.6 ft) to 10 m (32.8 ft). Anomalies that likely are associated with vertical conductors were observed on line 1 at 200, 290, 360, and 440 ft (fig. 4c). Similar anomalies on line 2 are at 85 ft and 170 ft (fig. 5c). A combination of deepening overburden interpreted from the HD and potential vertical conductors are noted at 440 ft and 610 ft (fig. 5c).

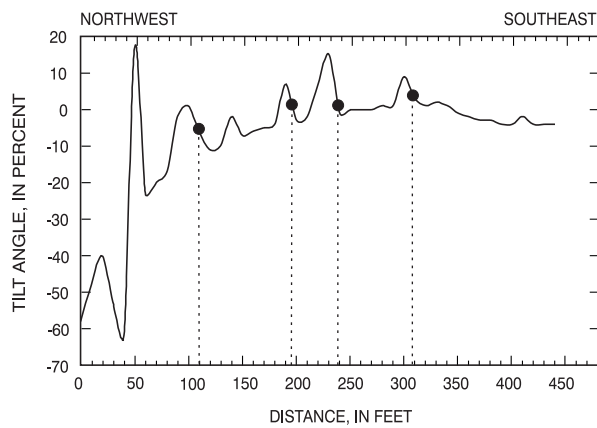
2-D resistivity surveys were collected at line 1 and line 2. Models were created to check interpretations for both lines. Line 1 survey interpretations indicate conductive anomalies in resistive bedrock that could be a result of near-horizontal sheeting fractures. A vertical conductive anomaly also is found on line 1 at 355 ft (fig. 6). Four major resistivity units from line 2 likely represent an unsaturated, and conductive-saturated overburden, and resistive-competent and conductive-saturated bedrock (fig. 7). Survey results indicate that near horizontal fractures in the bedrock could be present at the southeastern end of line 2. Near vertical, and dipping, conductive anomalies are indicated at 55-95 ft (not modeled), 460-500 ft, and 630-660 ft (fig. 7).

**SITE 1, LINE 1**

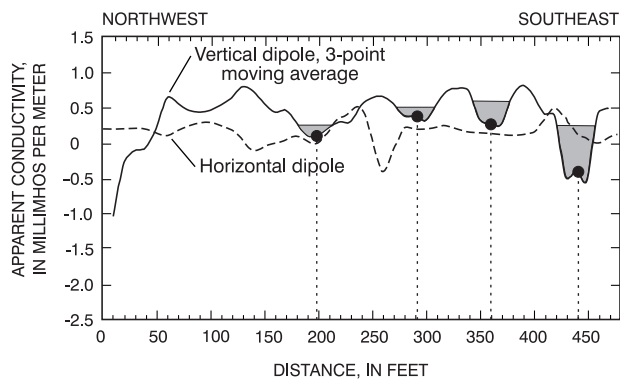
(A) Magnetometer survey--total field



(B) Very low frequency electromagnetic survey--tilt angle



(C) Electromagnetic (EM) terrain conductivity survey

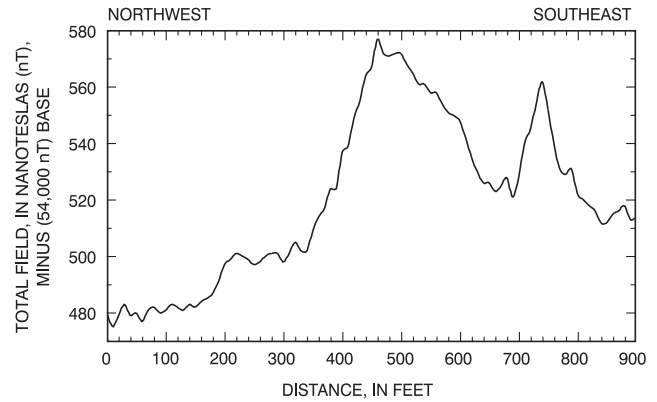


**EXPLANATION**  
 ■ Width of anomaly (10 meters)  
 ● Point of anomaly

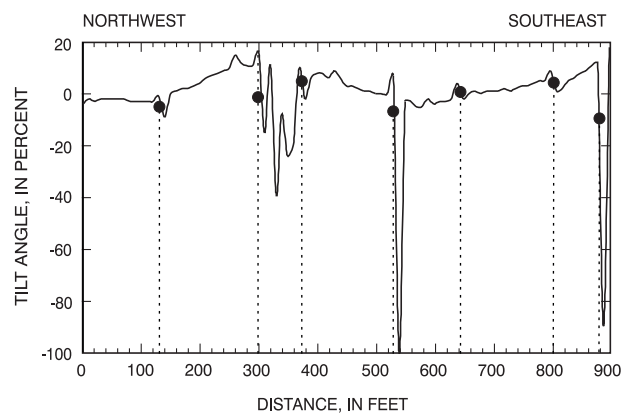
**Figure 4.** Magnetic and electromagnetic surveys at site 1 from line 1, Bedford, N.H. (A) magnetometer survey; (B) very low frequency (VLF) electromagnetic survey; (C) electromagnetic (EM) terrain conductivity survey with a 10-meter (32.8-foot) coil spacing. Site and line locations are shown on figures 1 and 2, respectively.

**SITE 1, LINE 2**

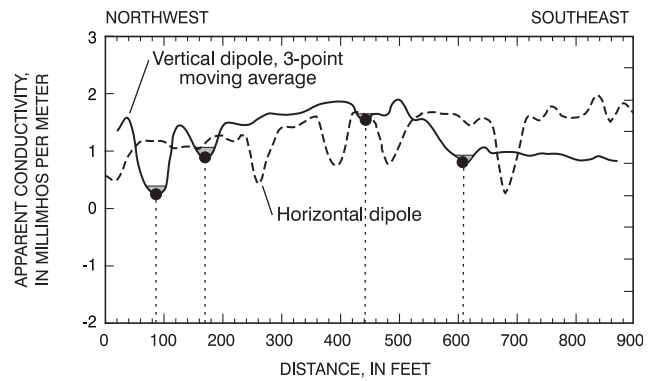
(A) Magnetometer survey--total field



(B) Very low frequency electromagnetic survey--tilt angle



(C) Electromagnetic (EM) terrain conductivity survey

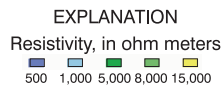
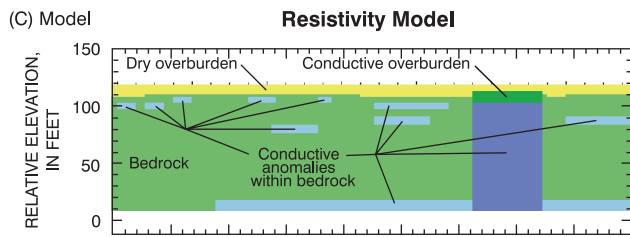
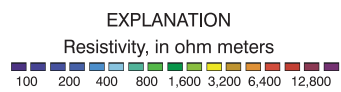
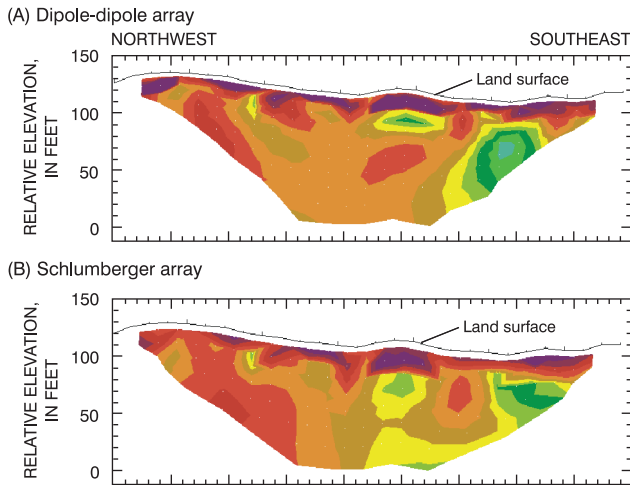


**EXPLANATION**  
 ■ Width of anomaly (10 meters)  
 ● Point of anomaly

**Figure 5.** Magnetic and electromagnetic surveys at site 1 from line 2, Bedford, N.H. (A) magnetometer survey; (B) very low frequency (VLF) electromagnetic survey; (C) electromagnetic (EM) terrain conductivity survey with a 10-meter (32.8-foot) coil spacing. Site and line locations are shown on figures 1 and 2, respectively.

**SITE 1, LINE 1**

**Inverted Resistivity Sections**



**Synthetic Inverted Resistivity Sections**

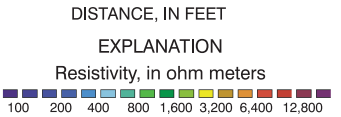
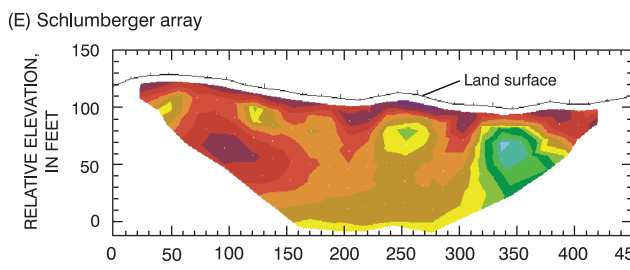
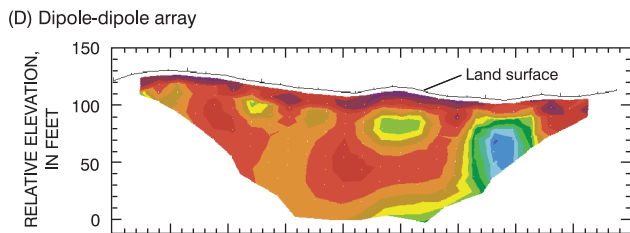


**Figure 6.** Cross sections showing (A and B) inverted resistivity sections of two-dimensional, direct-current resistivity data at site 1 from line 1, Bedford, N.H.; (C) model based on field data from A and B; and (D and E) synthetic resistivity output data from Model C. Site and line locations are shown on figures 1 and 2, respectively.

Square-array resistivity data were collected at two arrays centered on line 2. At the largest A-spacing of 10 m, array 1 (fig. 8a) shows a prominent primary and secondary conductive strike of 15° and 60°. At the largest A-spacing of 40 m, array 2 (fig. 8b) indicates a weak primary conductive strike of 345°. Measurements from array 2 show a decrease in the average resistivity from the 5-m A-spacing to the 10-m A-spacing, and an increase in resistivity from 10- through 40-m A-spacing. This sounding (fig. 8b) indicates three layers, resistive at the surface (unsaturated overburden), a conductive layer (saturated overburden), and a resistive lower layer (bedrock).

**Integration of Results**

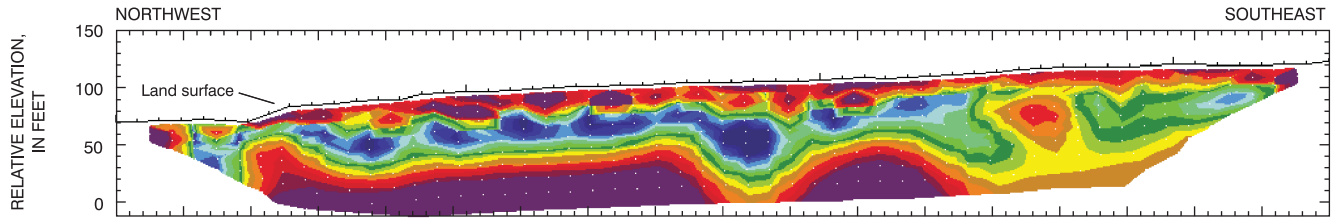
EM and VLF anomalies, indicative of conductive features in bedrock, appear along line 1 at 200 ft. A magnetic low, a conductive 2-D resistivity anomaly, and VLF and EM anomalies indicative of conductive features in bedrock are found along line 1 between 310 and 390 ft. Line 2 has near vertical, conductive EM and 2-D resistivity anomalies coincident with a magnetometer peak value between 460-500 ft. Fractured bedrock could be bisecting the line as indicated by the low bedrock seismic velocity between 335-565 ft. Conductive anomalies between 610 and 660 ft along line 2 from VLF, EM, and 2-D resistivity coincide with a magnetic low. Conductive features along lines have consistent responses, where the magnetic response varies between high and low with some features, along line 2.

Conductive strikes from square-array resistivity results with the same orientation as fractures identified in outcrop, or remotely sensed lineaments, likely are related to fracture zones. Interpretation of square-array resistivity surveys at array 1 indicate a primary conductive strike of approximately 15°±7.5° at the largest A-spacing, which is the same as the orientations of TOPO and SLAR lineaments (fig. 2). This strike also corroborates with the maximum fracture trend from geologic data. The peak fold axis trends 65° and is correlated with the deepest secondary strike anomaly trends from the square-array resistivity survey at array 1. Mapped lineament orientations at this site of 22° and 33° coincide with the maximum fracture peak from geological mapping data of 27°±7°. These include a 25,054-ft long Landsat lineament striking 33°, and a 10,900-ft long TOPO lineament striking 22°.

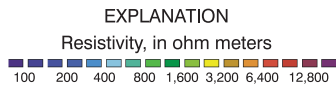
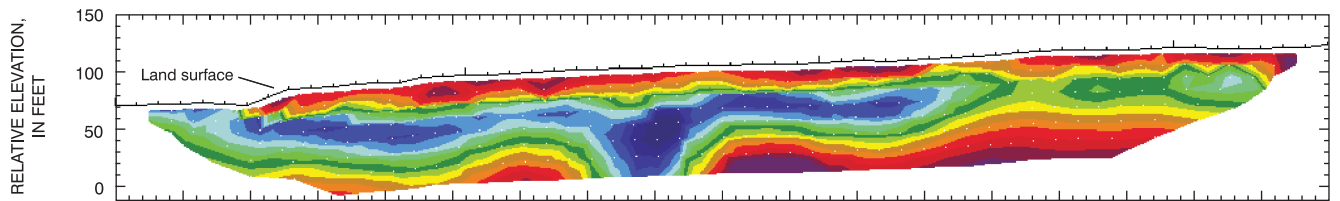
ITE 1, LINE 2

Inverted Resistivity Sections

a) Dipole-dipole array

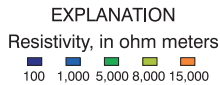
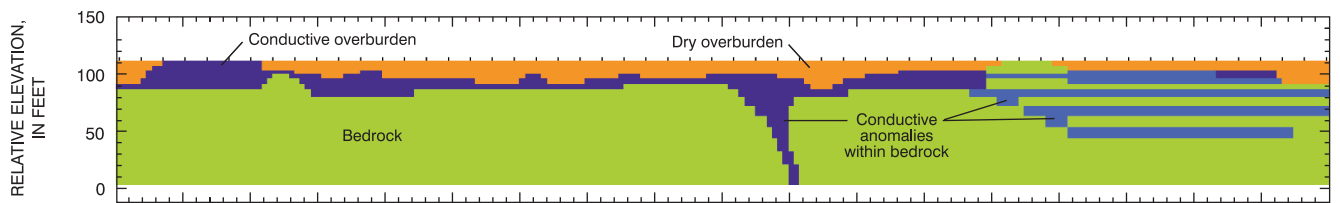


b) Schlumberger array



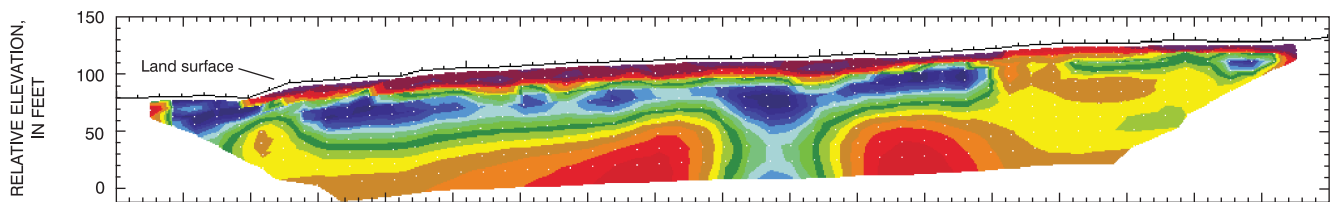
c) Model

Resistivity Model



Synthetic Inverted Resistivity Sections

d) Dipole-dipole array



e) Schlumberger array

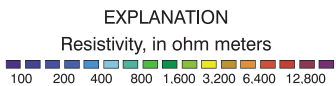
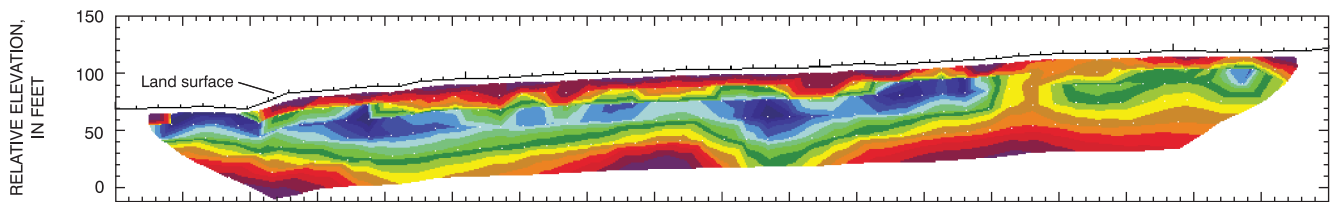


**Figure 7.** Cross sections showing (A and B) inverted resistivity sections of two-dimensional, direct-current resistivity data at site 1 from line 2, Bedford, N.H.; (C) model based on field data from A and B; and (D and E) synthetic resistivity output data from Model C. Site and line locations are shown on figures 1 and 2, respectively.

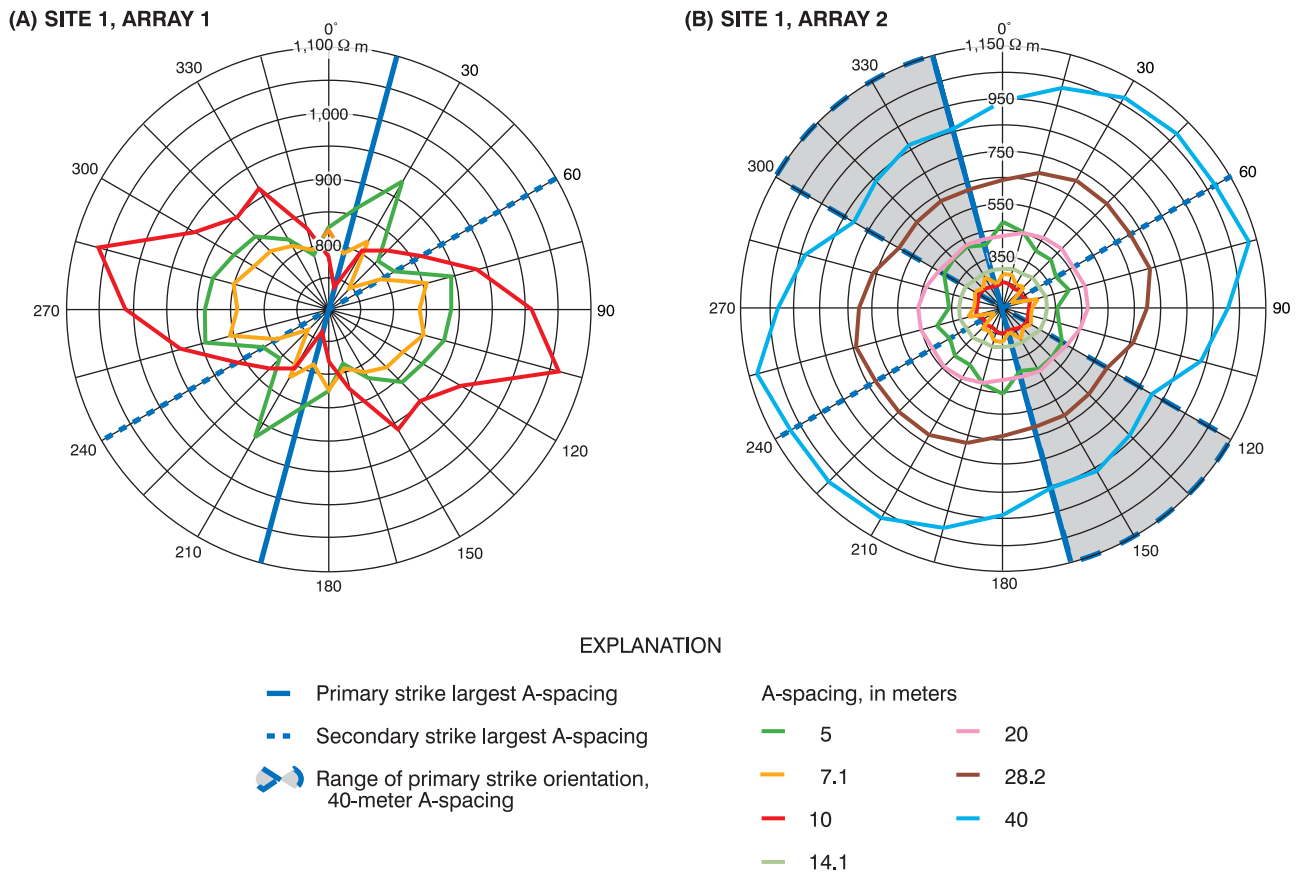


**Figure 8.** Polar plots showing azimuthal square-array direct-current resistivity at site 1 for arrays 1 and 2, Bedford, N.H. Apparent resistivity in ohm meters ( $\Omega$  m), is plotted as a function of azimuth, in degrees east of true north; (A) resistivity of square array 1, center at 700  $\Omega$  m; (B) resistivity of square array 2, center at 150  $\Omega$  m. Site and array locations are shown on figures 1 and 2, respectively.

Electromagnetic (EM and VLF) surveys indicate electrically conductive anomalies that are consistent with the presence of fractured bedrock. 2-D and square-array resistivity surveys, and geologic information corroborate to support the presence of a fractured-bedrock zone. These surveys indicate that lineaments are close to near-vertical conductive features, dipping southeast, identified with geophysical methods. These features may represent fractured-bedrock zones, which likely transmit water. Near-horizontal features in bedrock, interpreted as sheeting fracture zones, were identified with GPR and 2-D resistivity geophysical methods.

### Site 2, Windham, New Hampshire

Site 2 on Marblehead Road in Windham, N.H. (fig. 9), is a mostly wooded, valley-wetland setting, and ranges in elevation from about 170 to 210 ft in the area of the surveys. Walsh and Clark (1999) mapped the bedrock geology of this area with a contact

between the Berwick Formation, and the Ayer Granodiorite (fig. 9). The bedrock is exposed at the surface on topographic highs at this site. The overburden generally is less than 20 ft thick and is mapped as a till, which is unsorted to poorly sorted clay, silt, sand, pebbles, cobbles and boulders, with some gravel (Larson, 1984). Three mapped lineaments at the site were observed from a LOWALT platform trending 71°, 74°, and 355° (Ferguson and others, 1997), and one with a CIR platform, trending 77° (fig. 9). The 71°, 74°, and 77° trending lineaments were fracture correlated using the 1,000-ft buffer analysis technique (R.B. Moore and others, U.S. Geological Survey, written commun., 2001). Lineament criteria are visible at the site as a swale on line 1, trending 350°, and a shallow elongated valley trending 70°. Fracture data in a 4,000-ft radius of the site have three peak orientations: 310°±9° (100 percent, normalized height), 68°±11° (14 percent, normalized height), and 25°±34° (9 percent, normalized height). Fractures in

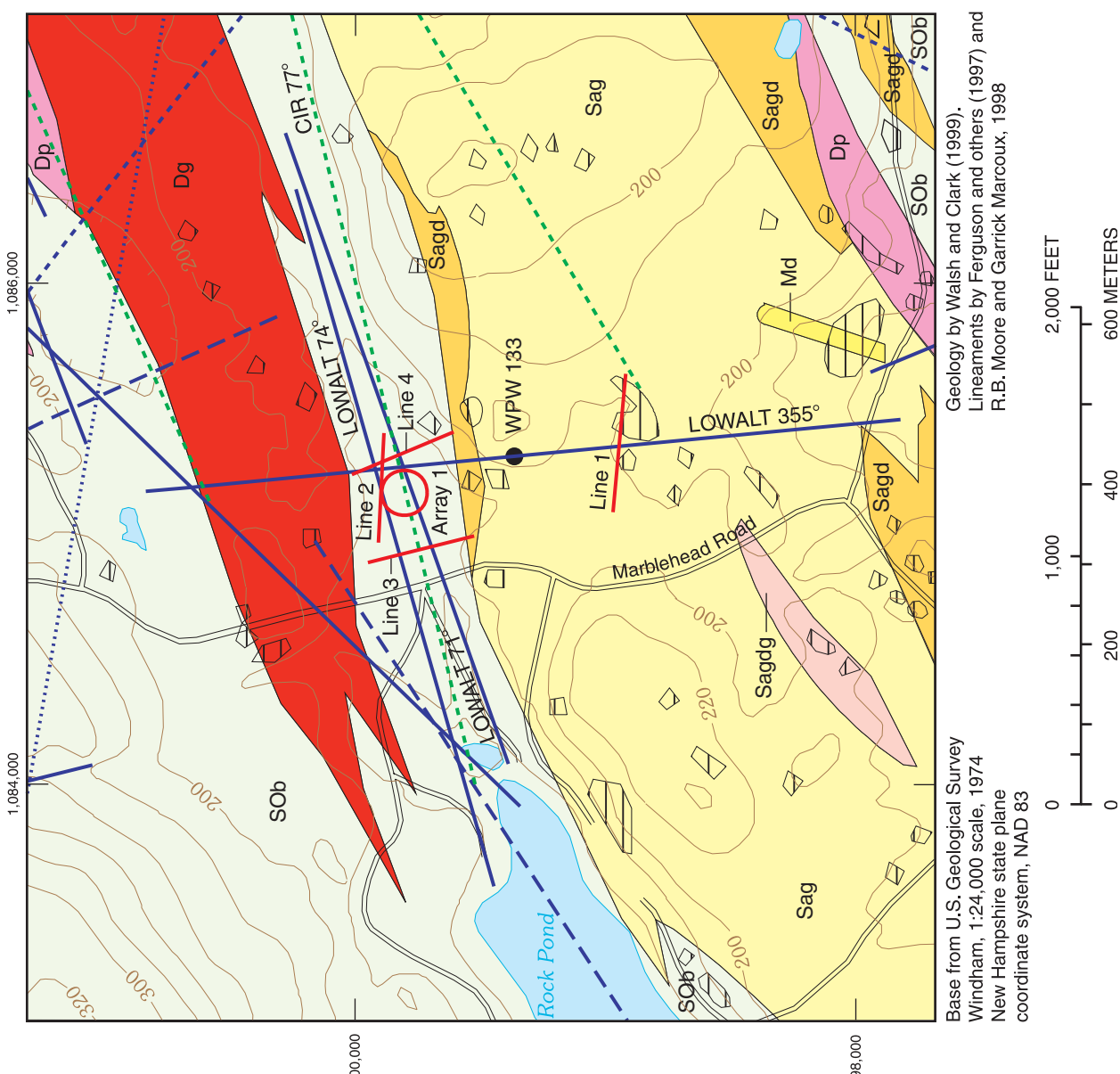
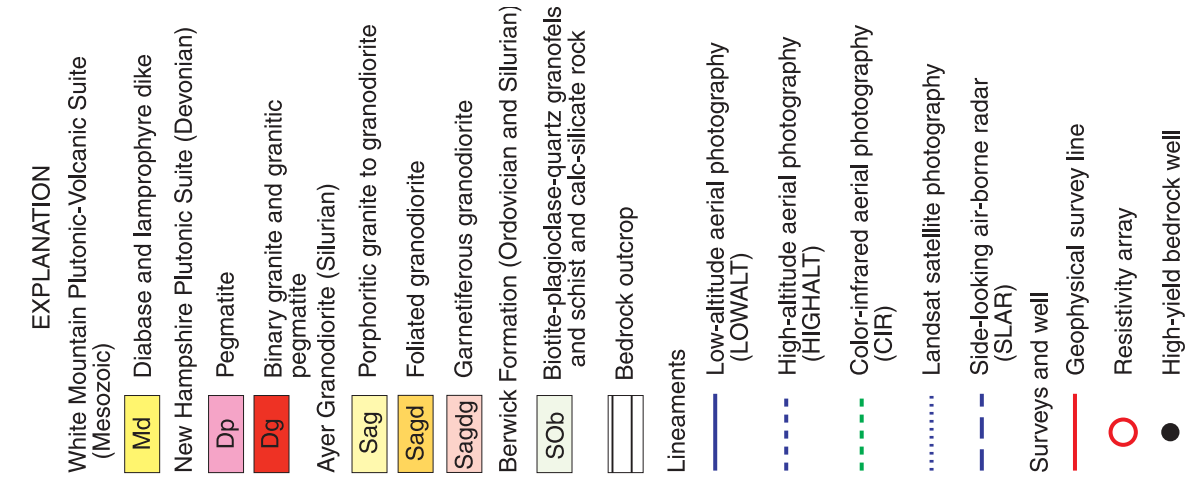


**Figure 9.** Geophysical survey locations, bedrock geology, and lineaments at site 2, Windham, NH. Site location is shown on figure 1.

an outcrop between line 3 and line 4 have a strike and dip of 70° and 19° dipping to the south, parting along foliation, and have a strike and dip of 67° and 35° dipping to the north.

Well WPW 133 (fig. 9) is drilled to a depth of 300 ft with a reported yield of 100 gal/min. Approximately 7 ft of overburden is present above the bedrock, and the static water level in the well is at 10 ft below landsurface. Probabilities of exceeding a yield of 40 gal/min from a 400-ft-deep well at this site ranged from 8 to 15 percent. A 14-percent probability is calculated for the 98.4-ft (30-m) square cell that well WPW 133 is in (R.B. Moore and others, U.S. Geological Survey, written commun., 2001). Variations in probability at the site most likely are caused by lithologic contacts and topography.

Four geophysical survey lines were located to bisect lineament locations on each side of well WPW 133 (fig. 9). Line 1 extends 570 ft from west to east and is on a trail in the woods to the south of WPW 133. It is on a topographic high with outcrops of the Ayer Granodiorite. Lines 2, 3, and 4 are in an east-west trending (70°) shallow valley. Logs from two monitoring wells reveal that the valley is filled by a 15-20-ft thick sequence of outwash and till. Line 2 extends 440 ft from west to east and is set in the woods, parallel to a monitoring-well access road to the north of well WPW 133. Line 3 is parallel to Marblehead Road, and extends 440 ft from north to south in a wooded area west of well WPW 133. Line 4 is parallel to line 3 in a wooded area to the east of well WPW 133, and extends 440 ft from north to south. An array center was chosen on the basis of availability of flat terrain and the location of anomalies from other techniques. The center of array 1 is at 200 ft along line 2, 90 ft to the south in the center of the valley (fig. 9).

### Geophysical Surveys and Interpretation

Seven geophysical surveys were used to characterize site 2. Overburden thickness and physical properties were derived from results of seismic refraction, GPR, EM, and 2-D resistivity surveys. Bedrock characteristics and anomalies that could be caused by bedrock fractures are seen in the seismic refraction, GPR, magnetometer, VLF, EM, 2-D resistivity and square-array resistivity survey results (figs. 11-19).

Seismic-refraction data were collected along line 1 and line 2 and at 90° to each line. These data were examined only with respect to average seismic wave velocity in bedrock along each line, to look at

variations in relation to orientation to a suspected fracture zone. Seismic refraction on line 1 was centered at 350 ft. The seismic velocity in the bedrock along line 1 is 11,500 ft/s, whereas the velocity normal to line 1 is 15,000 ft/s. Seismic refraction along line 2 is centered at 213 ft. The seismic velocity in bedrock along line 2 is 11,000 ft/s, and the velocity normal to line 2 is 9,500 ft/s.

GPR data were collected on lines 1, 2, 3, and 4; data from line 1 indicate features below the bedrock surface. A reflector below land surface from 0 to 160 ft along line 1 ends at a bedrock outcrop, which indicates that it is likely caused by the bedrock surface. A bedrock outcrop from 370 to 390 ft indicates that subhorizontal reflectors are below the bedrock surface from 375 to 500 ft along line 1. These reflectors are interpreted to be sheeting fractures (fig. 10).

Magnetometer measurements were made along all four lines at site 2 (figs. 11-14). The average magnetic field measure at this site during the surveys is 71 nT. Line 1 survey results indicate a magnetic low of 51 nT centered at 55 ft (fig. 11a). Data collected along line 4 indicate a magnetic low of 33 nT between 230-280 ft, and another low of 36 nT between 330-340 ft (fig. 14a).

VLF tilt-angle surveys at lines 1, 2, 3, and 4 indicate anomalies. Inflections along line 1 were detected at 70, 100, 140, 370, 405, and 430 ft (fig. 11b). Line 2 tilt-angle measurements have inflection points at 110, 240, 340, 380, and 415 ft (fig. 12b). Line 3 results indicate weak inflection anomalies at 255, 305, and 395 ft (fig. 13b). The VLF data from line 4 has a tilt-angle inflection point at 235 ft (fig. 14b).

EM surveys were collected on all lines at site 2. Along line 1, a VD anomaly at 380 ft indicates a near-vertical conductor (fig. 11c). Results of the VD survey from line 2 indicate a near-vertical conductor anomaly, possibly dipping east, at 180 ft (fig. 12c). Line 3 VD-survey results indicate a vertical conductor anomaly centered at 220 ft (fig. 13c). The results from survey line 4 indicate the bedrock is more conductive in the north than in the south (fig. 14c). The dip of features on lines 1-4 were not readily apparent from the EM data.

2-D resistivity was measured at lines 1, 2, 3, and 4. Models were created to verify interpretations of the data. A near-vertical fracture on line 1 is interpreted at 110 ft and an eastward-dipping fracture is interpreted as intersecting the bedrock surface at 345 ft (fig. 15).

## SITE 2, LINE 1

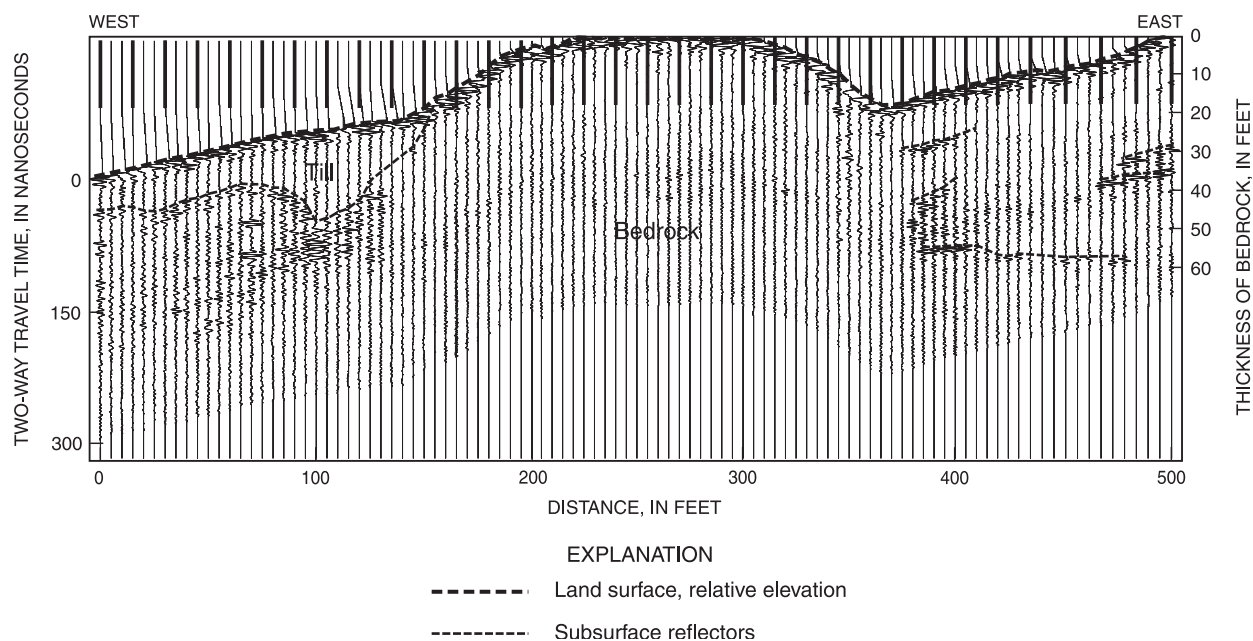


**Figure 10.** Processed ground-penetrating radar profile at site 2 from line 1, Windham, N.H. Site and line locations are shown on figures 1 and 9, respectively

Near-horizontal conductive features also can be interpreted from the dipole-dipole array at 345-450 ft that were not modeled (fig. 15a). A horizontal conductor at depth from 0 to 440 ft also was interpreted based on the Schlumberger array (fig. 15b). The model, created to check interpretations of the data from line 2 (fig. 16), displays the effect of fractures intersecting from different orientations. Based on the results from lines 3, 4, array 1, and lineament data, a fracture zone with a strike close to the strike of line 2 intersects the line from 190 to 440 ft. A conductive zone striking roughly perpendicular to line 2 intersects the bedrock surface at 110 ft along the line (fig. 16). Interpretations of line 3 indicate a fracture zone dipping to the south, and intersecting the surface of the bedrock at 200 ft (fig. 17). For line 4, a conductive south-dipping feature intersects the bedrock surface at 150 ft along the line (fig. 18).

Square-array resistivity data were collected at array 1. The primary conductive strike determined graphically is 75 $\times$  with a range of 60 $\times$  to 105 $\times$  at the largest A-spacing of 20 m (fig. 19). Increases in resistivity from the 5-m A-spacing through the 20-m A-spacing indicate a two layer model; conductive overburden and resistive bedrock (fig. 19).

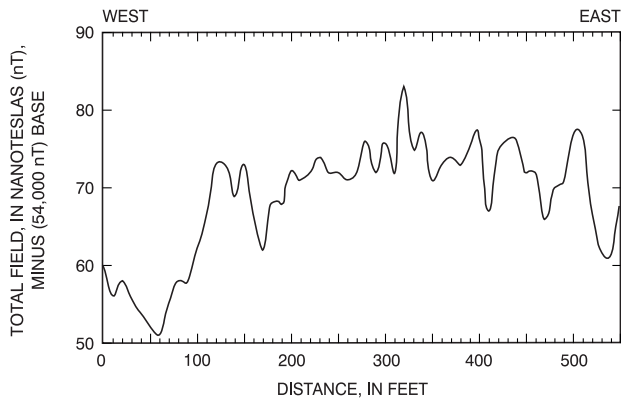
## Integration of Results

Line 1 at site 2 (fig. 11) has two locations containing anomalies from multiple techniques. 2-D resistivity and VLF anomalies indicative of conductive features in bedrock were found between 100 and 115 ft along the line. EM, VLF, and 2-D resistivity anomalies indicative of conductive features in bedrock are between 350 and 375 ft along line 1, whereas 2-D resistivity data indicate an eastward dip. Near-horizontal fractures begin in the GPR record at 375 ft and extend to at least 500 ft. The seismic-refraction velocity of bedrock parallel to line 1 is approximately 3,500 ft/s slower than the velocity normal to line 1 centered at 350 ft. This decrease in velocity is consistent with dominant fracture trends near parallel to the low-altitude lineament (fig. 9), striking roughly towards line 2 and the well.

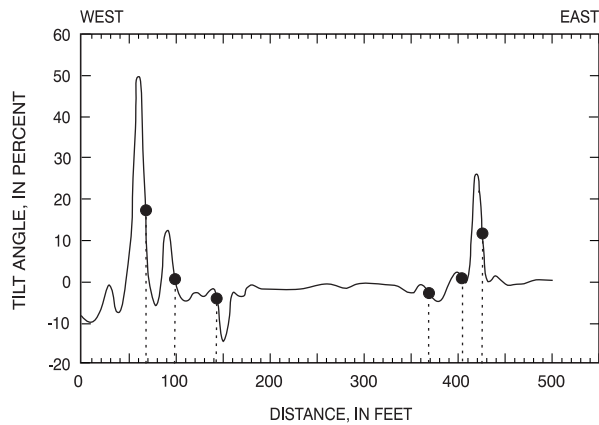
The line 2 survey is near-parallel to a suspected fracture zone, which bisects line 3 and line 4 intersecting line 2 at 270 ft. Interpretation of the data is difficult because line 2 may cross two bedrock-fracture zones at different orientations. EM and 2-D resistivity anomalies indicative of conductive features in bedrock are roughly normal to the line at 180 ft. 2-D resistivity indicated a possible eastward dip to the

**SITE 2, LINE 1**

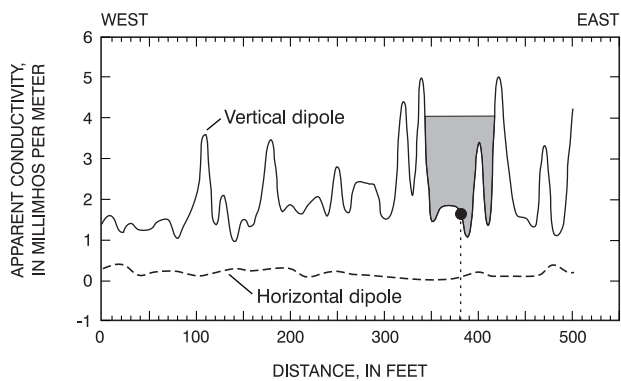
(A) Magnetometer survey--total field



(B) Very low frequency electromagnetic survey--tilt angle



(C) Electromagnetic (EM) terrain conductivity survey

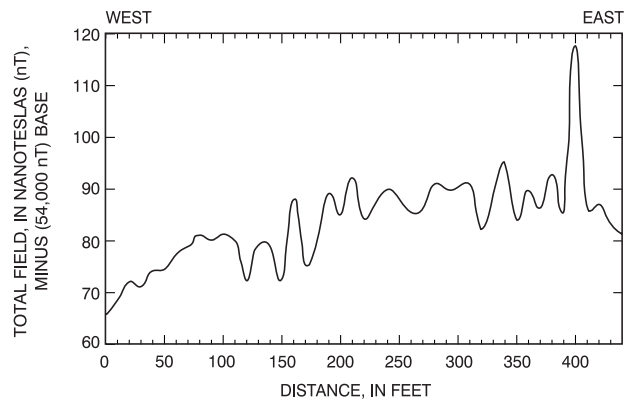


**EXPLANATION**  
 ■ Width of anomaly (20 meters)  
 ● Point of anomaly

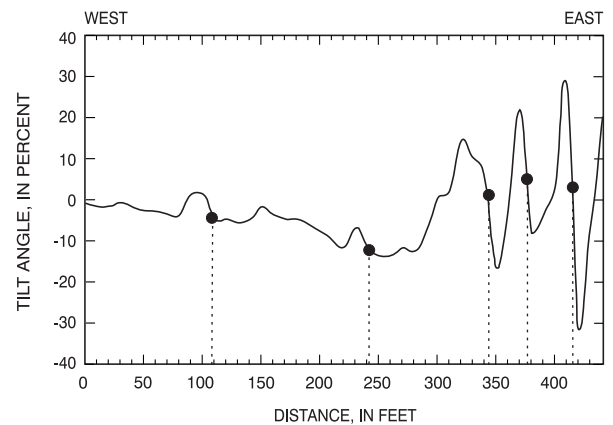
**Figure 11.** Magnetic and electromagnetic surveys at site 2 from line 1, Windham, N.H. (A) magnetometer survey; (B) very low frequency (VLF) electromagnetic survey; (C) electromagnetic (EM) terrain conductivity survey with a 20-meter (65.6-foot) coil spacing. Site and line locations are shown on figures 1 and 9, respectively.

**SITE 2, LINE 2**

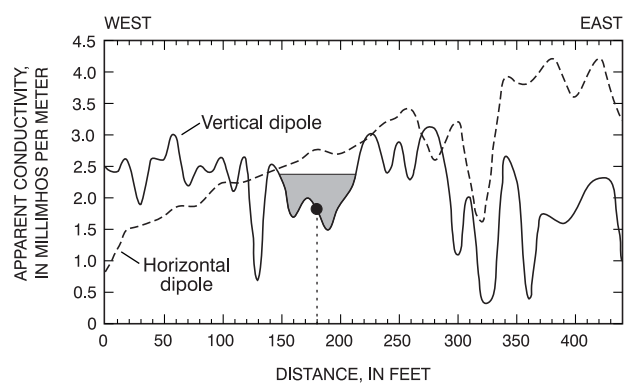
(A) Magnetometer survey--total field



(B) Very low frequency electromagnetic survey--tilt angle



(C) Electromagnetic (EM) terrain conductivity survey

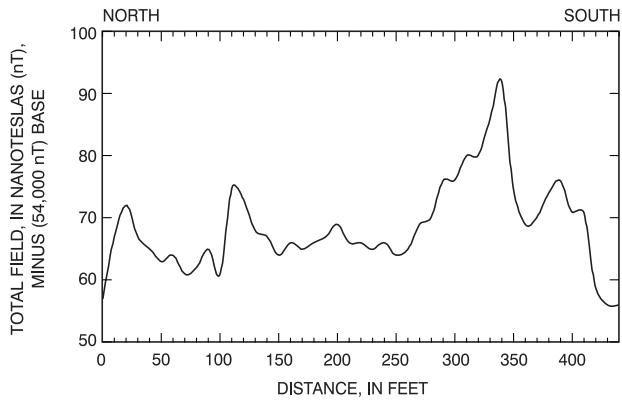


**EXPLANATION**  
 ■ Width of anomaly (20 meters)  
 ● Point of anomaly

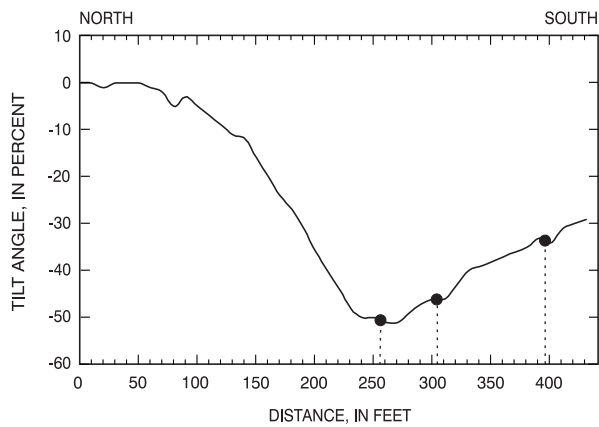
**Figure 12.** Magnetic and electromagnetic surveys at site 2 from line 2, Windham, N.H. (A) magnetometer survey; (B) very low frequency (VLF) electromagnetic survey; (C) electromagnetic (EM) terrain conductivity survey with a 20-meter (65.6-foot) coil spacing. Site and line locations are shown on figures 1 and 9, respectively.

**SITE 2, LINE 3**

(A) Magnetometer survey--total field



(B) Very low frequency electromagnetic survey--tilt angle



(C) Electromagnetic (EM) terrain conductivity survey

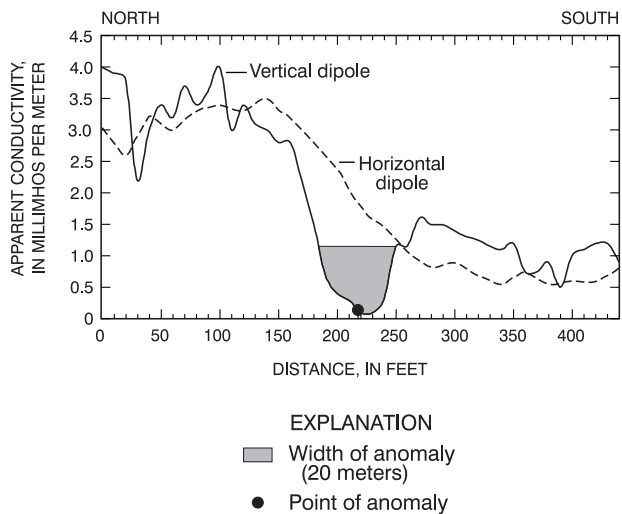
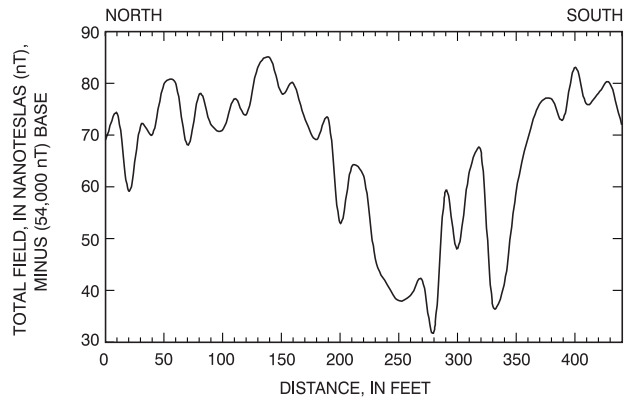


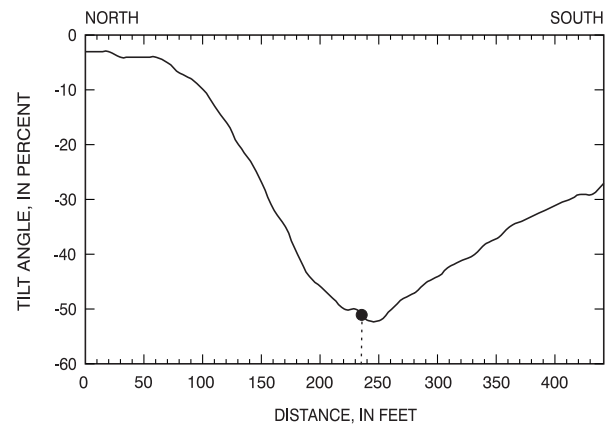
**Figure 13.** Magnetic and electromagnetic surveys at site 2 from line 3, Windham, N.H. (A) magnetometer survey; (B) very low frequency (VLF) electromagnetic survey; (C) electromagnetic (EM) terrain conductivity survey with a 20-meter (65.6-foot) coil spacing. Site and line locations are shown on figures 1 and 9, respectively.

**SITE 2, LINE 4**

(A) Magnetometer survey--total field



(B) Very low frequency electromagnetic survey--tilt angle



(C) Electromagnetic (EM) terrain conductivity survey

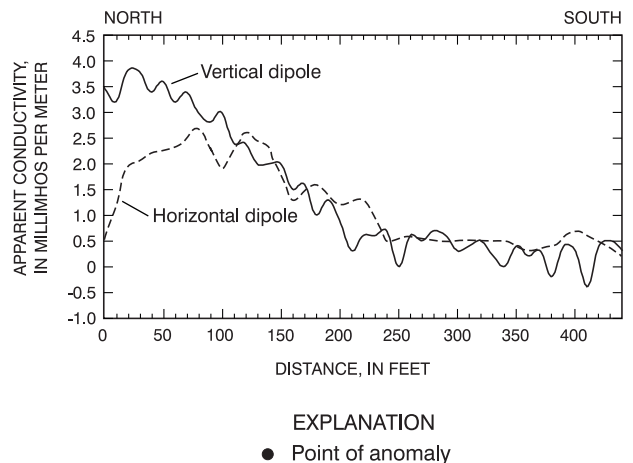
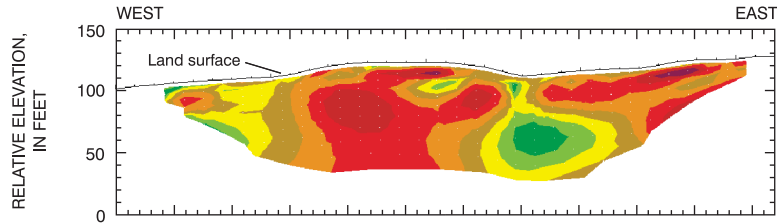


**Figure 14.** Magnetic and electromagnetic surveys at site 2 from line 4, Windham, N.H. (A) magnetometer survey; (B) very low frequency (VLF) electromagnetic survey; (C) electromagnetic (EM) terrain conductivity survey with a 20-meter (65.6-foot) coil spacing. Site and line locations are shown on figures 1 and 9, respectively.

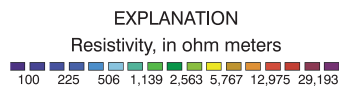
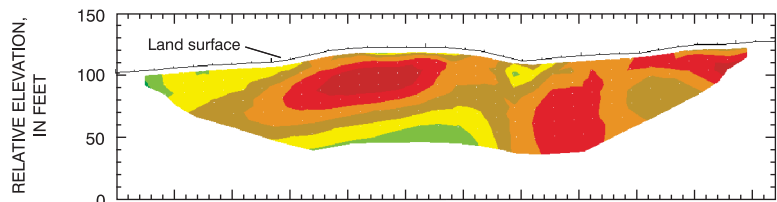
**SITE 2, LINE 1**

**Inverted Resistivity Sections**

(A) Dipole-dipole array

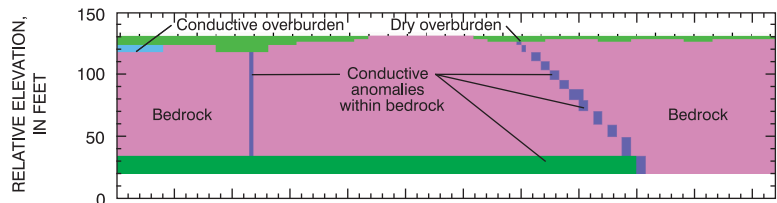


(B) Schlumberger array



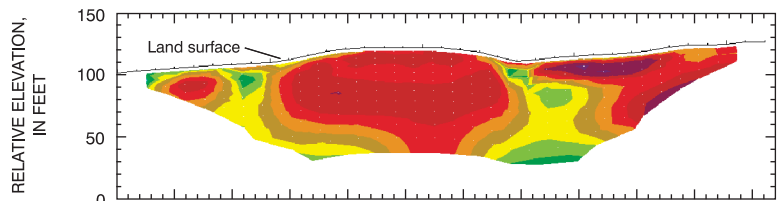
(C) Model

**Resistivity Model**



**Synthetic Inverted Resistivity Sections**

(D) Dipole-dipole array



(E) Schlumberger array

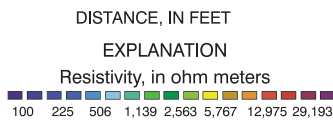
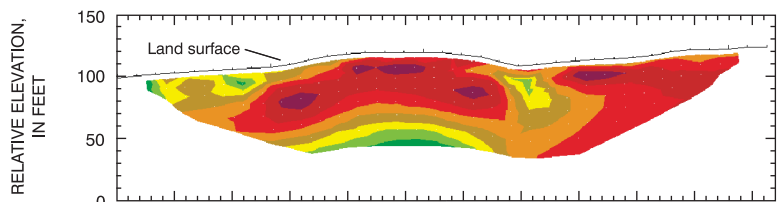
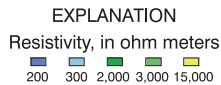
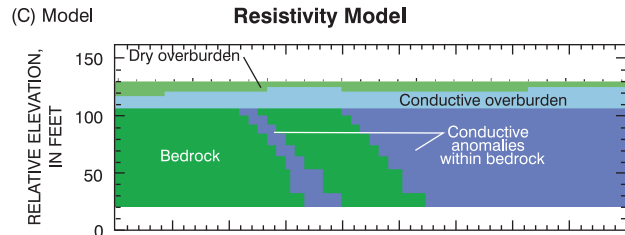
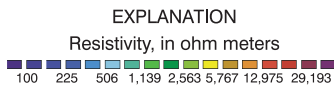
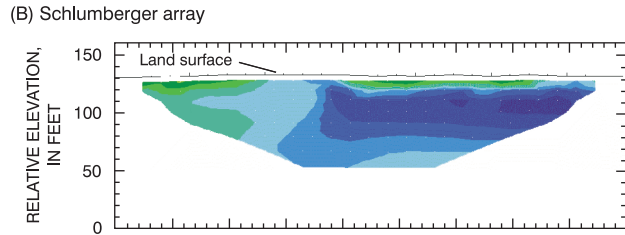
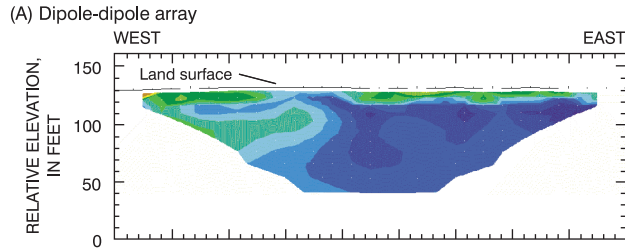


**Figure 15.** Cross sections showing (A and B) inverted resistivity sections of two-dimensional, direct-current resistivity data at site 2 from line 1, Windham, N.H.; (C) model based on field data from A and B; and (D and E) synthetic resistivity output data from Model C. Site and line locations are shown on figures 1 and 9, respectively.

**SITE 2, LINE 2**

**Inverted Resistivity Sections**



**Synthetic Inverted Resistivity Sections**

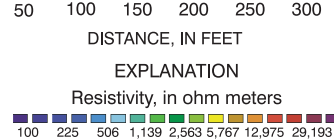
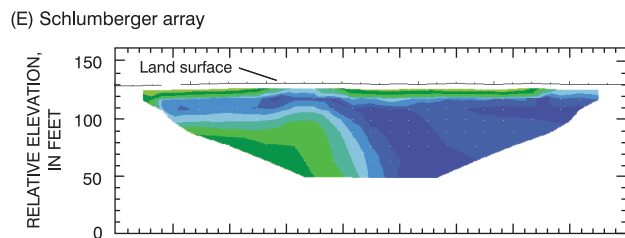
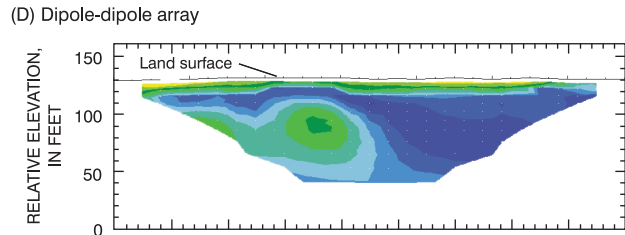
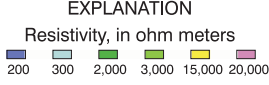
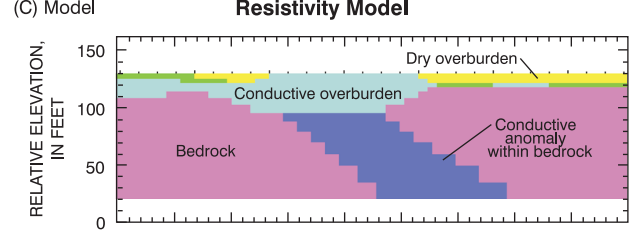
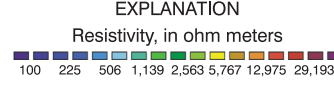
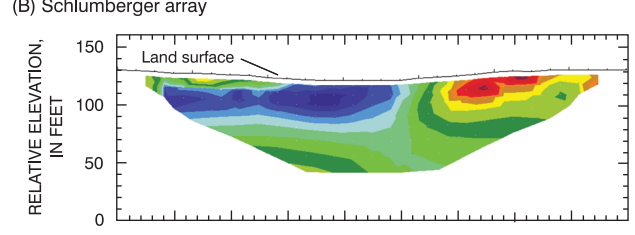
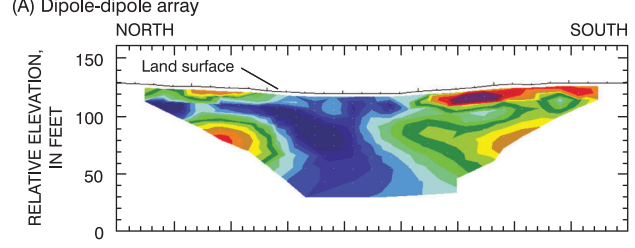


**Figure 16.** Cross sections showing (A and B) inverted resistivity sections of two-dimensional, direct-current resistivity data at site 2 from line 2, Windham, N.H.; (C) model based on field data from A and B; and (D and E) synthetic resistivity output data from Model C. Site and line locations are shown on figures 1 and 9, respectively.

**SITE 2, LINE 3**

**Inverted Resistivity Sections**



**Synthetic Inverted Resistivity Sections**

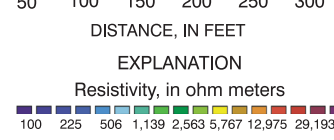
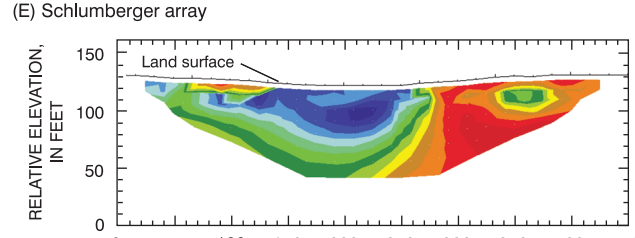
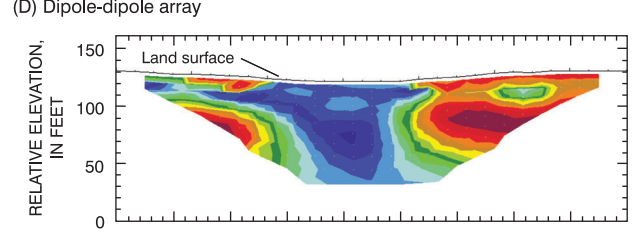
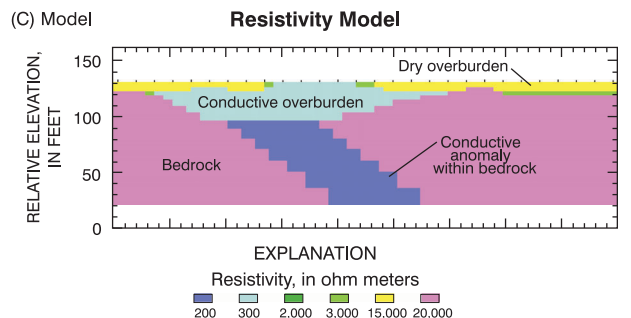
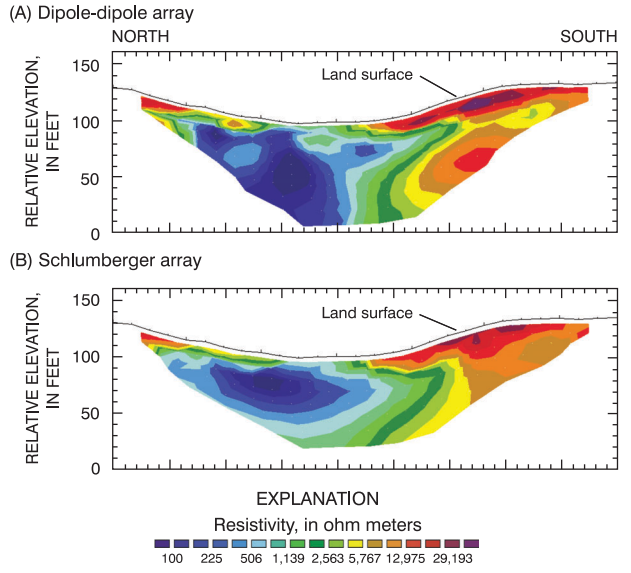


**Figure 17.** Cross sections showing (A and B) inverted resistivity sections of two-dimensional, direct-current resistivity data at site 2 from line 3, Windham, N.H.; (C) model based on field data from A and B; and (D and E) synthetic resistivity output data from Model C. Site and line locations are shown on figures 1 and 9, respectively.

**SITE 2, LINE 4**

**Inverted Resistivity Sections**



**Synthetic Inverted Resistivity Sections**

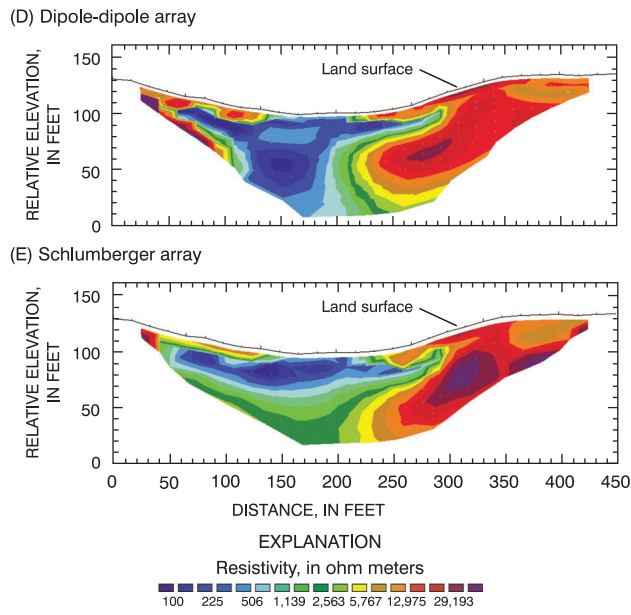


**Figure 18.** Cross sections showing (A and B) inverted resistivity sections of two-dimensional, direct-current resistivity data at site 2 from line 4, Windham, N.H.; (C) model based on field data from A and B; and (D and E) synthetic resistivity output data from Model C. Site and line locations are shown on figures 1 and 9, respectively.

**SITE 2, ARRAY 1**

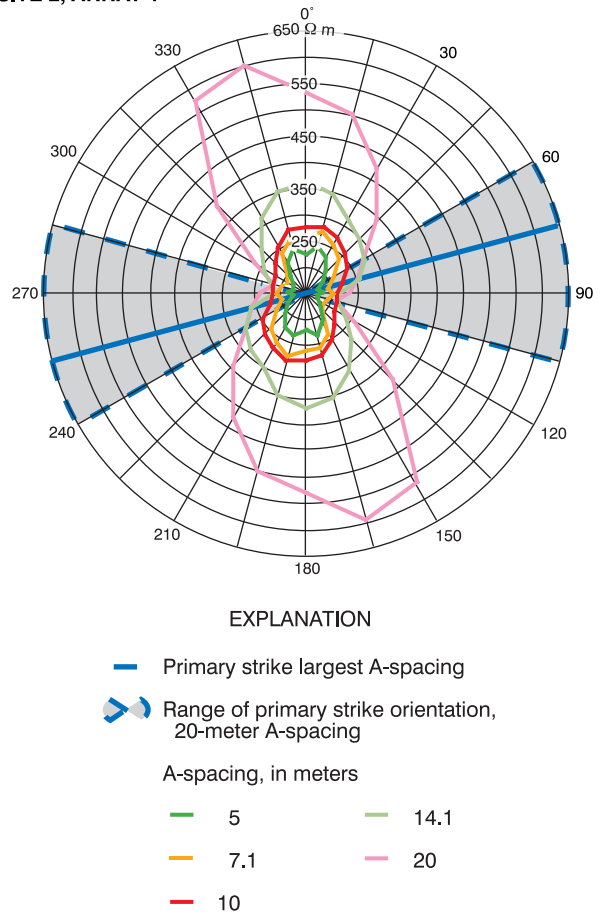


**Figure 19.** Polar plot showing azimuthal square-array direct-current resistivity at site 2 for array 1, Windham, N.H. Apparent resistivity in ohm meters ( $\Omega$  m), is plotted as a function of azimuth, in degrees east of true north, and resistivity center is at 150  $\Omega$  m. Site and array locations are shown on figures 1 and 9, respectively.

line 2 anomaly. The seismic-refraction velocity of bedrock along line 2 is approximately 1,500 ft/s faster than the velocity normal to line 2, which indicates that the dominant fracture trend is nearly parallel to line 2.

Line 3 has a steeply dipping conductive 2-D resistivity anomaly (fig. 17) that correlates with the location of an EM anomaly indicative of a conductive feature in bedrock (fig. 13b). Line 4 has a steeply dipping conductive 2-D resistivity anomaly (fig. 18) that correlates with the location of a VLF anomaly, indicative of a conductive feature in bedrock (fig. 14). A magnetic low identified along line 4 coincides with the deep, down-dip portion of the 2-D resistivity feature. The anomalies bisecting line 3 and line 4 appear to be the same continuous feature based on the primary conductive strike from the square-array resistivity and the location and orientation of lineaments.

Conductive strikes identified by square-array resistivity, with the same orientation as fractures identified in outcrop, or remotely sensed lineaments, likely are related to fracture zones. Array 1 has a primary strike direction that is the same as the three lineaments striking 71°, 74°, and 77°. These lineaments cross line 3 and line 4 on the location of steeply dipping anomalies identified with 2-D resistivity. Array 1 has a primary bedrock strike of 75° that has the same orientation as a small peak in the geologic-fracture data analysis (68°±11°), and both fractures dipping south and parting along foliation dipping north in an adjacent outcrop.

Electromagnetic (EM and VLF) surveys indicate electrically conductive anomalies that are consistent with fractured bedrock. DC-resistivity surveys and arrays, and geologic information also indicate fractured bedrock. These surveys show that the lineaments are close to dipping planar features that may represent fractured-bedrock zones. The possible fracture zones, indicated by lineaments LOWALT 74, LOWALT 71, and CIR 77, probably are a southward dipping fracture zone that allows for transmission of water to well WPW 133 (fig. 9). Near-horizontal conductive features in bedrock, that cannot be identified with a lineament analysis, were identified on line 1 with GPR and 2-D resistivity surveys. These near-horizontal features are interpreted as sheeting fracture zones and may serve to connect near-vertical fracture zones.

### Site 3, Pelham, New Hampshire

Site 3 on State Route 128 in Pelham, N.H., is set in grassy lots in a shallow valley containing Beaver Brook. The elevation ranges from 150 to 170 ft where the data were collected. Walsh and Clark (1999) mapped the bedrock geology of this area as the Berwick Formation (fig. 20). Overburden material at the site is mapped as a fine-grained (clay to fine sand) stratified drift. Transmissivity of the stratified-drift aquifer is less than 1,000 ft<sup>2</sup>/d (Stekl and Flanagan, 1992). Lineaments mapped at the site were SLAR trending 329° and 325° (Ferguson and others, 1997), and CIR trending 303° (fig. 20). The 303° trending lineament was fracture correlated using the domain-analysis technique (R.B. Moore and others, U.S. Geological Survey, written commun., 2001). These lineaments have identifying criteria visible at the site

such as a small wetland, and a valley trend of 300° at survey line 1, and a straight reach of stream with a trend of 320° south of line 2 (fig. 20). Fracture data in a 4,000-ft radius of the site has four peak orientations: 282°±8° (100 percent, normalized height), 304°±6° (90 percent, normalized height), 28°±4° (17 percent, normalized height), and 325°±13° (24 percent, normalized height).

At site 3, well PAW 131 was drilled to a depth of 240 ft and has a reported yield of 120 gal/min. The drilling log indicates that a fracture zone was intersected between 225 and 240 ft deep. The static water level in the well is at 12 ft and bedrock is at 11 ft below land surface. Well PAW 420 was drilled at 115 ft along line 2 at site 3 during this study. The overburden consisted of 7 ft of poorly sorted fine to coarse sands, gravels, and cobbles. The well was completed at 300 ft below land surface when a sufficient supply for domestic use was obtained at a reported yield of 30 gal/min. At 19 ft below the land surface, the well yield was 2 gal/min from fractures between soft and hard variations of the Berwick Formation. The high-producing zone for the well is at 277 ft in an open fracture. The open fracture is below an approximately 1-ft thick silicified zone with quartz-biotite black schist and quartzite above and Berwick granofels below (S.F. Clark, Jr., U.S. Geological Survey, written commun., 1999).

Probabilities of exceeding a yield of 40 gal/min from a 400-ft deep well at this site ranged from 12 to 19 percent. A 12-percent probability is calculated for the 98.4-ft (30-m) square cell that well PAW 131 is in (R.B. Moore and others, U.S. Geological Survey, written commun., 2001). Well PAW 420 is within a cell with a 13-percent probability. Variations in probability at the site appear to be caused by proximity to surface water and topography.

Two geophysical survey lines were located to cross lineaments on each side of well PAW 131. Line 1, which extends 440 ft from southwest to northeast, is along the property line of two developed lots and in a vacant lot to the northwest of well PAW 131. Line 2, southeast of PAW 131, is in a channel of Beaver Brook, and extends 440 ft from southwest to northeast. Well PAW 420 was drilled directly adjacent to line 2 at approximately 100 ft along the line. Two array locations were sited on electrically conductive anomalies after a preliminary analysis of other geophysical data; array 1 was set at 215 ft on line 1, array 2 was set at 200 ft on line 2 (fig. 20).

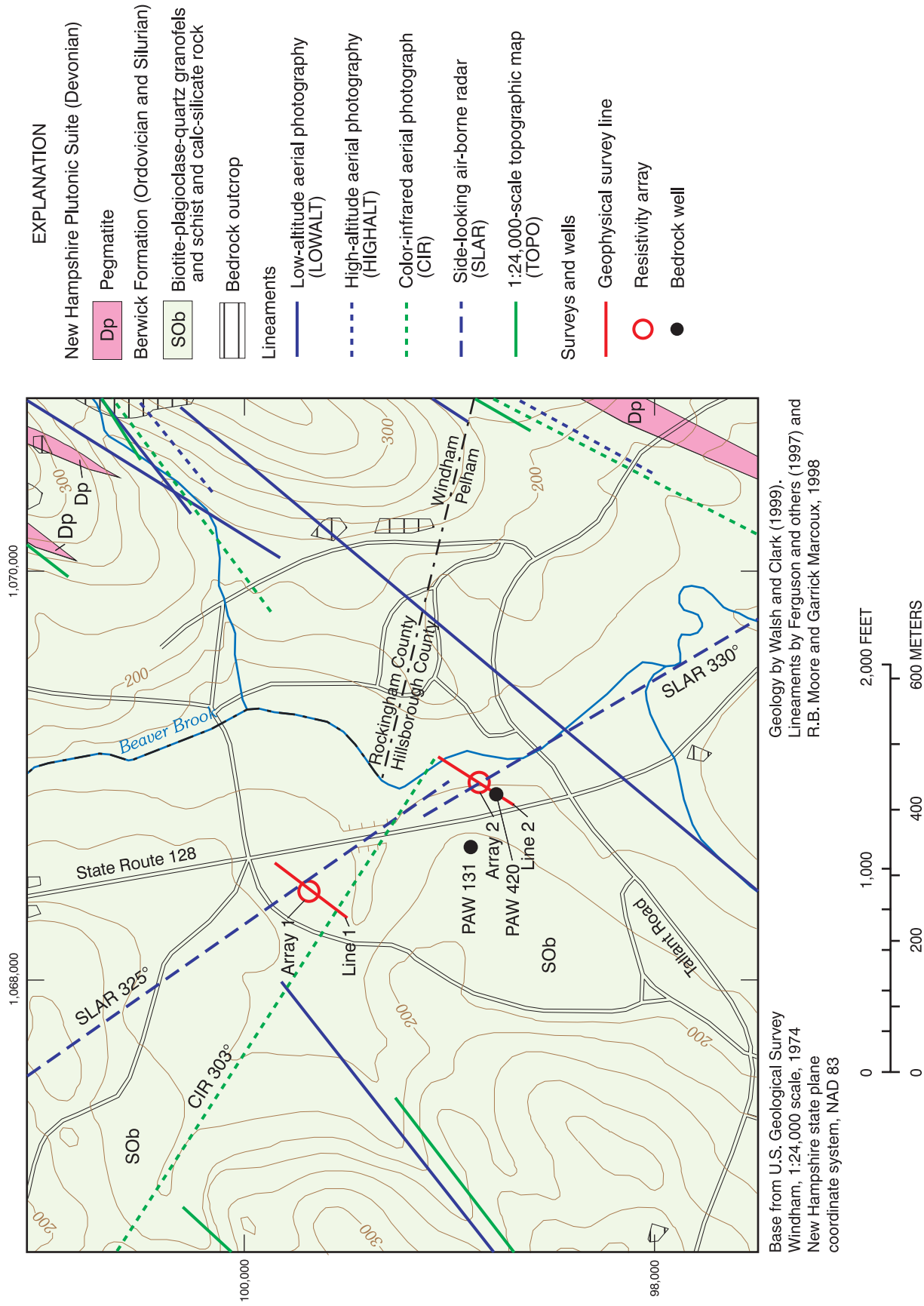


**Figure 20.** Geophysical survey locations, bedrock geology, and lineaments at site 3, Pelham, N.H. Site location is shown on figure 1.

## Geophysical Surveys and Interpretation

Six geophysical surveys were used to characterize site 3. Overburden thickness and physical properties were derived from the GPR, EM, and 2-D resistivity survey results. Bedrock properties were determined by magnetometer, 2-D resistivity, and square-array resistivity. Anomalies that could be caused by bedrock fractures are seen in the magnetometer, VLF, EM, 2-D resistivity and square-array resistivity survey results (figs. 21-25).

GPR data were collected on lines 1 and 2. The GPR record from line 1 indicates bedded sands, with attenuation of the record before the bedrock is detected. Reflectors from the bedded sands dip towards the center of the cross-section. The GPR record from line 2 has a reflector that is interpreted to be the bedrock surface. From 195 to 205 ft along line 2, this reflector drops from 7 to 14 ft in depth, indicating a depression in the bedrock surface. The GPR record did not return any clear reflectors in the bedrock and is not presented in this report.

Magnetometer measurements were made along line 1 and line 2 (figs. 21 and 22). The average magnetic field measure at this site during the surveys is 109 nT. Line 2 survey results indicate anomalous lows of  $\bar{n}35$  nT at 120 ft, and 50 nT at 300 ft (fig. 22a). The steel-well casing at 115 ft along line 2 from well PAW 420 could affect the anomaly at 120 ft, considering the magnetic high just before it along the line.

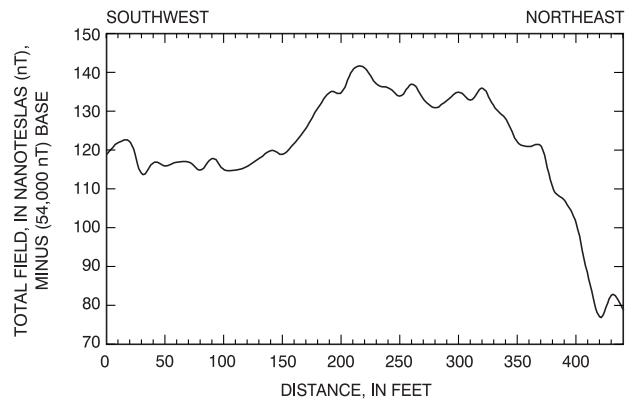
VLF tilt-angle measurements were made along lines 1 and 2. VLF data from line 1 indicates a weak inflection at 210 ft, but was dominated by power-line noise at its northeastern end (fig. 21b). An anomalous inflection is at 175 ft along line 2 (fig. 22b). The suspected fracture zone orientations at site 2 in relation to the transmitter are not ideal.

EM surveys were collected on lines 1 and 2 at site 3. The survey along line 1 was shortened because of interference from power lines (fig. 21c), and the remaining data may be affected. The EM results from line 2 indicate a near-vertical conductor anomaly at 155 ft along the line (fig. 22c).

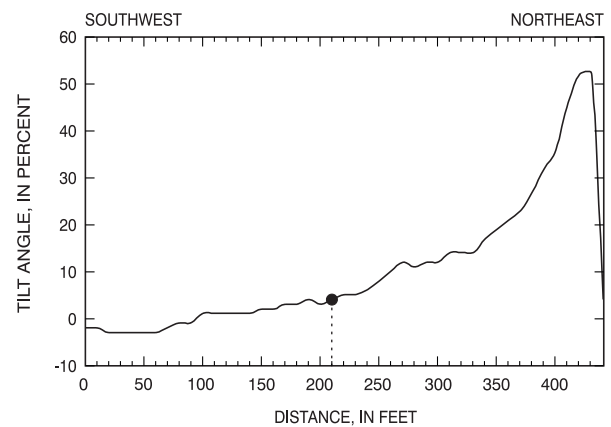
2-D resistivity surveys were run at lines 1 and 2. Four primary resistivity units from line 1 and line 2 can be represented by resistive unsaturated and conductive saturated sediments, and resistive competent and conductive fractured bedrock. Below the interpreted bedrock surface at 230 ft along line 1 is a conductive anomaly penetrating into the bedrock. This anomaly was interpreted with an apparent dip to the southwest (fig. 23). Near horizontal conductive

### SITE 3, LINE 1

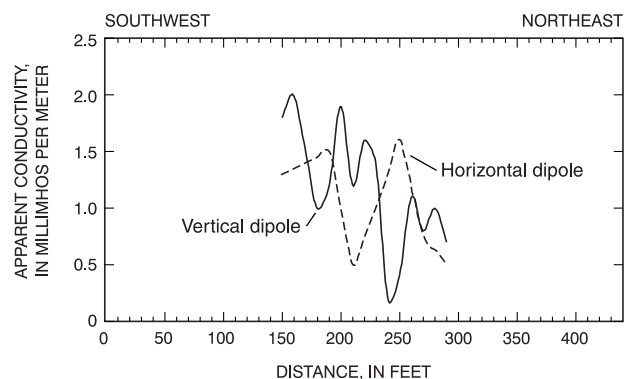
(A) Magnetometer survey--total field



(B) Very low frequency electromagnetic survey--tilt angle



(C) Electromagnetic (EM) terrain conductivity survey



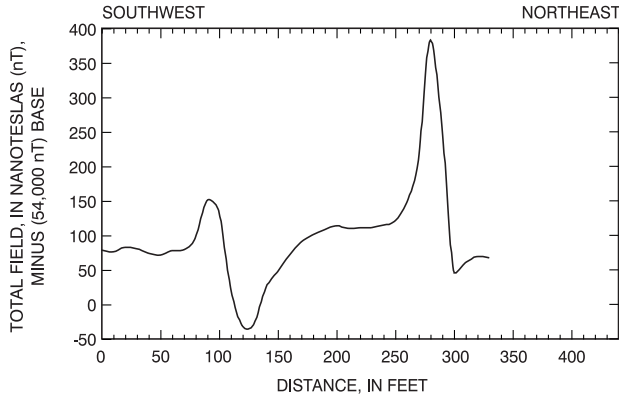
#### EXPLANATION

- Point of anomaly

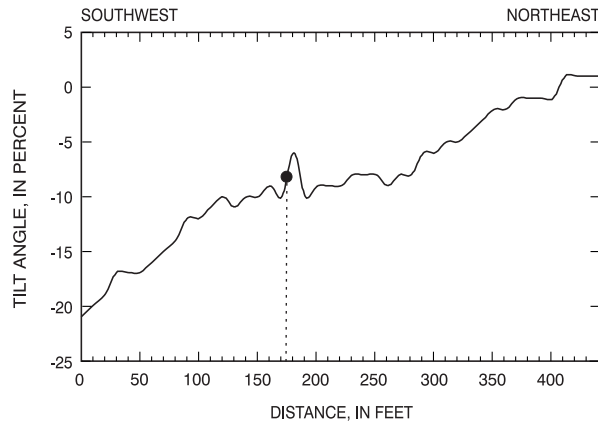
**Figure 21.** Magnetic and electromagnetic surveys at site 3 from line 1, Pelham, N.H. (A) magnetometer survey; (B) very low frequency (VLF) electromagnetic survey; (C) electromagnetic (EM) terrain conductivity survey with a 20-meter (65.6-foot) coil spacing. Site and line locations are shown on figures 1 and 20, respectively.

**SITE 3, LINE 2**

(A) Magnetometer survey--total field



(B) Very low frequency electromagnetic survey--tilt angle



(C) Electromagnetic (EM) terrain conductivity survey

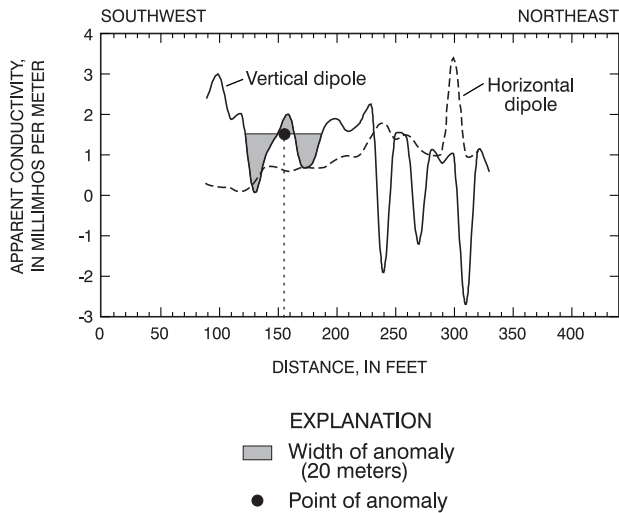
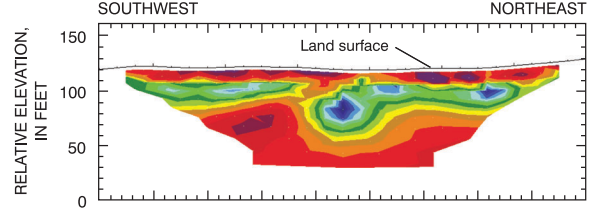


**Figure 22.** Magnetic and electromagnetic surveys at site 3 from line 2, Pelham, N.H. (A) magnetometer survey; (B) very low frequency (VLF) electromagnetic survey; (C) electromagnetic (EM) terrain conductivity survey with a 20-meter (65.6-foot) coil spacing. Site and line locations are shown on figures 1 and 20, respectively.

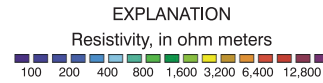
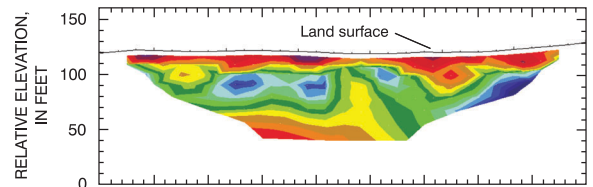
**SITE 3, LINE 1**

**Inverted Resistivity Sections**

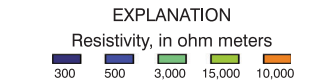
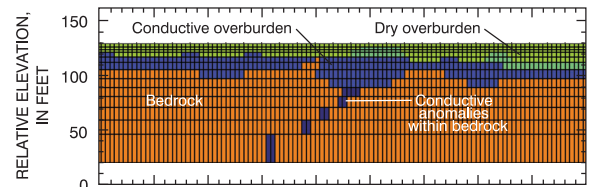
(A) Dipole-dipole array



(B) Schlumberger array

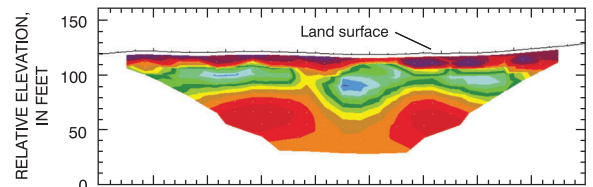


(C) Model



**Synthetic Inverted Resistivity Sections**

(D) Dipole-dipole array



(E) Schlumberger array

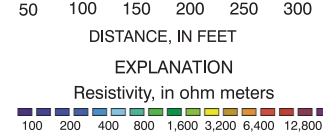
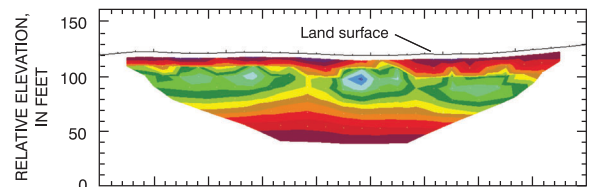
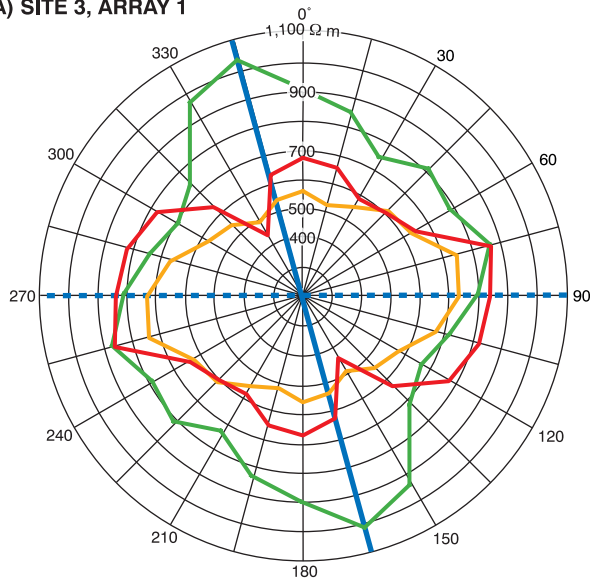


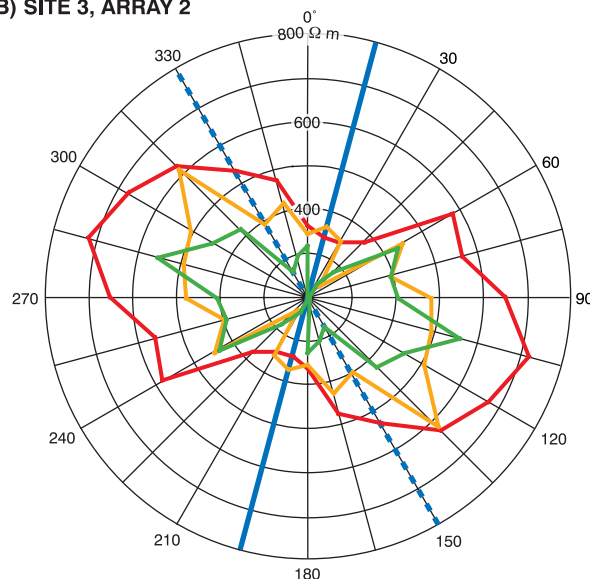
**Figure 23.** Cross sections showing (A and B) inverted resistivity sections of two-dimensional, direct-current resistivity data at site 3 from line 1, Pelham, N.H.; (C) model based on field data from A and B; and (D and E) synthetic resistivity output data from Model C. Site and line locations are shown on figures 1 and 20, respectively.



(A) SITE 3, ARRAY 1



(B) SITE 3, ARRAY 2



EXPLANATION

- |  |                      |
|--|----------------------|
| — Primary strike largest A-spacing       | A-spacing, in meters |
| - - - Secondary strike largest A-spacing | — 5                  |
|  | — 7.1                |
|  | — 10                 |

**Figure 25.** Polar plots showing azimuthal square-array direct-current resistivity at site 3 for arrays 1 and 2, Pelham, N.H. Apparent resistivity in ohm meters ( $\Omega$  m), is plotted as a function of azimuth, in degrees east of true north; (A) resistivity of square array 1, center at 200  $\Omega$  m; (B) resistivity of square array 2, center at 200  $\Omega$  m. Site and array locations are shown on figures 1 and 20, respectively.

Near-horizontal features in bedrock that cannot be identified with a lineament analysis were indicated by 2-D resistivity surveys. These near-horizontal features are identified as sheeting fracture zones, which may enhance the transmissivity of near-vertical fracture zones.

### Site 4, Goffstown, New Hampshire

Site 4 on Mountain Road in Goffstown, N.H., is set in a grassy field and wooded terrain. The site is on the south side of North Uncanoonuc Mountain, and ranges in elevation from about 850 to 930 ft between survey lines. Bedrock geology of this area consist of two variations of the Rangeley Formation, biotite schist and granofels, and rusty biotite-muscovite schist (fig. 26) (T.R. Armstrong and W.C. Burton, U.S. Geological Survey, written commun., 1999). The bedrock is exposed at the surface on the northern part of the study area. The overburden at this site is mapped as a till, which is unsorted to poorly sorted clay silt, sand, pebbles, cobbles and boulders, with some gravel (Koteff, 1970). Lineaments at the site

were identified from LOWALT and HIGHALT aerial photography (Ferguson and others, 1997) trending 27° (fig. 26). These lineaments were fracture correlated by domain-analysis techniques (R.B. Moore and others, U.S. Geological Survey, written commun., 2001). Fracture data in a 4,000-ft radius of the site has five peak orientations: 55°±9° (100 percent, normalized height), 315°±8° (87 percent, normalized height), 272°±11° (75 percent, normalized height), 24°±7° (57 percent, normalized height), and 335°±5° (64 percent, normalized height).

Well GNW 406 (fig. 26), drilled to a depth of 500 ft, has a reported yield of 75 gal/min. The static water level was at a depth of approximately 10 ft after drilling in April 1997, and was at a depth of 64 ft during the borehole-geophysical surveys in December 2000. The drillers' log indicates that the high-yield water-bearing zone is between 420 and 500 ft deep. Probabilities of exceeding a yield of 40 gal/min from a 400-ft deep well at this site ranged from 10 to 38 percent. A 38-percent probability is calculated for the 98.4-ft (30-m) square cell that well GNW 406 is in (R.B. Moore and others, U.S. Geological Survey,

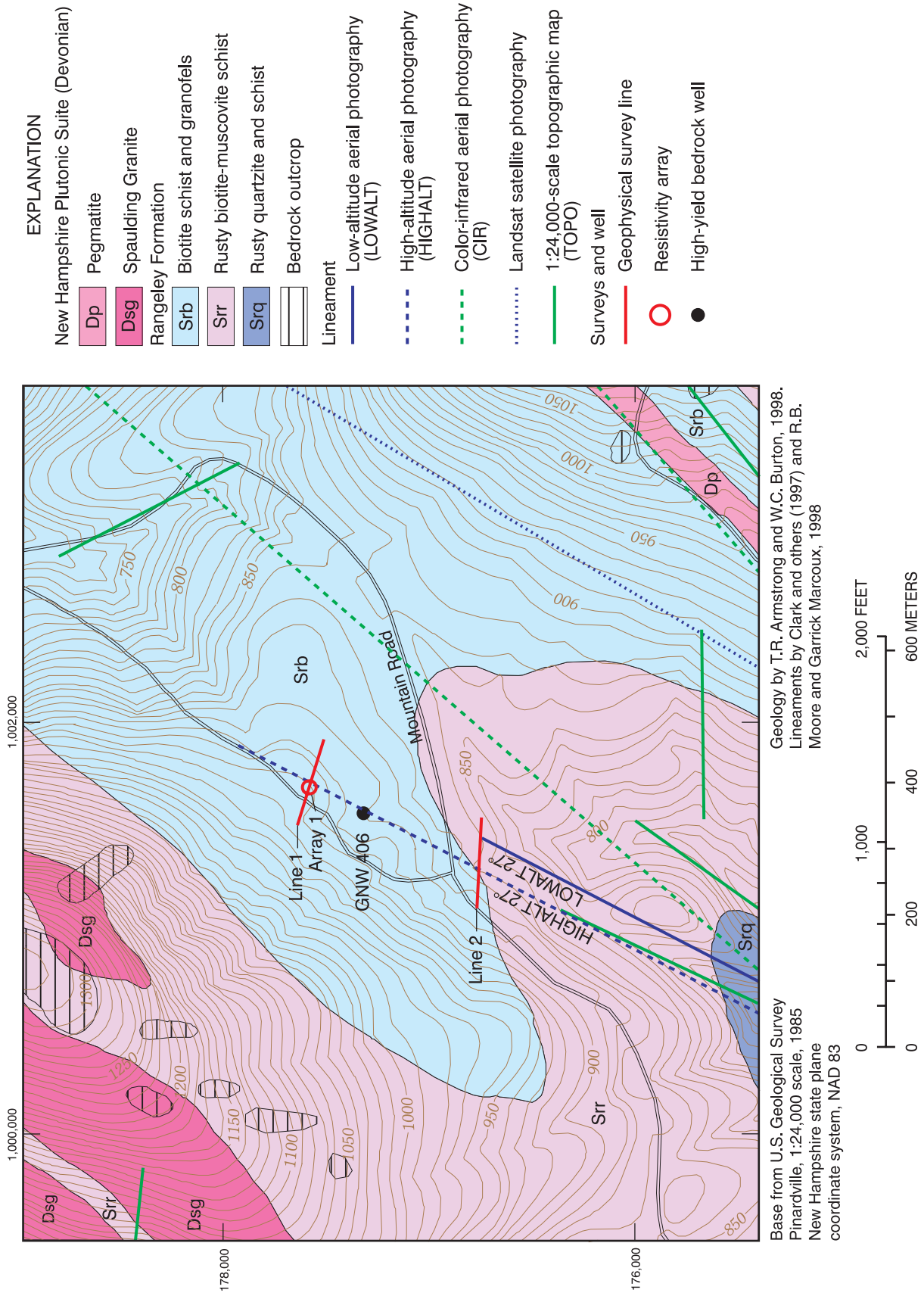


**Figure 26.** Geophysical survey locations, bedrock geology, and lineaments at site 4, Goffstown, N.H. Site location is shown on figure 1.

written commun., 2001). Variations in probability at the site are caused by fracture-correlated lineaments and topography. Two geophysical-survey lines were located to bisect lineaments on either side of the well. Line 1, extending 440 ft from west to east is in the field to the north of the well. Line 2 is in the woods to the south of the well, extending 440 ft from west to east. Array 1 was set on line 1 centered at 190 ft (fig. 26).

### Geophysical Surveys and Interpretation

Six surface and six borehole-geophysical surveys were used to characterize site 4 (figs. 27-31). Overburden thickness and physical properties were derived from GPR, EM, and 2-D resistivity survey results. Magnetometer, VLF, surface EM, 2-D resistivity, square-array resistivity, and borehole-geophysical survey results were used to determine bedrock properties, and identify anomalies that could be caused by bedrock fractures. Borehole-geophysical surveys including caliper, fluid temperature and resistivity, and EM borehole logs were used to characterize and help identify bedrock features seen in the OTV logs.

GPR was collected on lines 1 and 2. Line 1 was surveyed using a continuous profile method, taking advantage of the open field. Subsurface near-horizontal reflectors are seen throughout the line up to 20 ft in depth. Line 2 was collected using a point survey and did not yield consistent reflectors.

Magnetometer measurements were made along line 2 at site 4 (fig. 28a). The average magnetic field measured at this site during the survey is 352 nT. The magnetic field along the line 2 gradually rises, except for a low anomaly of approximately 340 nT between 250 and 330 ft (fig. 28a).

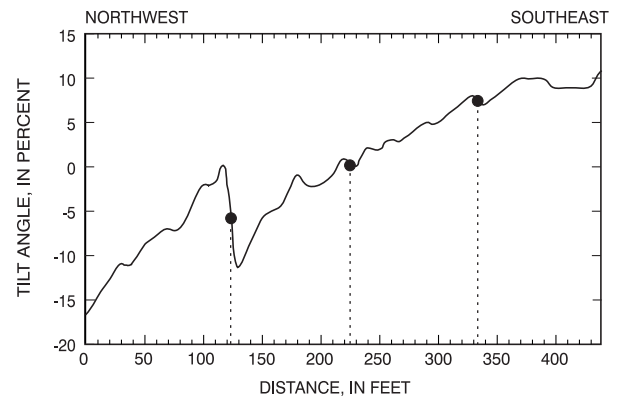
VLF tilt-angle surveys were made at lines 1 and 2. VLF tilt-angle inflections from line 1 are seen at 125, 225, and 335 ft (fig. 27a). VLF tilt-angle survey results from line 2 are obscured by interference from near-by overhead power lines and are not useful (fig. 28b).

EM surveys were collected on both lines at site 4. Line 1 VD anomalies (fig. 27c) that could indicate near-vertical conductors were seen at 160, 230, and 310 ft. VD survey results from line 2 (fig. 28c) indicated anomalies centered at 195 and 380 ft.

Models were created to check interpretation of the 2-D resistivity survey data at lines 1 and 2. Resistivity data from line 1 indicate there are three

### SITE 4, LINE 1

(A) Very low frequency electromagnetic survey—tilt angle



(B) Electromagnetic (EM) terrain conductivity survey

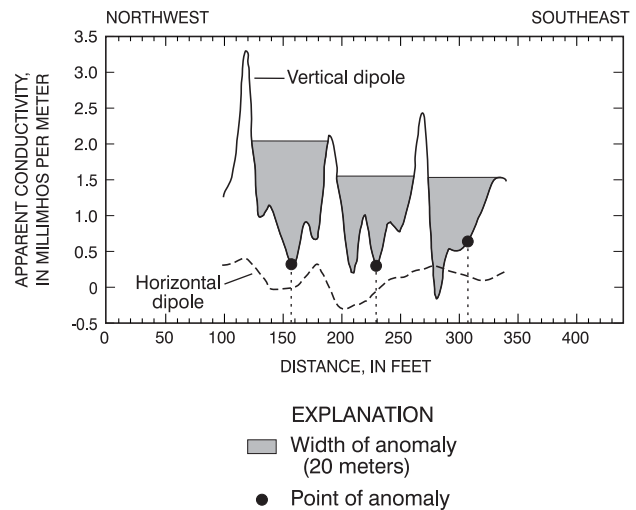


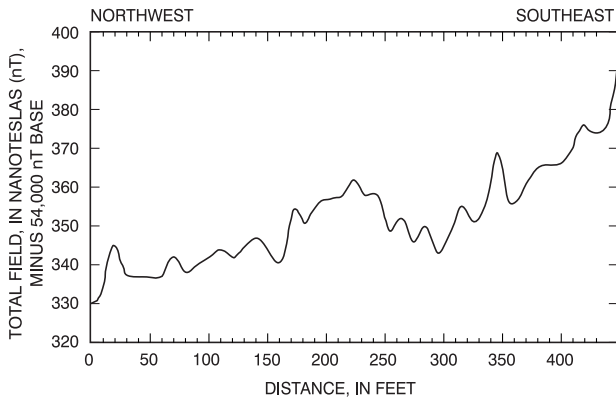
**Figure 27.** Magnetic and electromagnetic surveys at site 4 from line 1, Goffstown, N.H. (A) very low frequency (VLF) electromagnetic survey; (B) electromagnetic (EM) terrain conductivity survey with a 20-meter (65.6-foot) coil spacing. Site and line locations are shown on figures 1 and 26, respectively.

primary units, which likely represent unsaturated overburden and resistive competent and conductive fractured bedrock. A model fit with the field data was obtained by placing the water-table surface in the fracture zones below the top of bedrock at a depth between 40 and 50 ft (relative elevation between 80 and 90 ft). Near-vertical conductive features below the interpreted bedrock surface are interpreted at 190 and 315 ft. Several horizontal conductive features also were interpreted in the bedrock (fig. 29).

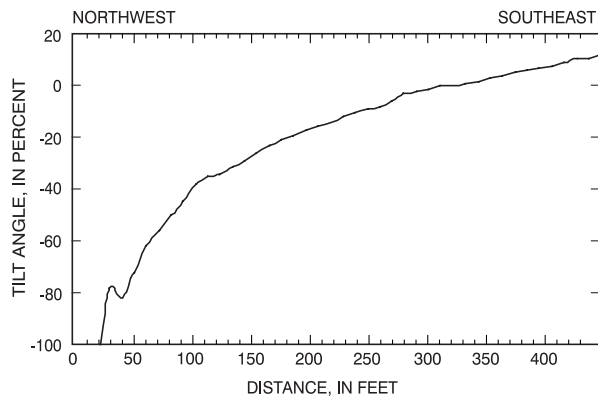
2-D resistivity results from line 2 indicate four units that likely represent resistive unsaturated and conductive saturated overburden, resistive competent

**SITE 4, LINE 2**

**(A) Magnetometer survey--total field**



**(B) Very low frequency electromagnetic survey--tilt angle**



**(C) Electromagnetic (EM) terrain conductivity survey**

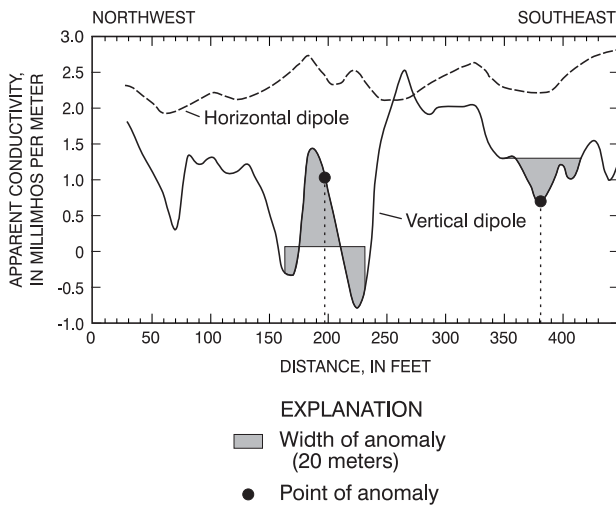
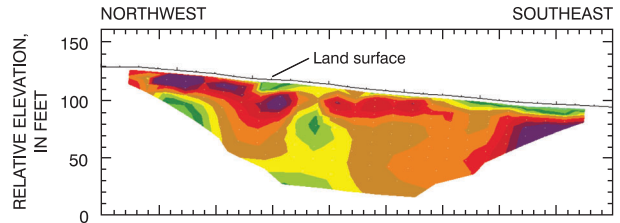


**Figure 28.** Magnetic and electromagnetic surveys at site 4 from line 2, Goffstown, N.H. (A) magnetometer survey; (B) very low frequency (VLF) electromagnetic survey; (C) electromagnetic (EM) terrain conductivity survey with a 20-meter (65.6-foot) coil spacing. Site and line locations are shown on figures 1 and 26, respectively.

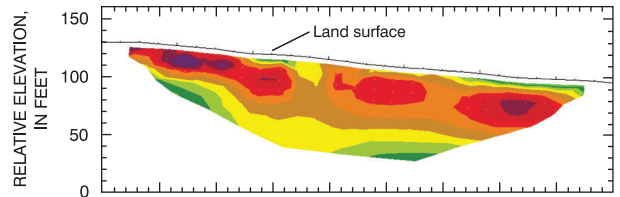
**SITE 4, LINE 1**

**Inverted Resistivity Sections**

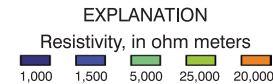
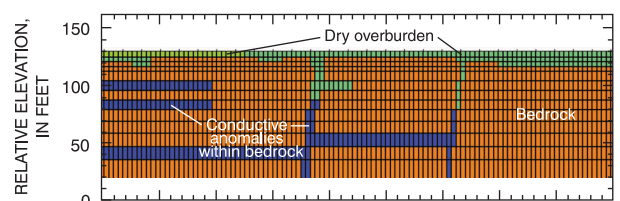
**(A) Dipole-dipole array**



**(B) Schlumberger array**

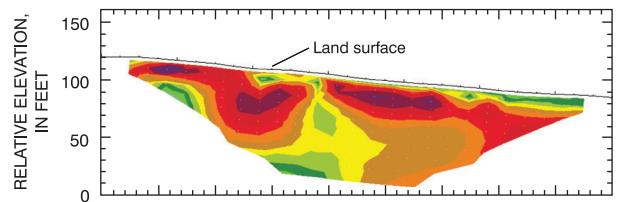


**(C) Model**



**Synthetic Inverted Resistivity Sections**

**(D) Dipole-dipole array**



**(E) Schlumberger array**

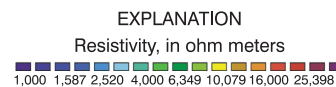
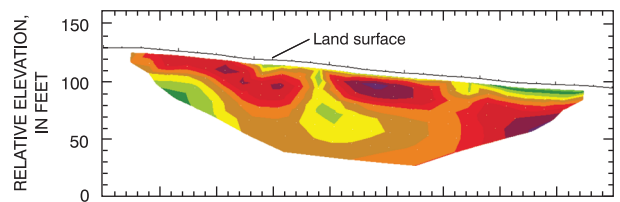


**Figure 29.** Cross sections showing (A and B) inverted resistivity sections of two-dimensional, direct-current resistivity data at site 4 from line 1, Goffstown, N.H.; (C) model based on field data from A and B; and (D and E) synthetic resistivity output data from Model C. Site and line locations are shown on figures 1 and 26, respectively.

**SITE 4, LINE 2**

**Inverted Resistivity Sections**

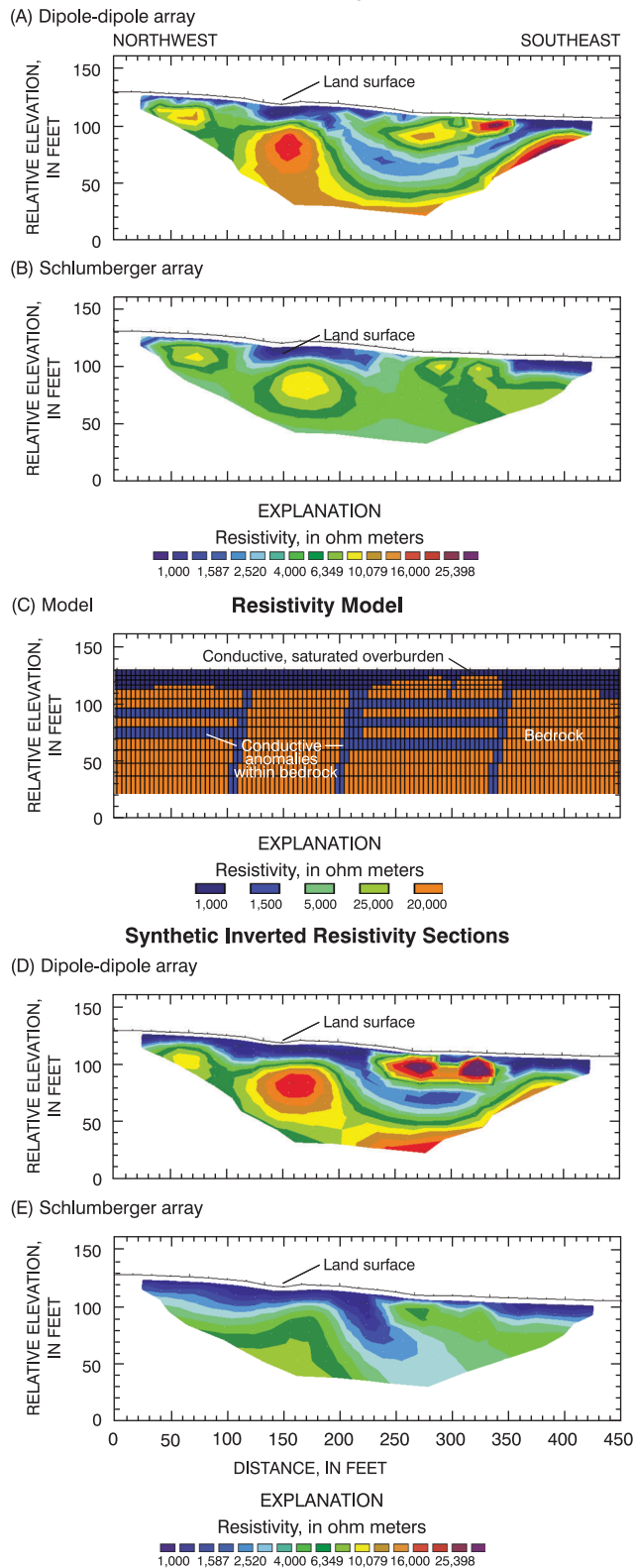


**Figure 30.** Cross sections showing (A and B) inverted resistivity sections of two-dimensional, direct-current resistivity data at site 4 from line 2, Goffstown, N.H.; (C) model based on field data from A and B; and (D and E) synthetic resistivity output data from Model C. Site and line locations are shown on figures 1 and 26, respectively.

bedrock, and conductive fractured bedrock. Near-vertical conductive anomalies below the bedrock surface are interpreted with a steep apparent dip to the west at 100, 210, and 360 ft (fig. 30). Horizontal conductive zones below the bedrock surface are interpreted, which are corroborated by the model results (fig. 30c).

Square-array resistivity data were collected at array 1. The primary conductive strike at the deepest A-spacing (7.1-m) was 60°, with a range of 30° to 60°. The shallow conductive strike measured with a 5-m A-spacing was oriented at 45° with a 15° to 45° range (fig. 31).

Caliper and EM conductivity logs for well GNW406 (appendix 1a) were used to identify fracture zones on OTV logs. Transmissive-fracture zones were identified by fluid-temperature and fluid-resistance logs (appendix 1a) at approximately 150, 295, and 330 ft. The orientations of several open fractures were

**SITE 4, ARRAY 1**

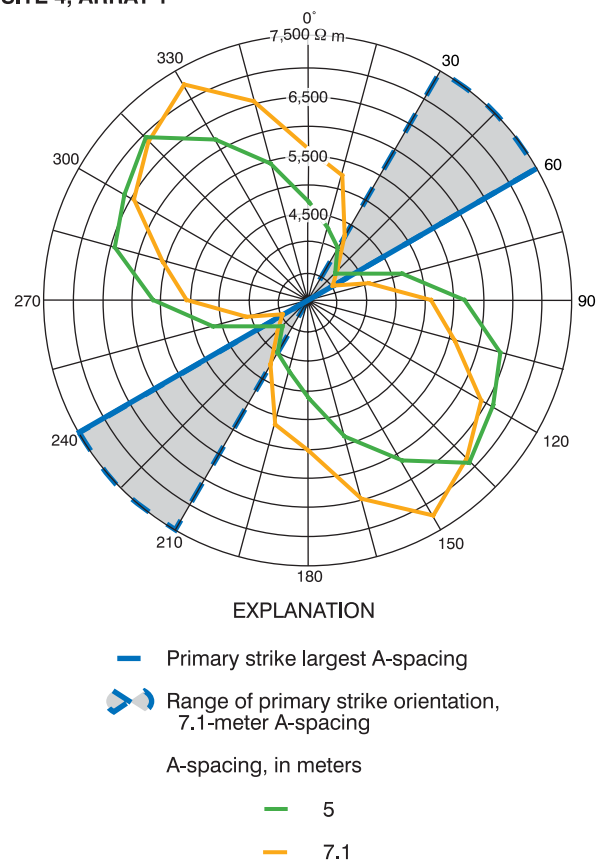


**Figure 31.** Polar plot showing azimuthal square-array direct-current resistivity at site 4 for array 1, Goffstown, N.H. Apparent resistivity in ohm meters ( $\Omega$  m), is plotted as a function of azimuth, in degrees east of true north, and resistivity center is at 3,000  $\Omega$  m. Site and array locations are shown on figures 1 and 26, respectively.

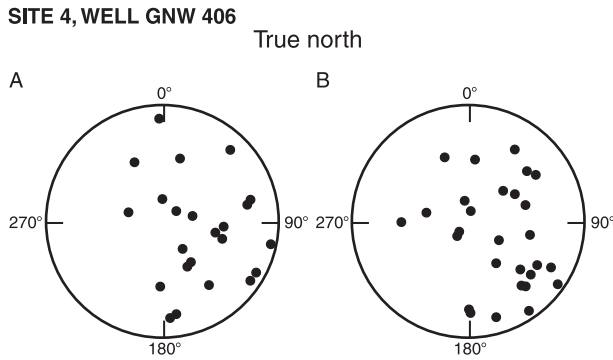


**Figure 32.** Lower hemisphere equal-area nets from bedrock well GNW 406 at site 4, Goffstown, N.H., showing (A) borehole fractures and (B) borehole contacts and foliation. Site and well locations are shown on figures 1 and 26, respectively.

determined using OTV logs. The OTV did not identify all of the fracture zones indicated with the other borehole techniques. Rock that is dark in color limits fracture identification with the OTV. Twenty-three fractures, and 28 contacts and foliation trends, were identified with the OTV log, with a broad range of orientations lacking definitive groups (fig. 32). In the high-yield zone between 420-500 ft below land surface, only two fractures were identified from the OTV log. At the bottom of the well, at 497 ft, the caliper-measured anomaly indicates a fracture zone that is not measurable with the OTV since the scanning window is above the bottom of the tool.

## Integration of Results

Line 1 has VLF and EM anomalies indicative of conductive-bedrock features at about 225 ft (fig. 27). 2-D resistivity and EM anomalies, also indicative of conductive features in bedrock, are found at about 310 ft (figs. 27 and 29). Line 2 has 2-D resistivity and EM anomalies indicative of conductive bedrock features located at about 195 ft (figs. 28 and 30). The magnetic low from the magnetometer-survey results corresponds with the interpreted sheeting fracture zones from the 2-D resistivity (figs. 28 and 30).

Array 1 has a primary bedrock strike of 60°, with essentially the same strike (55°±9°) as the maximum peak in the geologic-data analysis. The range of orientations from the square-array resistivity shallow conductive strike of 15° to 45° correlates with mapped lineament orientations between lines 1 and 2 of 27°, and the strike of a fracture peak in the geological data of 24°±7° (57 percent, normalized height). A

fracture identified in well GNW 406 at 90.6 ft depth, having a strike and dip of 209× (209×-180×=29°) and 65×, also correlates with the trends of the square-array resistivity, lineament, and geologic data peak.

Borehole-geophysical surveys identified transmissive fractures in well GNW 406. A wide scattering of fracture orientations were identified in the analysis of the borehole data (fig.32a). The average of all of the fracture trends (75°) and contact and foliation trends (85°) are close (when normalized for the right hand rule, indicating that fractures often follow contact and foliation in this borehole. The average dip of the fractures, contacts (38°) and foliation (36°) seen in the borehole are less than the dip of fracture zones that sometimes are indicated by lineaments. A negative, vertical-fracture-sampling bias must be considered because the borehole is near vertical. Fracture orientations could not be collected at the bottom of the well where a water-producing fracture may be located.

Electromagnetic (EM and VLF) surveys indicate electrically conductive anomalies that are consistent with fractured bedrock but were limited, by cultural noise. DC-resistivity surveys and arrays and geologic information indicated that the 27°-trending lineaments at this site overlie near-vertical conductive features that likely represent water-transmitting bedrock-fracture zones. Near-horizontal features in bedrock, which cannot be identified with a lineament analysis, were identified with 2-D resistivity and borehole-survey analysis. These near-horizontal features are identified as sheeting-fracture zones, which may transmit water to vertical fracture zones. Square array, geologic-outcrop fractures, and lineaments support a dominant northeast-trending water-bearing fracture zone at site 4 in Goffstown.

## Site 5, Goffstown, New Hampshire

Site 5 on Shirley Hill Road in Goffstown, is a relatively flat grassy field on the side of a hill at an elevation of about 730 to 750 ft in the surveyed area. The bedrock geology of this area is composed of the Rangeley Formation (T.R. Armstrong and W.C. Burton, U.S. Geological Survey, written commun., 1999). Three different variations of the Rangeley Formation have contacts at the site—biotite schist and granofels, migmatite schist and gneiss, and rusty biotite-muscovite schist (fig. 33). Bedrock is

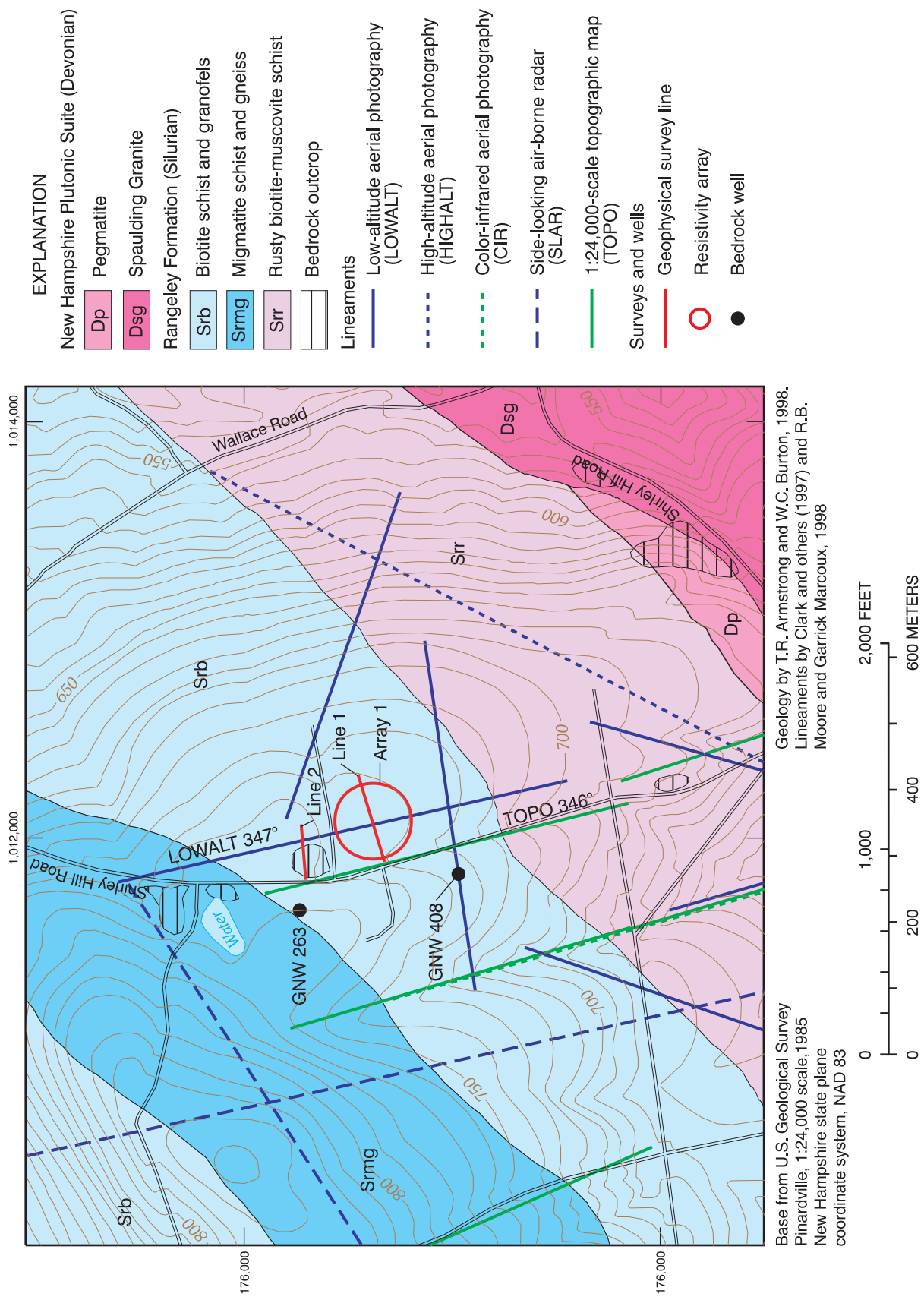


**Figure 33.** Geophysical survey locations, bedrock geology, and lineaments at site 5, Goffstown, N.H. Site location is shown on figure 1.

exposed in the northern most part of the surveyed area. The overburden at this site is till, which is unsorted to poorly sorted clay, silt, sand, pebbles, cobbles and boulders, with some gravel (Koteff, 1970). Mapped lineaments at the site were observed from LOWALT (Ferguson and others, 1997), and TOPO platforms trending  $347^\circ$  and  $346^\circ$ , respectively (fig. 33). These lineaments are visible at the site as swales trending about  $340^\circ$ . Fracture data in a 4,000-ft radius of the site has four peak orientations:  $34^\circ \pm 7^\circ$  (100 percent, normalized height),  $301^\circ \pm 6^\circ$  (32 percent, normalized height),  $5^\circ \pm 7^\circ$  (24 percent, normalized height), and  $340^\circ \pm 11^\circ$  (15 percent, normalized height). Fractures measured in an outcrop just south of the site on the side of Shirley Hill Road, have a strike and dip of  $355^\circ$  and  $80^\circ$ .

Well GNW 263 drilled to a depth of 150 ft has a reported yield of 80 gal/min. The static water level and bedrock are at a depth of 10 ft according to the drillers' log. Well GNW 408 was installed for domestic use during this study and provided an opportunity for logging by a geologist during its drilling and a survey with borehole-geophysical tools. The depth of the till, at GNW 408, was 21 ft and the well was completed at 200 ft into bedrock. The well was completed shortly after the demand for domestic use was met and exceeded in this case. A 20-gal/min producing zone was identified during drilling between 170 and 175 ft, and is described as a contact between a muscovite-quartz-feldspar granofels and a muscovite biotite granofels (S.F. Clark, Jr., U.S. Geological Survey, written commun., 1999).

The probability of exceeding a yield of 40 gal/min from a 400-ft-deep well at this site ranged from 12 to 14 percent. A 14-percent probability is calculated for the 98.4-ft (30-m) square cell that well GNW 263 is in (R.B. Moore and others, U.S. Geological Survey, written commun., 2001). Well GNW 408 is in a cell with a 12-percent probability. Variations in probability at the site appear to be caused by topography. Two geophysical-survey lines bisect lineament locations. Line 1 is in a field to the southeast of the GNW 263 and line 2 is in a field to the east of the well. A center location for array 1 was set in the swale at 230 ft on line 1 (fig. 33).

### Geophysical Surveys and Interpretation

Seven surface and six borehole geophysical surveys were used to characterize site 5. Overburden

thickness and physical properties were derived from GPR, EM, and 2-D resistivity survey results. Bedrock properties and anomalies that could be caused by bedrock fractures were observed in seismic-refraction, magnetometer, VLF, EM, 2-D resistivity and square-array resistivity, and borehole-geophysical survey results. Caliper, EM borehole, and a drillers' log was used to characterize and help identify bedrock fractures measured with the OTV logs.

Seismic-refraction data were collected in two orientations separated by  $90^\circ$  at lines 1 and 2. The bedrock seismic-wave velocities were compared at each orientation. Seismic-refraction-data collection at lines 1 and 2 were centered at 220 and 135 ft along the lines. The average velocity of the seismic wave in bedrock along, and normal to, line 1 is 13,500 and 14,000 ft/s respectively, and do not indicate a large velocity contrast. The average velocity of the bedrock along line 2 is 14,000 ft/s, and the average velocity normal to line 2 is 11,500 ft/s, which are indicative of a contrast.

GPR data were collected at the two lines at site 5 using a continuous profile method. Electrically conductive till attenuated the radar signal and useful radar records could not be identified.

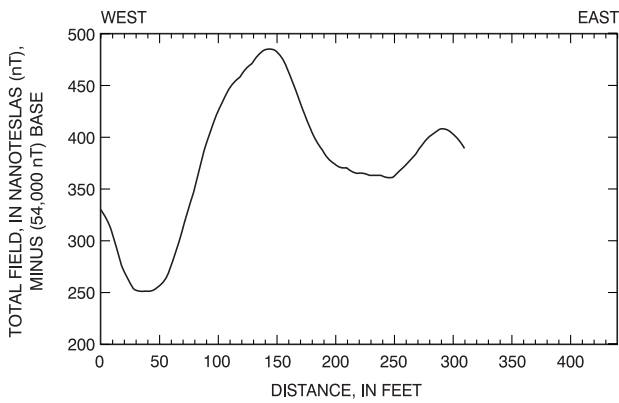
The average magnetic field measured at site 5 during the survey was 374 nT. Low magnetic anomalies of 250 nT between 30 and 60 ft, and of 350 nT between 200 and 250 ft were identified along line 1 (fig. 34a). Metal farm machinery parked on line 2 prevented a magnetic survey from being conducted.

VLF tilt-angle surveys were made at lines 1 and 2. Line 1 has VLF inflections at 130 and 155 ft (fig. 34b). Line 2 has an inflection centered at 165 ft (fig. 35a).

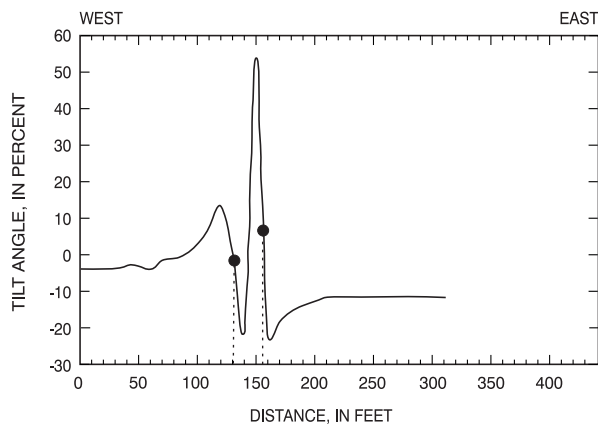
EM surveys also were collected on lines 1 and 2 at site 5. Apparent conductivity had a range from 26 to -28 mmho/m. Along line 1, an anomaly in the VD measurement that could be related to a near-vertical conductor was observed at 180 ft (fig. 34c). An additional EM survey done 50 ft to the south and parallel to line 1 produced similar results. The height of the peaks of the anomaly indicates a dip to the west. Along line 2, an anomaly in the VD measurement with a 20-m (65.6-ft) coil spacing that could be related to a near-vertical subsurface conductor was centered at 160 ft (fig. 35b). The height of the peaks of the anomaly is consistent with the line 1 anomalies, indicating a dip to the west. EM measurements with a 40-m (131.2 ft) coil spacing also were made along

**SITE 5, LINE 1**

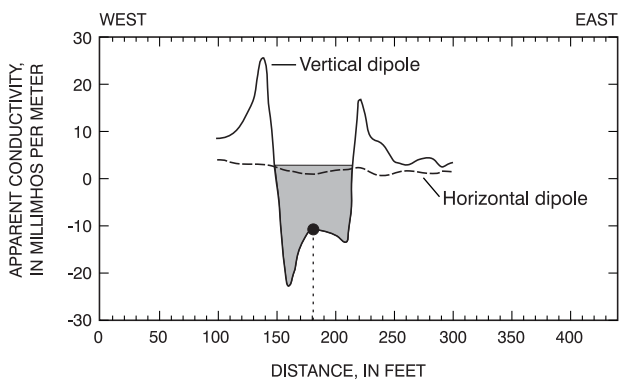
(A) Magnetometer survey--total field



(B) Very low frequency electromagnetic survey--tilt angle



(C) Electromagnetic (EM) terrain conductivity survey

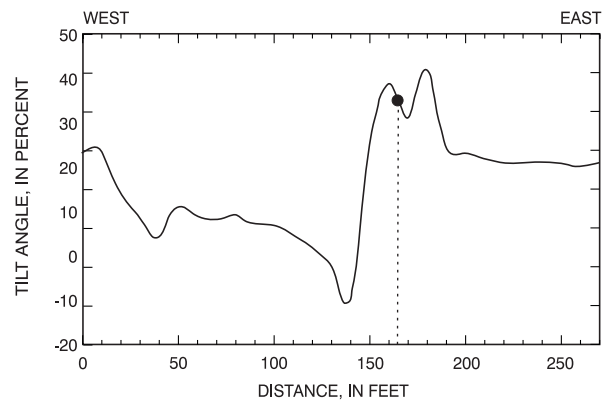


**EXPLANATION**  
 ■ Width of anomaly (20 meters)  
 ● Point of anomaly

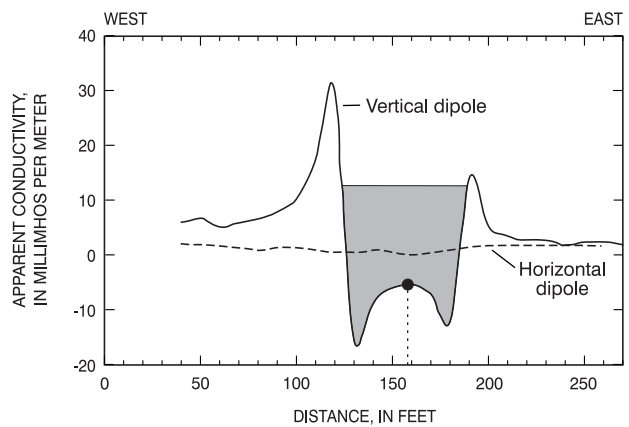
**Figure 34.** Magnetic and electromagnetic surveys at site 5 from line 1, Goffstown, N.H. (A) magnetometer survey; (B) very low frequency (VLF) electromagnetic survey; (C) electromagnetic (EM) terrain conductivity survey with a 20-meter (65.6-foot) coil spacing. Site and line locations are shown on figures 1 and 33, respectively.

**SITE 5, LINE 2**

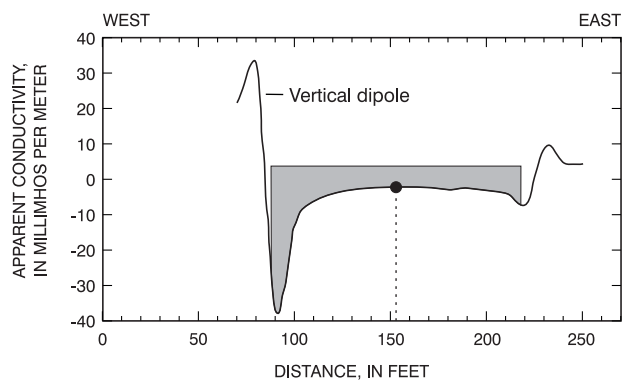
(A) Very low frequency electromagnetic survey--tilt angle



(B) Electromagnetic (EM) terrain conductivity survey



(C) Electromagnetic (EM) terrain conductivity survey



**EXPLANATION**  
 ■ Width of anomaly equal to coil spacing  
 ● Point of anomaly

**Figure 35.** Magnetic and electromagnetic surveys at site 5 from line 2, Goffstown, N.H. (A) very low frequency (VLF) electromagnetic survey; (B) electromagnetic (EM) terrain conductivity survey with a 20-meter (65.6-foot) coil spacing; (C) electromagnetic (EM) terrain conductivity survey with a 40-meter (131.2-foot) coil spacing. Site and line locations are shown on figures 1 and 33, respectively.

line 2 (fig. 35c). The 40-m-coil spacing surveys at a greater depth than the 20-m-coil spacing and indicates that a west-dipping anomaly continues at depth.

2-D resistivity surveys were done at lines 1 and 2. Models were used to verify interpretations of the data. Resistivity data from lines 1 and 2 show four resistivity units, likely representing resistive-unsaturated, and conductive-saturated sediments, and resistive-competent and conductive-fractured bedrock. Below the interpreted bedrock surface, at around 190 ft along the line, is a conductive anomaly penetrating into the bedrock (fig. 36). Resistivity data from line 2 (fig. 37) indicate a horizontal conductive feature between 140 and 180 ft at a depth of about 20 ft. A steep, west-dipping conductive feature in bedrock is interpreted at 160 ft (fig. 37).

Square-array resistivity data were collected at array 1. A-spacings of 5-40 m were used. Resistivity data from array 1 surveyed with a 40-m A-spacing has a primary conductive strike of  $0^\circ$ , and a secondary strike of  $30^\circ$ . The anomaly forming the secondary strike ranged from  $15^\circ$  to  $45^\circ$ . The surveys with small A-spacings indicate a primary conductive strike of  $30^\circ$  and a secondary conductive strike of  $0^\circ$  (fig. 38).

Caliper and EM conductivity logs were used in well GNW 408 to identify fracture zones on OTV logs (appendix 1b). A total of 12 fractures, including 6 open-fracture orientations were determined using the OTV log. Two groups of fractures (fig. 39a) that were identified on the OTV log, have a range of strikes and dips between  $317\text{-}342^\circ$  and  $25\text{-}42^\circ$ , dipping NE, and  $202\text{-}225^\circ$  and  $22\text{-}51^\circ$ , dipping NW. A group of contacts and foliation trends were identified that have a range of strikes and dips of  $180\text{-}210^\circ$  and  $21\text{-}58^\circ$ , dipping NW (fig. 39b). These trends indicate that the large group of fractures are coincident with foliation or contacts. A fracture on a contact that was identified as producing 20 gal/min during drilling from the OTV log has a strike and dip of  $180^\circ$  and  $21^\circ$ . Strong borehole EM-conductivity anomalies are identified above and below this water-bearing zone.

### Integration of Results

Line 1 has conductive 2-D resistivity, EM, and VLF anomalies from 160-180 ft. Conductive anomalies on line 2 appear near 160 ft along the line from the results of 2-D resistivity, EM (20- and 40-m coil spacing) and VLF surveys. At site 5, a number of geophysical anomalies (VLF, EM, and 2-D resistivity)

were particularly distinct; the EM anomaly was especially large and distinct.

Conductive-striking bedrock features interpreted from square-array resistivity results have the same orientation as fractures identified in outcrop and remotely sensed lineaments. These features likely are related to fracture zones. The deep primary strike from array 1 of  $0^\circ \pm 7.5$  is less than  $6.5^\circ$  of the orientation of the lineament it is centered on, which has a strike of  $347^\circ$ , and is the same as fractures measured in outcrops adjacent to the site ( $355^\circ$ ,  $80^\circ$ ). The secondary strike from array 1 has the same orientation as the axis of foliation seen in a neighboring outcrop, and coincides with the orientation of the largest geologic-data fracture peak for the site. Secondary strikes in the square-array resistivity data, at depth, range from  $15^\circ$  to  $45^\circ$  and may be explained by a fold-axis trend of  $43^\circ$ . The LOWALT lineament between lines 1 and 2 strikes  $347^\circ$  and correlates with a small fracture peak from geological mapping data. This peak has a strike of  $340^\circ \pm 11^\circ$  (15 percent, normalized height).

Borehole-geophysical surveys identified a group of fractures with an average strike ( $330^\circ$ ) that matches a peak in the geologic-outcrop fracture data. This peak has a strike of  $340^\circ \pm 11^\circ$  (15 percent, normalized height).

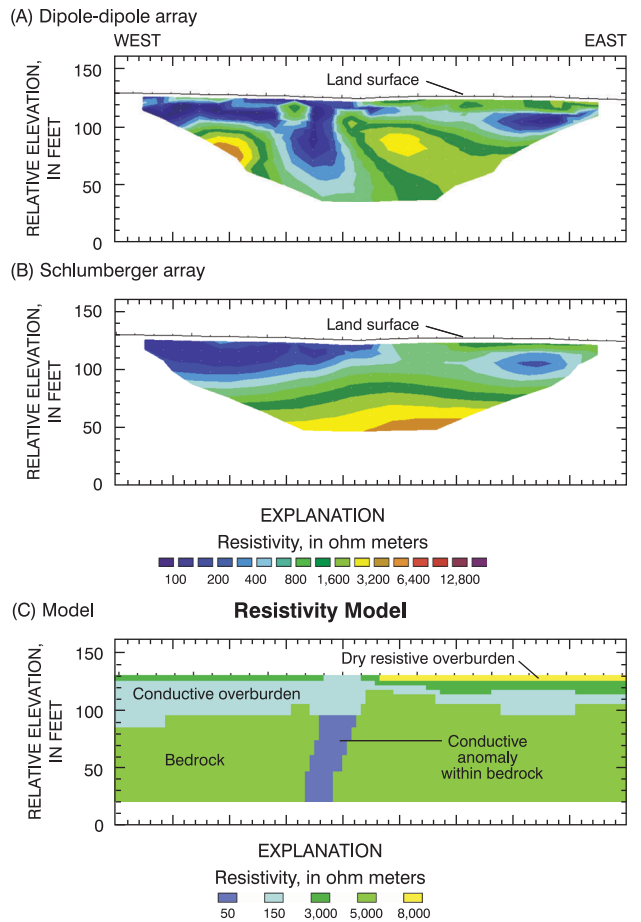
Electromagnetic (EM and VLF) and DC-resistivity (2-D and square-array) surveys and geologic information indicate strong electrically conductive anomalies that are consistent with fractured bedrock. These surveys indicate that lineaments likely represent steep-westward-dipping conductive bedrock features. These features may represent fractured-bedrock zones likely to transmit water.

### Site 6, Salem, New Hampshire

Site 6 on Brady Road in Salem, N.H., is a flat, and often wet, grassy field at an elevation of about 130 ft. The water table in the overburden at the site ranges in depth from 0-2 ft below the land surface. Overburden material at the site is mapped as a coarse-grained (medium sand to cobble gravel) stratified drift. Saturated thickness ranged from 20 to greater than 40 ft; transmissivity of the stratified-drift aquifer is between 1,001 and 4,000  $\text{ft}^2/\text{d}$  (Stekl and Flanagan, 1992). Lyons and others (1997) mapped the bedrock

**SITE 5, LINE 1**

**Inverted Resistivity Sections**



**Synthetic Inverted Resistivity Sections**

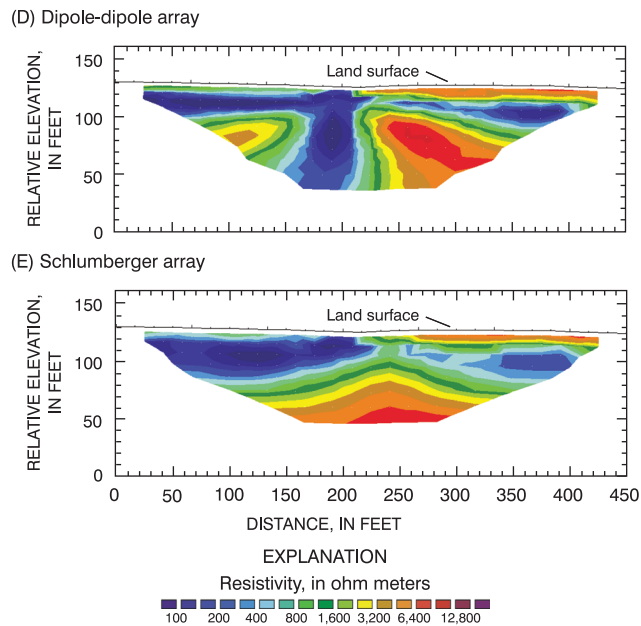
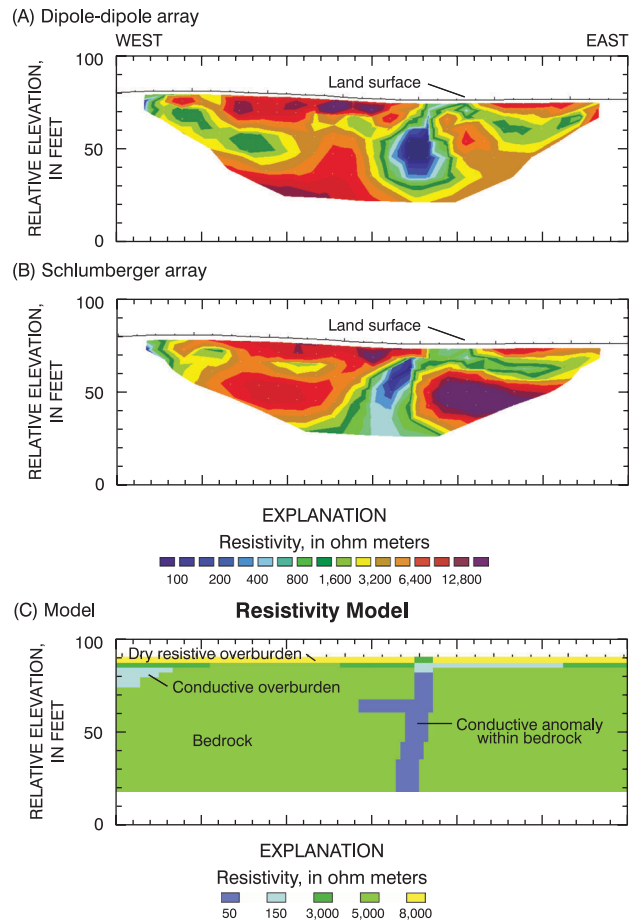


**Figure 36.** Cross sections showing (A and B) inverted resistivity sections of two-dimensional, direct-current resistivity data at site 5 from line 1, Goffstown, N.H.; (C) model based on field data from A and B; and (D and E) synthetic resistivity output data from Model C. Site and line locations are shown on figures 1 and 33, respectively.

**SITE 5, LINE 2**

**Inverted Resistivity Sections**



**Synthetic Inverted Resistivity Sections**

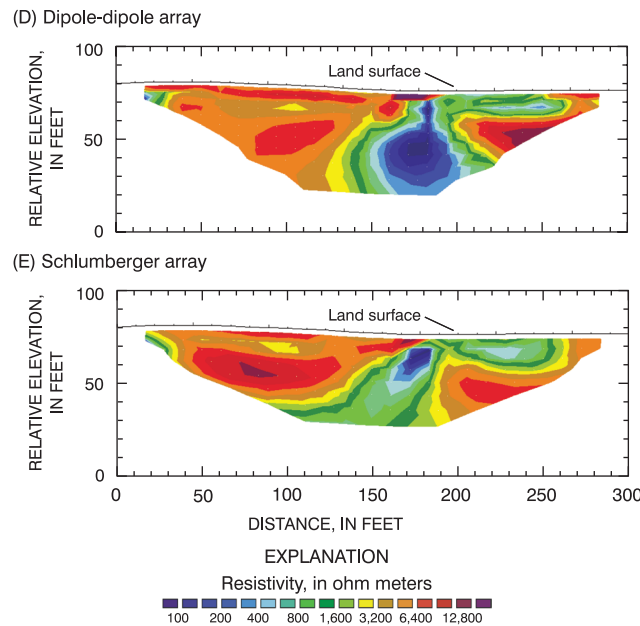


**Figure 37.** Cross sections showing (A and B) inverted resistivity sections of two-dimensional, direct-current resistivity data at site 5 from line 2, Goffstown, N.H.; (C) model based on field data from A and B; and (D and E) synthetic resistivity output data from Model C. Site and line locations are shown on figures 1 and 33, respectively.

**SITE 5, ARRAY 1**

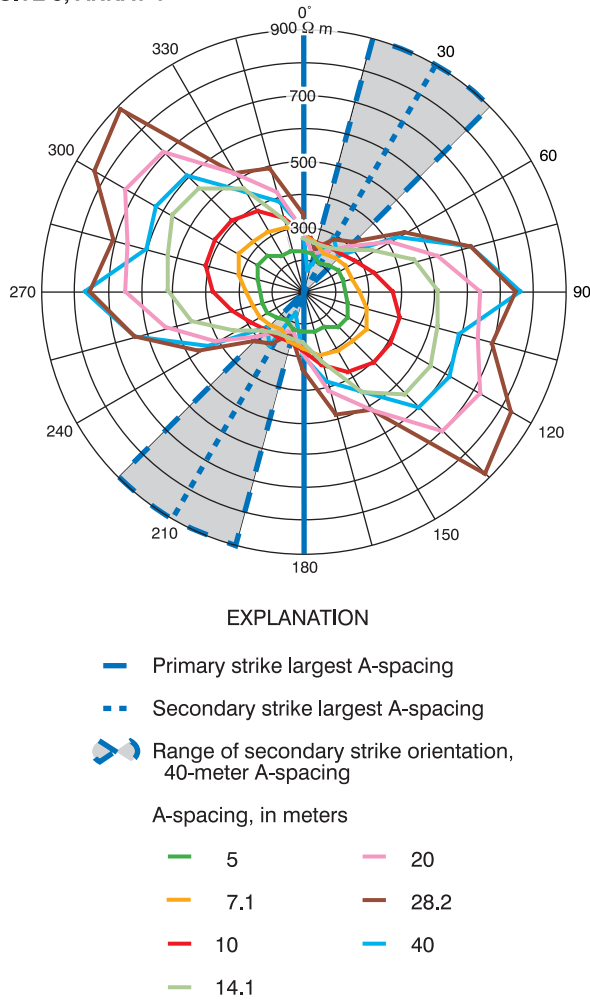


**Figure 38.** Polar plot showing azimuthal square-array direct-current resistivity at site 5 for array 1, Goffstown, N.H. Apparent resistivity in ohm meters ( $\Omega m$ ), is plotted as a function of azimuth, in degrees east of true north, and resistivity center is at 100  $\Omega m$ . Site and array locations are shown on figures 1 and 33, respectively.

geology of this area as the Berwick Formation of the Merrimack Group. Mapped lineaments at the site were observed from LOWALT and HIGHALT platforms (Ferguson and others 1997), trending  $44^\circ$  and  $353^\circ$ , respectively (fig. 40). Fracture data inside a 4,000-ft radius of the site has three peak orientations:  $37^\circ \pm 6^\circ$  (100 percent, normalized height),  $294^\circ \pm 7^\circ$  (67 percent, normalized height), and  $278^\circ \pm 4^\circ$  (50 percent, normalized height). The closest fracture measured in outcrop is more than 3,000 ft away.

Well SAW 207 was drilled to a depth of 533 ft at site 6 (fig. 40) and has a reported yield of 630 gal/min. The depth to bedrock at well SAW 207 is approxi-

mately 18 ft. A nearby test well SAW 272 was available for borehole-geophysical surveys. Well SAW 272 was drilled through 17 ft of overburden to a depth of 345 ft in bedrock and has a reported yield of 150 gal/min. Sediment accumulation or rock fragments at the bottom of the well SAW 272 likely account for the borehole tools being unable to reach a depth greater than 335 ft. Three geophysical survey lines bisected lineaments (fig. 40). All of the lines are to the south of the wells in the open field. Line 1 extends 750 ft from northwest to southeast. Line 2 extends 440 ft from northwest to southeast. Line 3 extends 440 ft from west to east. Array 1 was centered between the western ends of lines 2 and 3 (fig. 40).

### Geophysical Surveys and Interpretation

Six surface and six borehole geophysical surveys were used to characterize site 6. Overburden thickness and physical properties were derived from GPR, EM, and 2-D resistivity survey results. Seismic-refraction, EM, 2-D resistivity, and square-array resistivity surveys were used to determine bedrock properties. Anomalies that could be caused by bedrock fractures are seen in the VLF, EM, 2-D resistivity and square-array resistivity survey results. Caliper, fluid temperature and resistivity, and EM borehole logs were used to characterize and help identify bedrock fractures measured in the OTV logs.

Seismic-refraction modeling was used to identify a bedrock seismic velocity of 9,800 ft/s parallel to line 1 (K.J. Ellefsen, U.S. Geological Survey, written commun. 1997). This velocity is just

**SITE 5, WELL GNW 408**

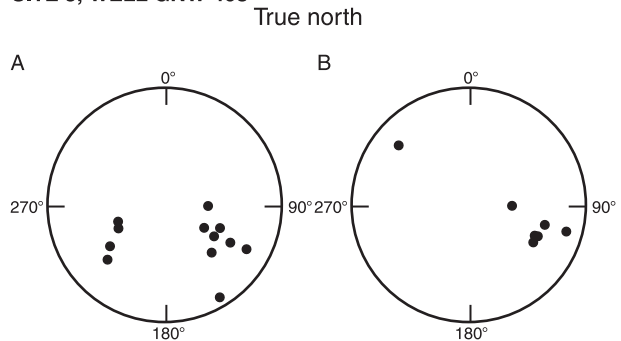


**Figure 39.** Lower hemisphere equal-area nets from bedrock well GNW 408 at site 5, Goffstown, N.H., showing (A) borehole fractures and (B) borehole contacts and foliation. Site and well locations are shown on figures 1 and 33, respectively.

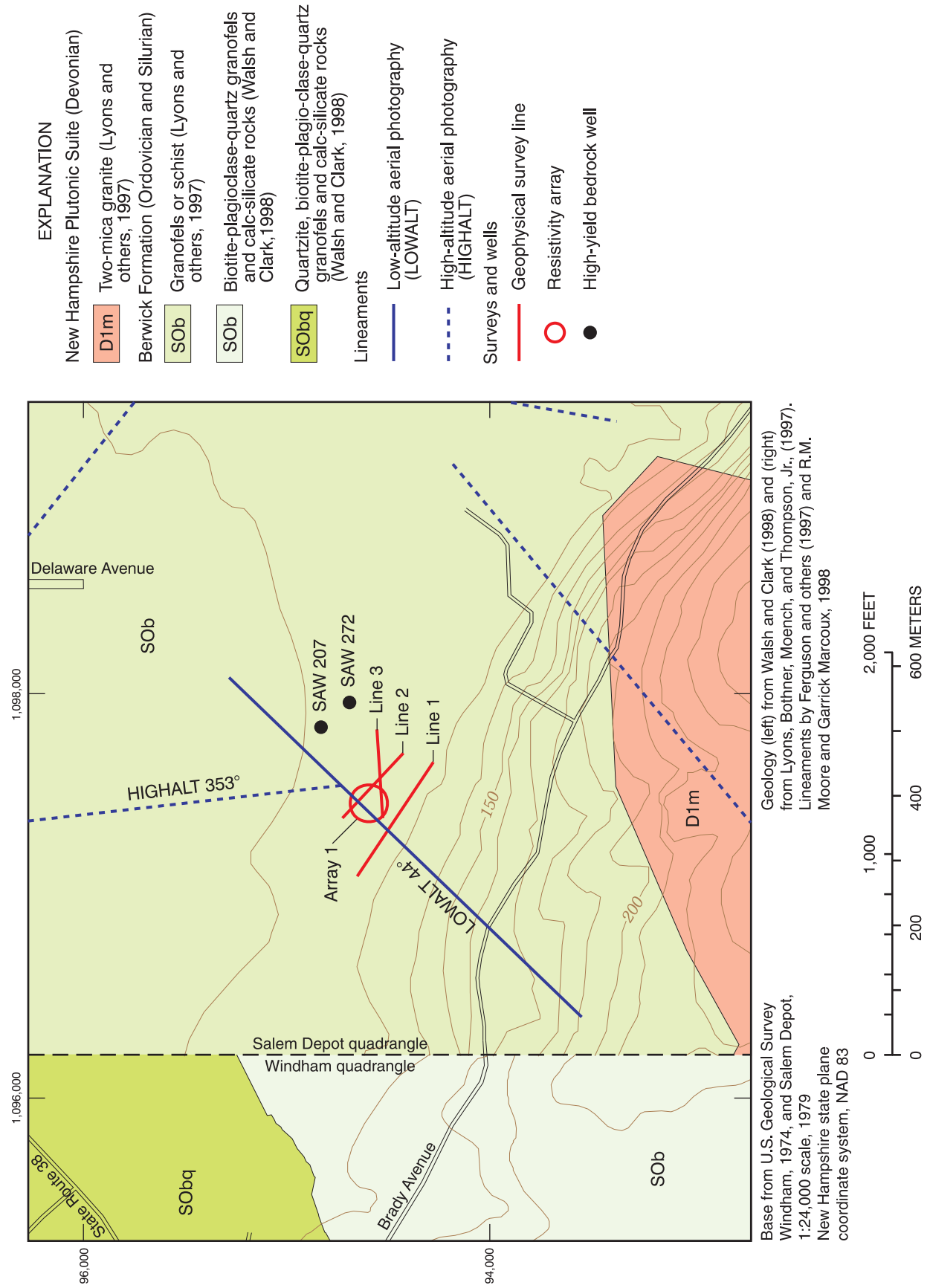
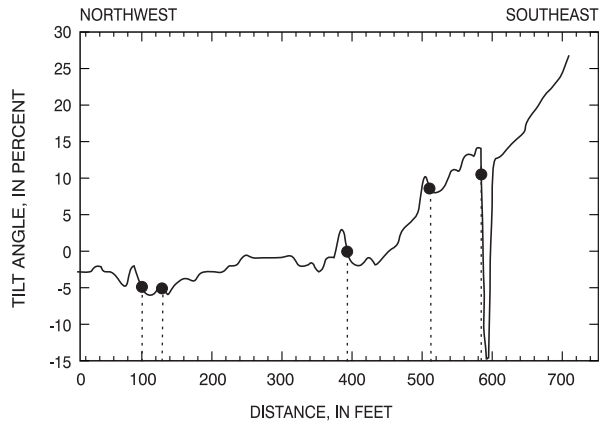


**Figure 40.** Geophysical survey locations, bedrock geology, and lineaments at site 6, Salem, N.H. Site location is shown on figure 1.

**SITE 6, LINE 1**

(A) Very low frequency electromagnetic survey--tilt angle



(B) Electromagnetic (EM) terrain conductivity survey

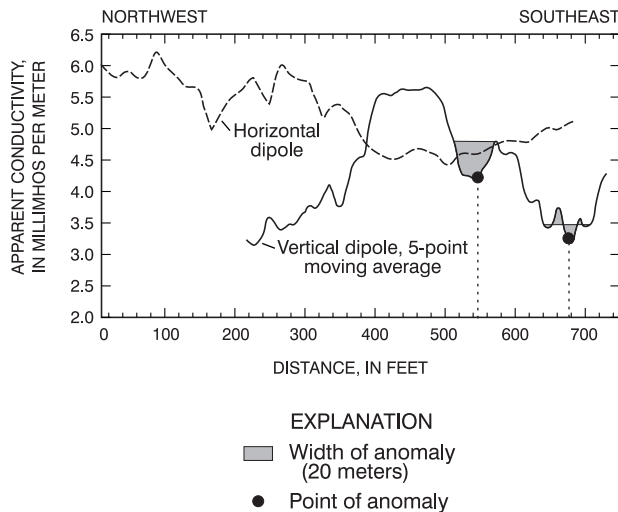


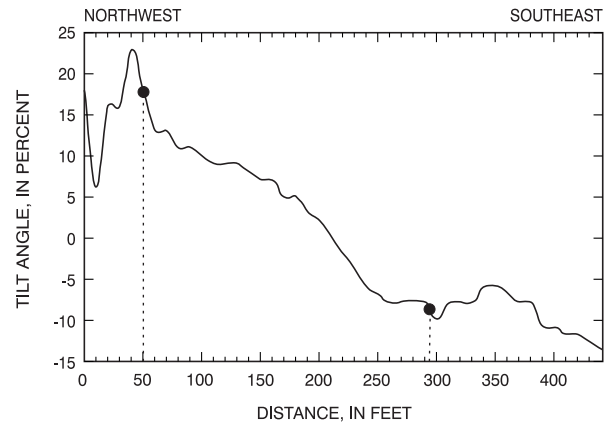
**Figure 41.** Electromagnetic surveys at site 6 from line 1, Salem, N.H. (A) very low frequency (VLF) electromagnetic survey; (B) electromagnetic (EM) terrain conductivity survey with a 20-meter (65.6-foot) coil spacing. Site and line locations are shown on figures 1 and 40, respectively.

below the low end of the range of bedrock velocities (10,000 to 20,000 ft/s) typically found in New Hampshire (Medalie and Moore, 1995). A low trough in the bedrock was noted beneath the LOWALT lineament.

GPR was collected on all lines at site 6. Lines 2 and 3 were collected using a continuous profile method, line 1 was collected using the point-survey method. Reflectors were identified in the overburden but the signal was attenuated before reaching bedrock.

**SITE 6, LINE 2**

Very low frequency electromagnetic survey--tilt angle



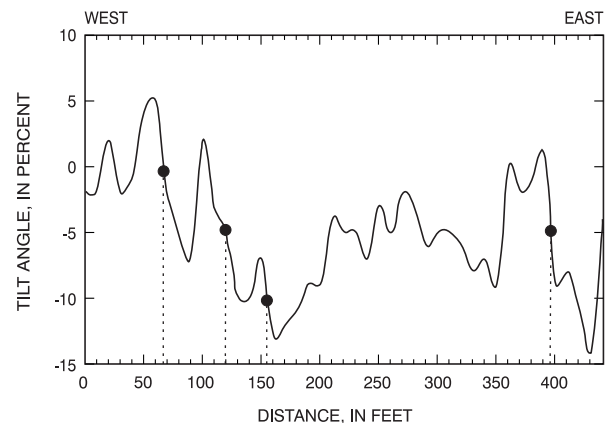
**EXPLANATION**

● Point of anomaly

**Figure 42.** Very low frequency (VLF) electromagnetic survey at site 6 from line 2, Salem, N.H. Site and line locations are shown on figures 1 and 40, respectively.

**SITE 6, LINE 3**

Very low frequency electromagnetic survey--tilt angle



**EXPLANATION**

● Point of anomaly

**Figure 43.** Very low frequency (VLF) electromagnetic survey at site 6 from line 3, Salem, N.H. Site and line locations are shown on figures 1 and 40, respectively.

VLF tilt-angle surveys were made at all lines (figs. 41-43). Line 1 has inflections at 100, 130, 395, 515, and 580 ft (fig. 41a). Line 2 tilt-angle results indicated inflection anomalies at 50 and 295 ft (fig. 42). Inflection anomalies are at 65, 120, 155, and 395 ft (fig. 43) from the survey of line 3.

EM surveys were collected along line 1 (fig. 41b). Vertical-conductor anomalies with the VD survey results were at 545 and 675 ft.

2-D resistivity surveys were used to characterize lines 1, 2, and 3. Models were created to support interpretations of the data. Resistivity data from line 1, 2, and 3 indicate three resistivity units: thin resistive unsaturated zone, conductive saturated zone, and resistive bedrock. Line 1 also has a fourth resistivity unit interpreted as fractured bedrock. Below the interpreted bedrock surface, at about 270 ft along the line, is a conductive anomaly with an apparent dip to the southeast (fig. 44). Line 2 data indicates a topographic high in the bedrock surface at 230 ft along the line (fig. 45). Anomalies in the bedrock were not identified with survey results from line 2 or 3 (fig. 46), only changes in the elevation of the bedrock surface were identified, with the bedrock being the deepest at the west end of line 3.

Square-array resistivity data were collected at array 1. Surveys were made with A-spacings of 5-20 m. Resistivity data from array 1 has a primary conductive strike of  $75^\circ$  when surveyed with the largest A-spacing (20 m). The secondary strike from array 1 at the 20-m A-spacing is  $300^\circ$  with a range of  $285^\circ$  to  $330^\circ$  (fig. 47).

Caliper, fluid temperature, fluid resistivity, and EM conductivity logs for well SAW 272 were used to identify and confirm fracture zones indicated on the OTV logs (appendix 1C). A cluster of fractures were identified on the lower hemisphere equal area net that have a range of strikes and dips of  $201\text{-}211^\circ$  and  $46\text{-}85^\circ$ , dipping NW (fig. 48). A group of contacts and foliation trends were identified, which have a range of strikes and dips of  $191\text{-}229^\circ$  and  $38\text{-}78^\circ$ , dipping NW. Fractures in the group fall within the range of strikes for the group of contacts and foliations. There also were widely scattered fractures and contacts and foliation outside of the identified groups (fig. 48). The largest fracture zone, at 264.5 ft, was identified as transmissive with fluid-temperature and resistivity logs from ambient and pumping borehole conditions. Caliper and EM logs correlate with this fracture zone, which was observed in the OTV log on a contact, with a strike and dip of  $240^\circ$  and  $64^\circ$ .

## Integration of Results

2-D resistivity results from line 1 indicate a prominent conductive east-dipping feature in the bedrock at 270 ft; however, results from lines 2 and 3 did not indicate major anomalies. Locations of anomalous results from different surface-geophysical methods could not be correlated at this site. The closest anomalies using VLF and EM were 35 ft apart on line 1 at 545 and 580 ft along the line. Thick, saturated overburden may obscure the VLF and EM survey results at this site.

Conductive strikes from square-array resistivity results that have the same orientation as fractures identified in outcrop, or remotely sensed lineaments, likely are related to fracture zones. The strike of the 20-m A-spacing secondary anomaly from array 1 ( $300^\circ$ ) has the same orientation as a fracture peak in the mapped geologic data at this site striking  $294^\circ \pm 7^\circ$  (67 percent, normalized height). The LOWALT lineament at the site with an orientation of  $44^\circ$  is just outside the error range for the maximum fracture peak at  $37^\circ$ , with a  $\pm 6^\circ$  error range.

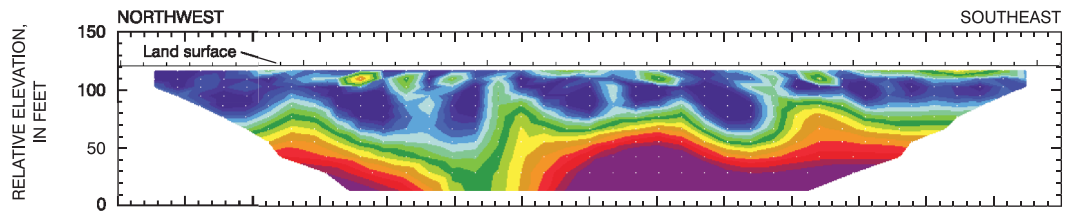
Borehole surveys from well SAW 272 show that the strikes and dips (average,  $206^\circ$  and  $60^\circ$ ) of a group of fractures are generally coincident with a group of foliation and contacts (average  $214^\circ$  and  $62^\circ$ ). The largest transmissive fracture zone characterized in the borehole data, (at a depth of 264.5 ft), dips towards, and if projected, would intersect well SAW 207 and may contribute to its yield. This fracture, which is coincident with a contact, is within  $7.5^\circ$  of the orientation of the primary strike from the square-array resistivity survey.

Although the locations of anomalies detected by electromagnetic (EM and VLF) surveys do not correlate spatially at site 6, they do indicate fractured bedrock. The lack of agreement between techniques may be caused by thick conductive overburden obscuring bedrock signatures. Because the overburden covering bedrock is thick, the geologic data used at this site may represent more regional rather than site specific conditions. DC-resistivity surveys and arrays and borehole data more clearly indicate fractured bedrock than other geophysical surveys at site 6 in Salem.

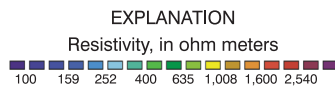
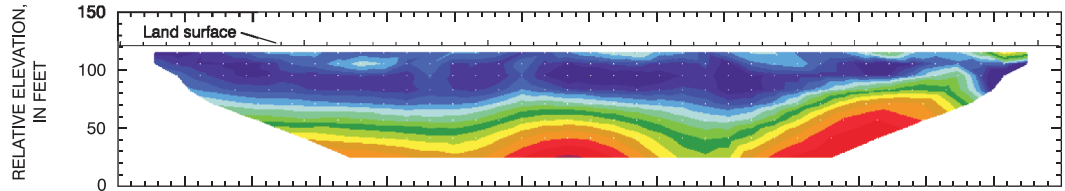
**SITE 6, LINE 1**

**Inverted Resistivity Sections**

(A) Dipole-dipole array

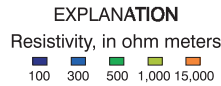
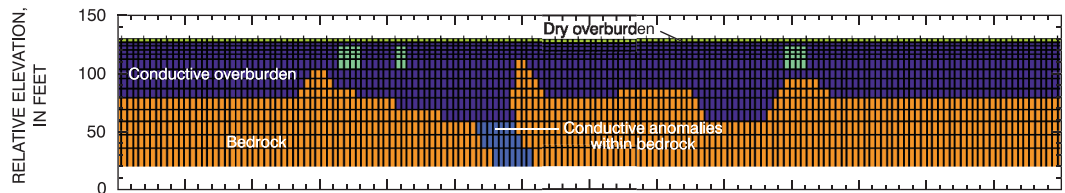


(B) Schlumberger array



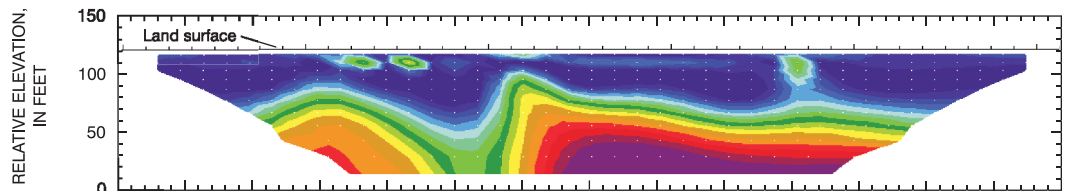
**Resistivity Model**

(C) Model



**Synthetic Inverted Resistivity Sections**

(D) Dipole-dipole array



(E) Schlumberger array

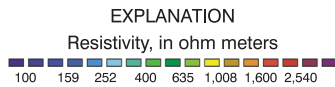
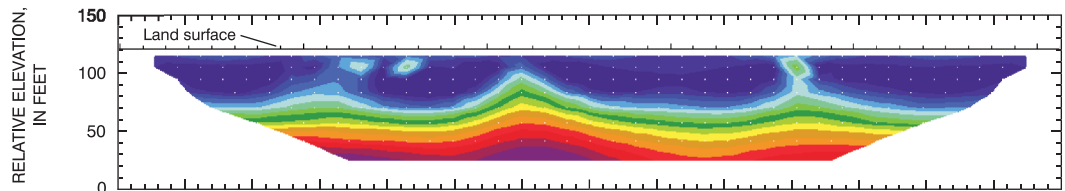


**Figure 44.** Cross sections showing (A and B) inverted resistivity sections of two-dimensional, direct-current resistivity data at site 6 from line 1, Salem, N.H.; (C) model based on field data from A and B; and (D and E) synthetic resistivity output data from Model C. Site and line locations are shown on figures 1 and 40, respectively.



SITE 6, ARRAY 1

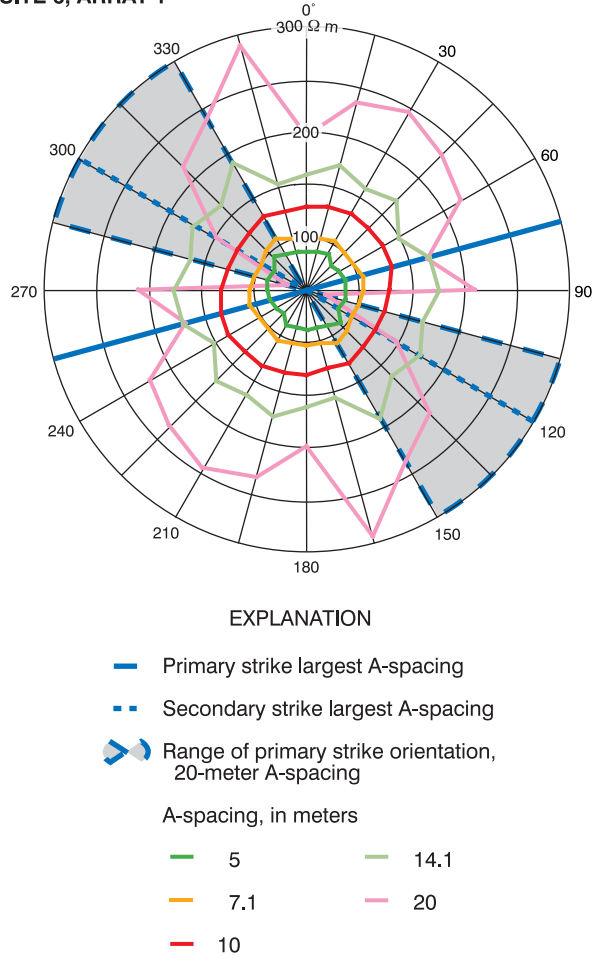


**Figure 47.** Polar plot showing azimuthal square-array direct-current resistivity at site 6 for array 1, Salem, N.H. Apparent resistivity in ohm meters ( $\Omega$  m), is plotted as a function of azimuth, in degrees east of true north, and resistivity center is at  $50 \Omega$  m. Site and array locations are shown on figures 1 and 40, respectively.

SITE 6, WELL SAW 272

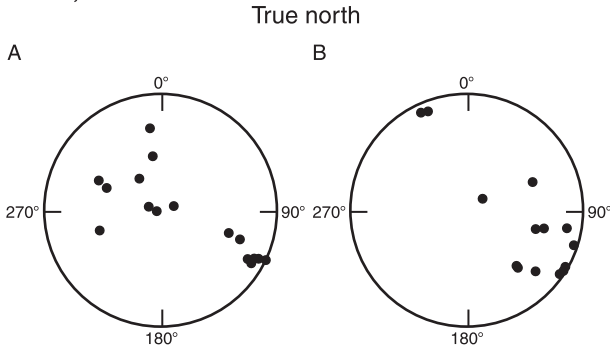


**Figure 48.** Lower hemisphere equal-area nets from bedrock well SAW 272 at site 6, Salem, N.H., showing (A) borehole fractures and (B) borehole contacts and foliation. Site and well locations are shown on figures 1 and 40, respectively.

## SUMMARY AND CONCLUSIONS

Bedrock aquifer ground-water resources in New Hampshire have been assessed statewide by the U.S. Geological Survey, in cooperation with the New Hampshire Department of Environmental Services, to identify areas that are favorable for more intensive investigation. This study identified site-specific anomalies in geophysical-survey results from sites 1, 4, and 5 in the Pinardville 7.5-minute quadrangle, and sites 2, 3, and 6 in the Windham 7.5-minute quadrangle that indicate the location of bedrock-fracture zones that are potentially water bearing.

At four of the sites, geophysical anomalies were closely correlated with geologic-fracture data and lineament locations and orientations. High-yielding bedrock wells at all of the sites indicate highly transmissive fracture zones in those areas. Surface-geophysical methods used in this study were able to identify the locations of fracture zones at these sites.

Seismic-refraction and ground-penetrating radar were used primarily to characterize the overburden, and provided limited bedrock characteristics. At some site locations, velocities of seismic waves through bedrock indicated a dominant fast trend near parallel to a specific fracture orientation. Where seismic wave velocities were slow, measurements often were nearly perpendicular to an interpreted fracture zone. Where overburden was thin or absent, GPR results located near-horizontal bedrock fractures zones that geologic mapping and lineament analysis could not identify. Conductive overburden sediments, particularly till, generally obscured GPR penetration to bedrock.

VLF and EM surveys provide a rapid means to locate conductive features such as water-filled fractures. VLF surveys identified several likely fracture zones, however, these surveys were susceptible to cultural interference and were often difficult to interpret. In addition to providing qualitative information about the thickness and conductivity of the overlying formations, EM surveys identified several fracture zones, and in some cases, their dip direction. The EM surveys can be done relatively quickly and are easy to interpret. Whereas other techniques, for example a lineament analysis, may indicate the surface expression of a fracture zone, geophysical methods sometimes help identify the dip direction of that zone. Dip direction is the next most valuable piece of information required to target a well through a fracture zone.

The collection of various layers of data and inversion processing of 2-D resistivity surveys yielded results that indicate overburden types and saturation, depths to bedrock, and most importantly, depths and dips of fracture zones. Modeling was used to back up interpretations of resistivity data and incorporate known information from well data and surface observations of overburden materials and bedrock outcrop into the analysis. Incorporating multiple pieces of information increased the confidence in 2-D resistivity interpretations. Of the seven surface geophysical methods investigated, analysis of 2-D resistivity surveys provided the most quantitative information on fracture-zone location and dip direction.

The orientation of conductive-geophysical anomalies identified with square-array resistivity showed varying agreement between geologic fracture and lineament data. At some sites, available indicators (outcrop fracture measurements and lineaments) to strikes of features were confirmed, whereas at other sites, they were not. At arrays where conductive-fracture zones were not interpreted, other features could cause the azimuthal-square-array resistivity anomalies if the horizontal layer assumption (bedrock surface and overburden) of the model was violated.

Borehole-geophysical data identified transmissive-fracture zones at the three sites surveyed. Borehole-survey data reinforce interpretations drawn from surface geophysical, geological outcrop, and remote-sensing surveys. Two sites had agreement between orientations of anomalies from surface geophysics, borehole-geophysical-survey feature orientations, and geologic data. At site 6, with no outcrops nearby, a large transmissive-fracture zone located with borehole geophysics was projected towards another high-yielding well that was not accessible for logging.

The various geophysical surveys described in this report illustrate how geophysical methods can be integrated to help define the hydrogeology at different sites in crystalline rock. These survey results were analyzed in conjunction with other data, such as geologic outcrop, well logs, and remotely sensed data to interpret the location of subsurface fracture zones at high-yield well sites.

## SELECTED REFERENCES

- Ayotte, J.D., and Dorgan, T.H., 1995, Geohydrology of the Flints Pond aquifer, Hollis, New Hampshire: U.S. Geological Survey Open-File Report 95-363, 22 p.
- Ayotte, J.D., Mack, T.M., and Johnston, C.M., 1999, Geophysical surveys of Country Pond and adjacent wetland, and implications for contaminant-plume monitoring, Kingston, New Hampshire: U.S. Geological Survey Open-File Report 99-51, 16 p.
- Beres, Milan, Jr., and Haeni, F.P., 1991, Application of ground-penetrating-radar methods in hydrogeologic studies: *Ground Water*, v. 29, no. 3, p. 375-386.
- Bisdorf, R.J., 1985, Electrical techniques for engineering applications: *Bulletin of the Association of Engineering Geologists*, v. XXII, no. 4, p. 421-433.
- Chapman, M.J., and Lane, J.W., 1996, Use of directional borehole radar and azimuthal square-array D.C. resistivity methods to characterize a crystalline bedrock aquifer, *in* Symposium on the application of Geophysics to Environmental and Engineering Problems, Keystone, Colo., April 28 through May 2, 1996, Proceedings: Keystone, Colo., p. 833-842.
- Clark, S.F., Jr., Ferguson, E.W., Moore, R.B., 1997, Lineament map of area 2 of the New Hampshire bedrock aquifer assessment, southeastern New Hampshire: U.S. Geological Survey Open-File Report 96-490, 1 sheet, scale 1:48,000.
- Clark, S.F., Jr., Moore, R.B., Ferguson, E.W., and Picard, M.Z., 1996, Criteria and methods for fracture-trace analysis of the New Hampshire bedrock aquifer: U.S. Geological Survey Open-File Report 96-479, 12 p.
- Dahlin, Torleif, 1996, 2-D Resistivity surveying for environmental and engineering applications: *First Break*, v. 14, no. 7, July 1996, p. 275-283.
- Drew, L.J., Karlinger, M.R., Armstrong, T.R., and Moore, R.B., 1999, Relations between igneous and metamorphic rock fracture patterns and ground-water yield from the variability of water-well yields, Pinardville Quadrangle, New Hampshire: *Natural Resource Research*, v. 8, no. 2, 1999.
- Ferguson, E.W., Clark, S.F., Jr., and Moore, R.B., 1997, Lineament map of area 1 of the New Hampshire bedrock aquifer assessment, southeastern New Hampshire: U.S. Geological Survey Open-File Report 96-489, 1 sheet, scale 1:48,000.
- Frohlich, R.K., 1989, Magnetic signatures of zones of fractures in igneous metamorphic rocks with an example from southeastern New England: *Tectonophysics*, no. 163, p. 1-12.
- Haberjam, G.M., and Watkins, G.E., 1967, The use of a square configuration in resistivity prospecting, *in* 29th European Association of Exploration Geophysicists

- Meeting, Stockholm, June 1967, Proceedings: Stockholm, European Association of Exploration Geophysicists, 23 p.
- Haeni, F.P., 1988, Application of seismic-refraction techniques to hydrologic studies: U.S. Geological Survey Techniques of Water-Resources Investigations, book 2, chap. D2, 86 p.
- 1995, Application of surface-geophysical methods to investigations of sand and gravel aquifers in the glaciated northeastern United States: U.S. Geological Survey Professional Paper 1415-A, 70 p.
- Haeni, F.P., Lane, J.W., Jr., and Lieblich, D.A., 1993, Use of surface-geophysical and borehole-radar methods to detect fractures in crystalline rocks, Mirror Lake Area, Grafton County, New Hampshire, *in* Hydrogeology of Hard Rocks, International Association of Hydrologists, XXIVth Congress, Oslo, Norway, June 1993, Proceedings: Oslo, Norway, International Association of Hydrologists, 11 p.
- Hansen, B.P., and Lane, J.W., 1995, Use of surface and borehole geophysical surveys to determine fracture orientation and other site characteristics in crystalline bedrock terrain, Millville and Uxbridge, Massachusetts: U.S. Geological Survey Water-Resources Investigations Report 95-4121, no. 25, 11 p.
- Hansen, B.P., Stone, J.R., and Lane, J.W., Jr., 1999, Characteristics of fractures in crystalline bedrock determined by surface and borehole geophysical surveys, Eastern Surplus Superfund Site, Meddybemps, Maine: U.S. Geological Survey Water-Resources Investigations Report 99-4050, 55 p.
- Iris Instruments, 1993, T-VLF Operating manual (Release 1.0): Orleans, France, 32 p.
- Johnson, C.D., Dunstan, A.H., Mack, T.J., and Lane, J.W., Jr., 1999, Borehole-geophysical characterization of a fractured-bedrock aquifer, Rye, New Hampshire: U.S. Geological Survey Open-File Report 98-558, 61 p.
- Keyes, W.S., 1988, Borehole geophysics applied to ground-water investigations: U.S. Geological Survey Open-File Report 87-539, 305 p.
- Koteff, Carl, 1970, Surficial geologic map of the Milford Quadrangle, Hillsborough County, New Hampshire: U.S. Geological Survey, 1 sheet, scale 1:24,000.
- Lane, J.W., Jr., Haeni, F.P., and Watson, W.M., 1995, Use of a square-array direct-current resistivity method to detect fractures in crystalline bedrock in New Hampshire: *Ground Water*, v. 33, no. 3, p. 476-485.
- Larson, G.T., 1984, Surficial geologic map of the Windham Quadrangle, Rockingham and Hillsborough Counties: New Hampshire Department of Resources and Economic Development, 1 sheet, 1:24,000 scale.
- Loke, M.H., 1999, Electrical imaging surveys for environmental and engineering studies, A practical guide to 2-D and 3-D Surveys: Penang, Malaysia, <http://www.agiusa.com/literature.shtml>, 57 p.
- 1999, RES2DMOD vers. 2.2 Rapid 2-D resistivity forward modelling using the finite-difference and finite-element methods: Penang, Malaysia, <http://www.agiusa.com/files/pub/res2dmodmanual.pdf>, 22 p.
- Lyons, J.B., Bothner, W.A., Moench, R.H., and Thompson, J.B., Jr., 1997, Bedrock geologic map of New Hampshire: U.S. Geological Survey State Geologic Map, 2 sheets, scale 1: 250,000 and 1:500,000.
- Mack, T.J., Johnson, C.D., and Lane, J.W., Jr., 1998, Geophysical characterization of a high-yield fractured-bedrock well, Seabrook, New Hampshire: U.S. Geological Survey Open-File Report 98-176, 22 p.
- McNeill, J.D., 1980, EM-34 Survey interpretation techniques: Geonics limited technical note TN-8, rev. January 1983, 16 p.
- Medalie, Laura, and Moore, R.B., 1995, Ground-water resources in New Hampshire: Stratified-drift aquifers: U.S. Geological Survey Water-Resources Investigations Report 95-4100, 31 p.
- Moore, R.B., and Clark, S.F., Jr., 1996, Assessment of ground-water supply potential of bedrock in New Hampshire: U.S. Geological Survey Fact Sheet FS 95-002, 2 p.
- Powers, C.J., Singha, Kamini, and Haeni, F.P., 1999, Integration of surface geophysical methods for fracture detection in bedrock at Mirror Lake, New Hampshire, *in* Toxic Substances Hydrology Program Meeting, March 8-12, 1999, Proceedings: Charleston, S.C., U.S. Geological Survey, p. 757-768.
- Powers, C.J., Wilson, Joanna, Haeni, F.P., and Johnson, C.D., 1999, Surface-geophysical characterization of the University of Connecticut Landfill, Storrs, Connecticut: U.S. Geological Survey Water-Resources Investigations Report 99-4211, 34 p.
- Salvini, Francesco, 2000, The Structural Data Integrated System Analyzer software (DAISY 2.19): Rome, Italy, Università degli Studi "Roma Tre," Dipartimento di Scienze Geologiche.
- Salvini, Francesco, Billi, Andrea, and Wise, D.U., 1999, Strike-slip fault propagation cleavage in carbonate rocks: the Mattinata Fault Zone, Southern Apennines, Italy: *Journal of Structural Geology*, v. 21, p. 1731-1749.
- Scott, H.J., 1971, Seismic refraction modeling by computer, *in* Annual International Society of Engineering Geology Meeting, 41st, Houston, Tex., November 9, 1971, Proceedings: Houston, Tex., Society of Engineering Geology, p. 271-284.
- Spratt, J.G., 1996, Application of surface geophysical methods to delineate fracture zones associated with

- photolinear features in West-Central Florida *in* Bell, R.S., and Cramer, M.H., eds., Symposium on the application of geophysics to engineering and environmental problems, Keystone, Colo., April 28 - May 2, 1996: Keystone, Colo., Environmental and Engineering Geophysical Society, p. 907-916.
- Stekl, P.J., and Flanagan, S.M., 1992, Geohydrology and water quality of stratified-drift aquifers in the Lower Merrimack and Coastal River Basins, southeastern New Hampshire: U.S. Geological Survey Water-Resources Investigations Report 91-4025, 137 p.
- Taylor, K.C., Minor, T.B., Chesley, M.M., Matanawi, Korblaah, 1999, Cost effectiveness of well site selection methods in a fractured aquifer: *Groundwater*, v. 37, no. 2, March-April 1999, p. 271-274.
- Walsh, G.J., and Clark, S.F., Jr., 1999, Bedrock geologic map of the Windham Quadrangle, Rockingham and Hillsborough Counties, New Hampshire: U.S. Geological Survey Open-File Report 99-8, 1 sheet, 1:24,000 scale.
- 2000, Contrasting methods of fracture trend characterization in crystalline metamorphic and igneous rocks of the Windham Quadrangle, New Hampshire: *Northeastern Geology and Environmental Sciences*, v. 22, no. 2, 2000, p. 109-120.
- Wright, J.L., 1994, VLF Interpretation Manual: Terraplus U.S.A., Inc., 83 p.
- Zohdy, A.A.R., Eaton, G.P., and Mabey, D.R., 1974, Application of surface geophysics to ground-water investigations: U.S. Geological Survey Techniques of Water-Resources Investigations, book 2, chap. D1, 86 p.

---

---

**APPENDIX 1. Graphs showing borehole geophysical logs of  
three sites in New Hampshire**

---

---

SITE 4, WELL GNNW 406

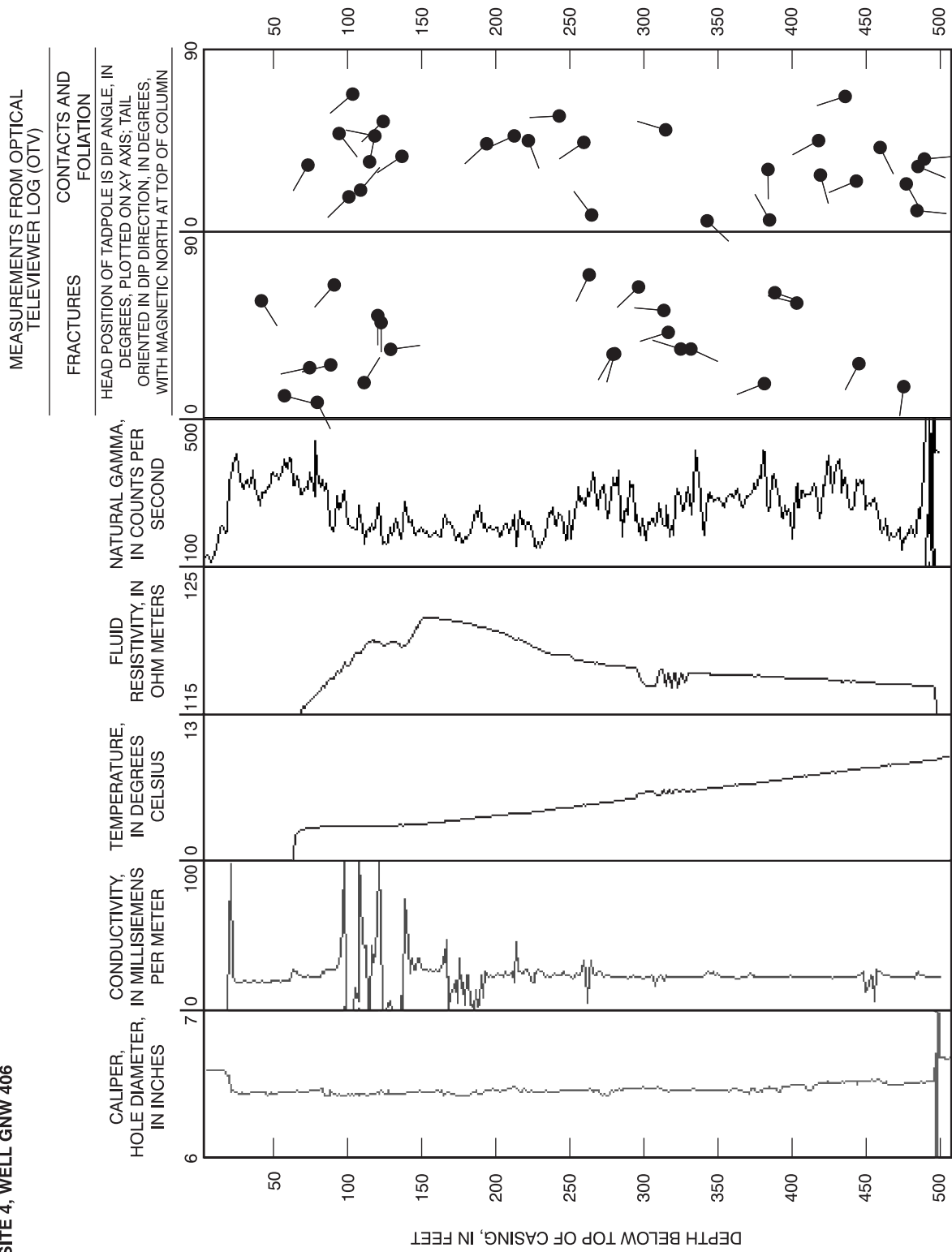


Figure 1A. Borehole geophysical logs of well GNNW 406 at site 4, Goffstown, N.H. Site and line locations are shown on figures 1 and 26, respectively.

SITE 5, WELL GNW 408

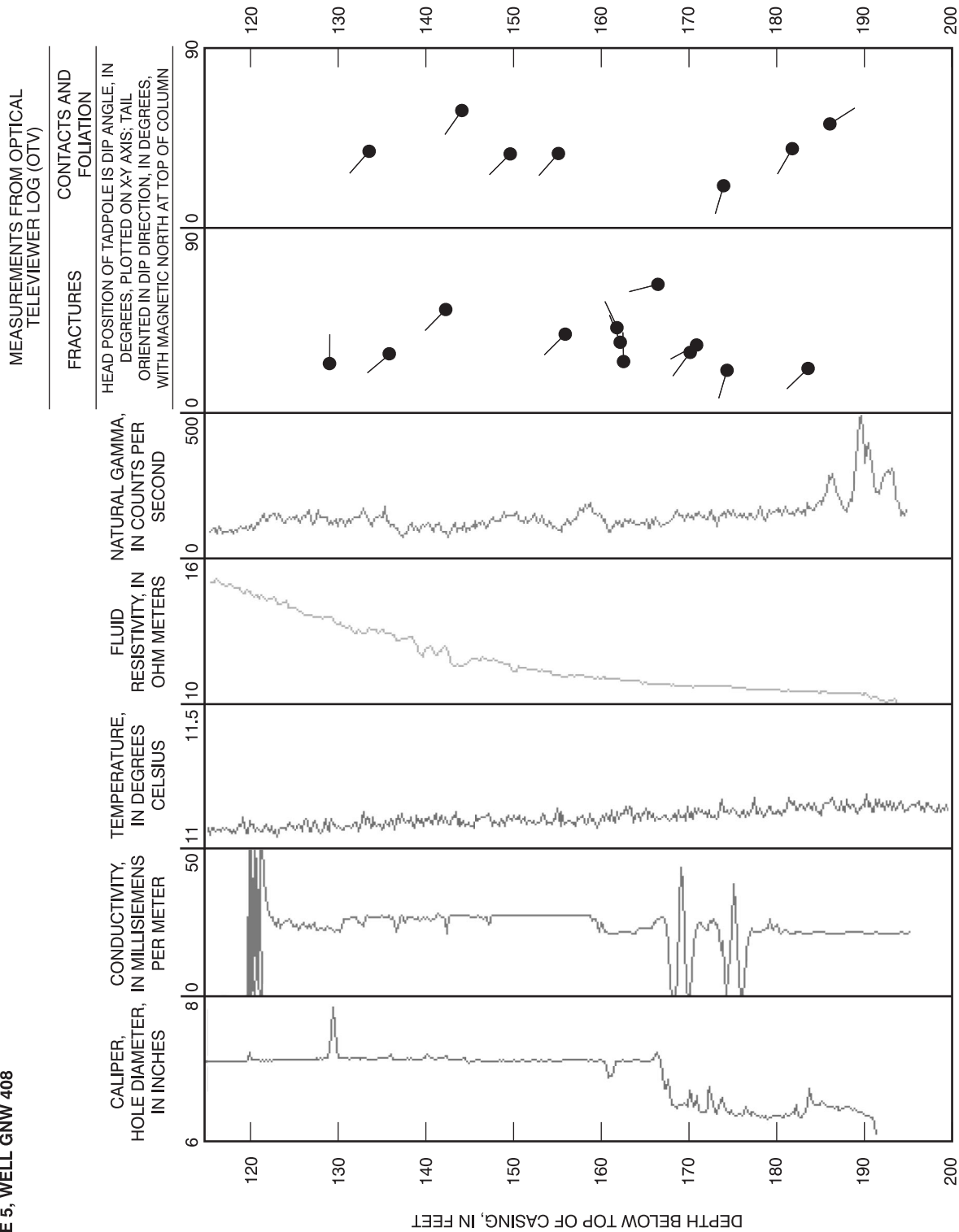


Figure AB. Borehole geophysical logs of well GNW 408 at site 5, Goffstown, N.H. Site and line locations are shown on figures 1 and 33, respectively.

SITE 6, WELL SAW 272

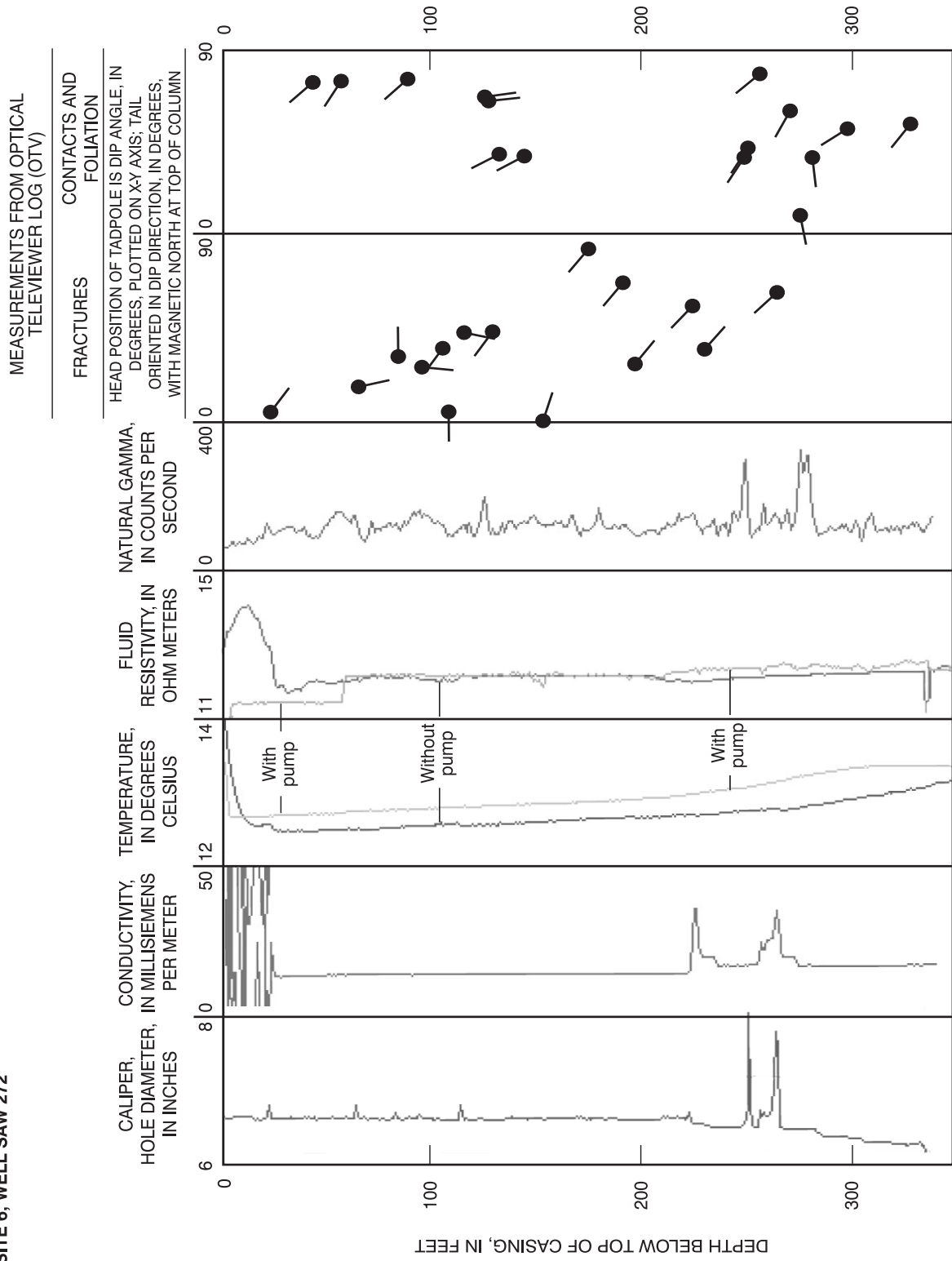


Figure 1c. Borehole geophysical logs of well SAW 272 at site 6, Salem, N.H. Site and line locations are shown on figures 1 and 40, respectively.



GEOPHYSICAL INVESTIGATIONS OF WELL FIELDS TO CHARACTERIZE FRACTURED-BEDROCK AQUIFERS IN SOUTHERN NEW HAMPSHIRE—  
Degnan, J.R., Moore, R.B., and Mack, T.J.  
USGS Water-Resources Investigations Report 01-4183